OUKA
The University of Osaka
Institutional Knowledge Archive

Title	STUDY ON CHEMICAL EFFECT OF RECOIL PARTICLE
Author(s)	Takemi, Hirokatsu
Citation	大阪大学, 1973, 博士論文
Version Type	VoR
URL	https://hdl.handle.net/11094/1902
rights	
Note	

The University of Osaka Institutional Knowledge Archive : OUKA

https://ir.library.osaka-u.ac.jp/

The University of Osaka

STUDY ON CHEMICAL EFFECT OF RECOIL PARTICLE

1973

Hirokatsu Takemi

STUDY ON CHEMICAL EFFECT OF RECOIL PARTICLE

by

Hirokatsu TAKEMI

NOTICE

This work is the thesis for fulfillment of the degree of doctor of engineering by the author and derives from the studies made under the research director, Professor Mutsuaki SHINAGAWA, in the postgraduate course of Nuclear Engineering Faculty of Engineering, Osaka University.

Contents

Chapter I. Introduction

It is known that the product induced by radioactive decay or nuclear reaction has some kinetic energies and charges characterized in the nuclear transformation. The products of α-decay, for instance, usually have about 0.1 MeV of kinetic energy. They may also be in unusually high charge state. Thus, in β^--decay of ^{41}A, ^{41}K atoms with charges as high as +8 have been detected. In passing through matter, these products come into equilibrium with their surroundings, and the resulting species have been detected by physical and chemical methods.

In 1934, L.Szilard and T.A.Chalmers showed that in the irradiation of ethyl iodide with neutron, some proportion of the ^{128}I formed in the $^{127}I(n,\gamma)^{128}I$ reaction could be extracted from the ethyl iodide by shaking it with an aqueous reducing solution containing a trace of free iodine as a carrier. This phenomenon was explained on the ground that the iodine – carbon bond was broken by recoil energy of ^{128}I. This type of process as well as some (γ,n), $(n,2n)$ and (d,n) reactions have been widely used for the separation isotopes.

Such reactions mentioned above usually arise under the background of contaminative radiations, e.g. high dose γ-rays beside neutron flux in reactor. These radiations induce the ionization, excitation or radicalization to dissociate the medium as the result of the interaction.

Considering the chemical phenomena occured in nuclear

reactor from a point of energy transference, the interaction between charged particles associated with nuclear transformation and chemical matrix is important to apply the energy of nuclear process for chemical preparation. In general, the energy imparted to the newly formed recoil atom is usually much excess for chemical bond energy. In fission it is of more or less 100 MeV. When a few nucleons are emitted, it is of order of 0.1 MeV or less, and in (n,γ) reaction or β^--decay it is of order of 100 eV. Until the atom disperses most of this energy, it is unable to enter into stable chemical combination. The most chemically significant stage in the slowing down process is therefore the final stage, when an energitic atom loses its energy mainly by collision with matrix atom.

The present thesis involves the studies on behaviors of recoil atoms associated with α-decay and on $^{10}B(n,\alpha)^7Li$ reaction in chemical matrix. The paper consists of three parts. Part one (Chap. II and III) is concerned with the behavior of α-recoil atoms in air, i.e. the gaseous electro-deposition process of recoil atoms in thorium decay series. Part two (Chap. IV) is described the interaction of α- and γ-rays with celluloid film, one of the most sensitive materials suffering the radiation damage in polymers from a point of solid state track detector. Part three (Chap. V) deals with chemical preparation by using the $^{10}B(n,\alpha)^7Li$ reaction, i.e. hydrazine formation from an aqueous solution of ammonia with boron compounds added.

The experimental studies given in each part are discussed mainly at following three points: (1) chemical effect associated with α-decay, (2) detection of charged particle with polymer and (3) application of nuclear energy for chemical preparation.

(1) Chemical effect associated with α-decay

Alpha decay reduces two units in the atomic number and gives a recoil energy of about 0.1 MeV to the atom. As for the chemical reaction, this is a very high level of energy and breaks chemical bonds to make the recoil atom free from the mother molecule. It collides successively with the neighboring atoms, losing energy in the process and giving rise to ionization. After 100 collisions, corresponding to a range of the order of 10 $\mu g/cm^2$, it is reduced to thermal energy, and about 3000 ion-pairs are formed along the track.

The accepted theory postulates that the recoil atom interacts mainly with the electrons of the medium through which it passes. This leads to the Bohr's equation in which the recoil range is proportional to the first power of the recoil energy.

The number of charges on the recoil atom tends to fluctuate as the atom moves through the medium. A loss of two units of charges might be expected in the initial α-decay, but in many cases the final charge is one in positive, and the recoil atoms can be collected on a negatively charged metal plate. Recoil emanation atoms are usually uncharged

at the end of their path. After dispersing the excess energy along a recoil track, an α-decay product may take part in chemical reactions with its neighbors. The effects observed are often rather obvious ones, because the elements concerned are of relatively simple chemistry. The $^{212}Bi \xrightarrow{\alpha} {}^{208}Tl$ decay in thorium series however provides an example of less predictable chemistry since it has complication in decay scheme. In chapter II, it is attempted to apply the selective gaseous electro-deposition of thorium decay series nuclides under atmosphere using RdTh source. Chapter III deals with the conditions of their electro-deposition using ^{212}Pb source under pressure below atmospheric.

(2) Detection of charged particle with polymer

When charged particle irradiates on a dielectric material, it produces minute trails of damage (ca. 10 ~ 100 Å in diameter) in the material. These damage trails, which are initially visible only under an electron microscope, are then usually enlarged a thousandfold by subjecting the material to a suitable etching process so that become visible under an ordinary microscope. This is one of the reasons why many dielectric materials have been widely used as the detection of heavy charged particle in several disciplines, including nuclear physics and chemistry.

The mechanism for the formation of radiation damage and this etchability have been discussed. In particular, the mechanism in polymeric dielectric materials has been proposed

on the grounds of the σ-rays produced from the secondary reaction of charged particle with them. At the present time a comprehensive theory of latent track formation in polymer is not available since the exact chemical and physical properties of preferentially etchable region depend strongly on the charge and speed of the particle, on the chemical structure of the polymer, on the physical state of materials during irradiation and on the environmental conditions. Chapter IV deals with celluloid film which is one of the most sensitive polymer to the radiation damage as solid state track detector, particularly alpha energy analysis for several α-emitter sources and the effect of γ-rays and its related α-track registering sensitivity.

(3) Application of nuclear energy for chemical preparation

The application of nuclear energy for chemical preparation has been considered from several stand points of energy transference. Most of the proposals which have been suggested involve the use of energy as process heat, as ionizing or radical forming radiation in the form of γ-rays or particle beam. Of all the type of energy that released in the fission process, the most important as energy source is the kinetic energy of fission fragments. This energy is very large in LET and in release energy comparing with other radiation. It is therefore advisable to use the chemical system that G-value is very small and its reaction is endothermic. No fullscale reactor of the type has yet been

built and the development of the technology is at present in a very early stage. One of the principal reason for this is that there is a lack of basic information concerning the behavior of chemical systems under this influence of fission fragment radiolysis. A major disadvantage of this radiolysis is the contamination caused by the fission products.

The $^{10}B(n,\alpha)^{7}Li$ reaction on the other hand does not give rise to radioactive products. The LET value in this reaction is considerably high with about 280 keV/μ in a medium of unit density ($\sim$0.28 keV/μ for ^{60}Co γ-rays, $\sim$4000 keV/μ for fission recoils). When the added boron compound used is dissolved in the system, the average kinetic energy of 2.33 MeV of the reaction is completely absorbed in the surroundings and some additive effect for the products may be expected. In chapter V, it is attempted to apply the energy of α and Li recoils in $^{10}B(n,\alpha)^{7}Li$ reaction to the hydrazine formation from ammonia-water system.

Chapter II. Selective Gaseous Electro-Deposition of Thorium Decay Series Nuclides[1]

2-1 Introduction

One method of preparing radioactive nuclides is to collect disintegrated recoil species on a negatively charged plate. For instance, ThB has been separated from Tn, RaB from Rn, AcB from RdAc and ^{206}Tl from ^{210}Bi by this method[2]. More recently, Briand et al. have succeeded in separating radioactive nuclide ^{216}At of very short half-life (300 μs) by automatic collection in vacuum as it was emitted by second order α recoil[3]. Ghiorso et al.[4] have collected on a negatively charged metal belt the 102nd element, produced from ^{246}Cm bombarded by ^{12}C ion beam. They have also collected ^{257}Lr produced from ^{252}Cf bombarded by ^{10}B ion beam.

Shinagawa et al.[5] have determined the most suitable conditions for the electro-deposition of radioactive decay products of the Th decay series under normal temperature and pressure, and have explained that the deposited radioactive substance has a positive charge in the gaseous phase.

In this chapter, some daughter nuclides of RdTh are to separate using a capsule equipped with three electrodes, one of which is constituted by the source plancet; RdTh has been chosen as parent substance. Decayed nuclides such as ^{212}Pb and ^{208}Tl are made to deposit on the nickel target plate under different experimental conditions (applied voltage, intervals between the electrodes, time allowed for deposition,

presence or absence of grid) under normal atmospheric pressure. The mechanism of the electro-deposition process under electric field with and without a grid is discussed on the basis of the decay pattern shown by each nuclide.

2-2 Experimental

2-2-1 Apparatus

Figure 2.1 shows the apparatus used for the experiment. It is made up of three electrodes installed in a glass capsule (50 mm diam., 160 mm high). The parent RdTh substance is placed on nickel plate, over which is placed an inverted cup with a pin hole (0.5 mm diam.) at the center. The target plate is made of nickel (40 mm diam., 0.5 mm thick, purity 99.9 %) and the grid is a net made of stainless steel wire (0.1 mm diam. mesh intervals of 0.5 mm) and bordered with a nickel ring. In Fig. 2.1, the symbols d, D and V represent the distances and the applied voltage between the parts indicated. The range of voltage applied was from -1500 to +1500 V D.C. in reference to the source plate which was held earthed. The interval D between the pin hole slit and the target plate was set in the range between 15 and 150 mm.

2-2-2 Sample and Method

As sample, 1 mCi of RdTh (Crystalline chloride with Th-232 carrier obtained from the Radio Chemical Center, England) was used. The daughter nuclides of RdTh were electro-deposited on the target surface under different experimental conditions. The relative amount of electro-deposition of RdTh

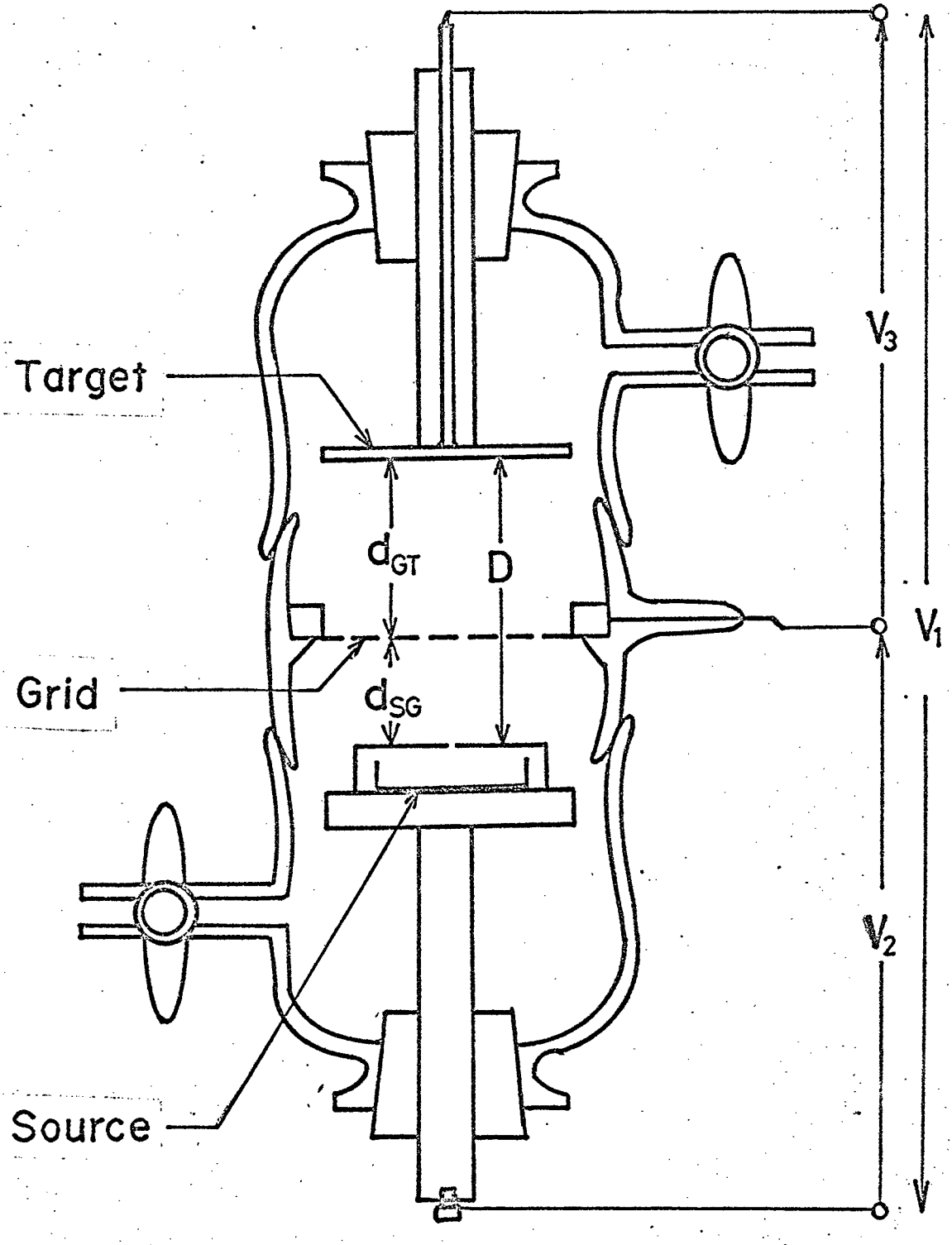

Fig. 2.1 Experimental glass capsule with source, grid and target

daughter nuclides on each electrode was measured by γ-ray spectrometer (Hitachi Ltd., NaI(Tl) crystal 1" x 1", 400 channels P.H.A.). On the other hand, the target plate was surveyed autoradiographically.

The γ-ray spectrum of the RdTh source revealed the photopeaks of the daughter nuclides ^{212}Pb (0.24 MeV), ^{208}Tl (0.58 MeV) and ^{212}Bi (0.73 MeV) as well as that of the parent substance, as seen in Fig. 2.2. Figure 2.3 presents the γ-ray spectra of the deposits on the target after different periods of cooling time T. The photopeaks of ^{212}Pb as denoted by A in Fig. 2.3 are seen to be influenced by the Compton scattering of ^{208}Tl ($T_{1/2}$ = 3.1 min), and to reduce this effect, the activities of ^{212}Pb were measured after T = 30 min. The relative amounts of activities for the γ-ray photopeaks were obtained by Covell's method[6].

Upon correction of such factors as time allowed for electro-deposition, for cooling, and time taken for the measurements, the activities at the end of the electro-deposition could be estimated, and were considered to represent the activities of deposited nuclides, and these values have been adopted in the ensuing descriptions. The statistical errors within the standard deviations were estimated for all measured radioactivities. Thus the deviations of ^{212}Pb(A) and ^{208}Tl(B) values were all within the circles marked in the figures, and those of B/A values are indicated by conventional signs.

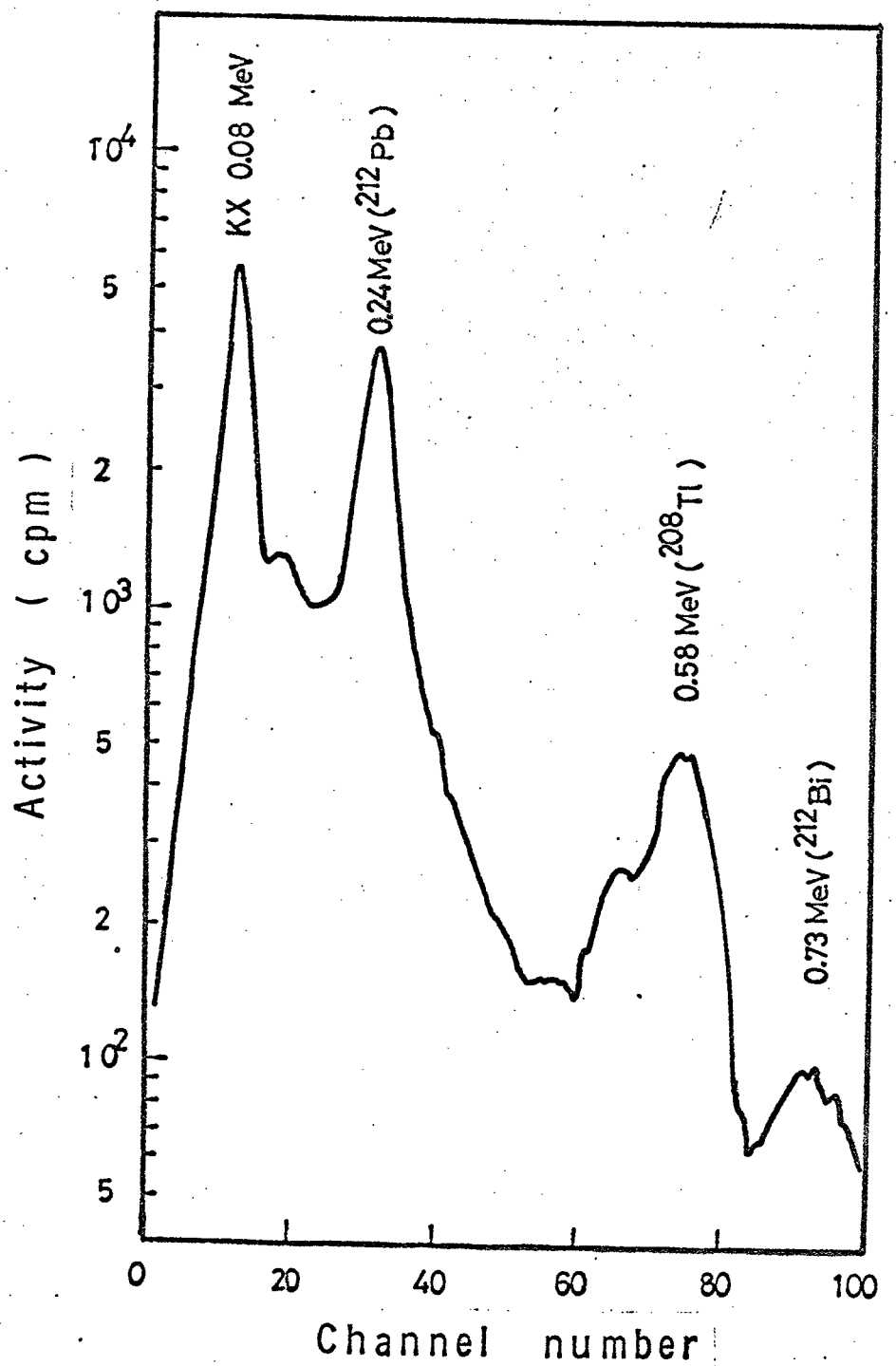

Fig. 2.2 Gamma-ray spectrum of RdTh source

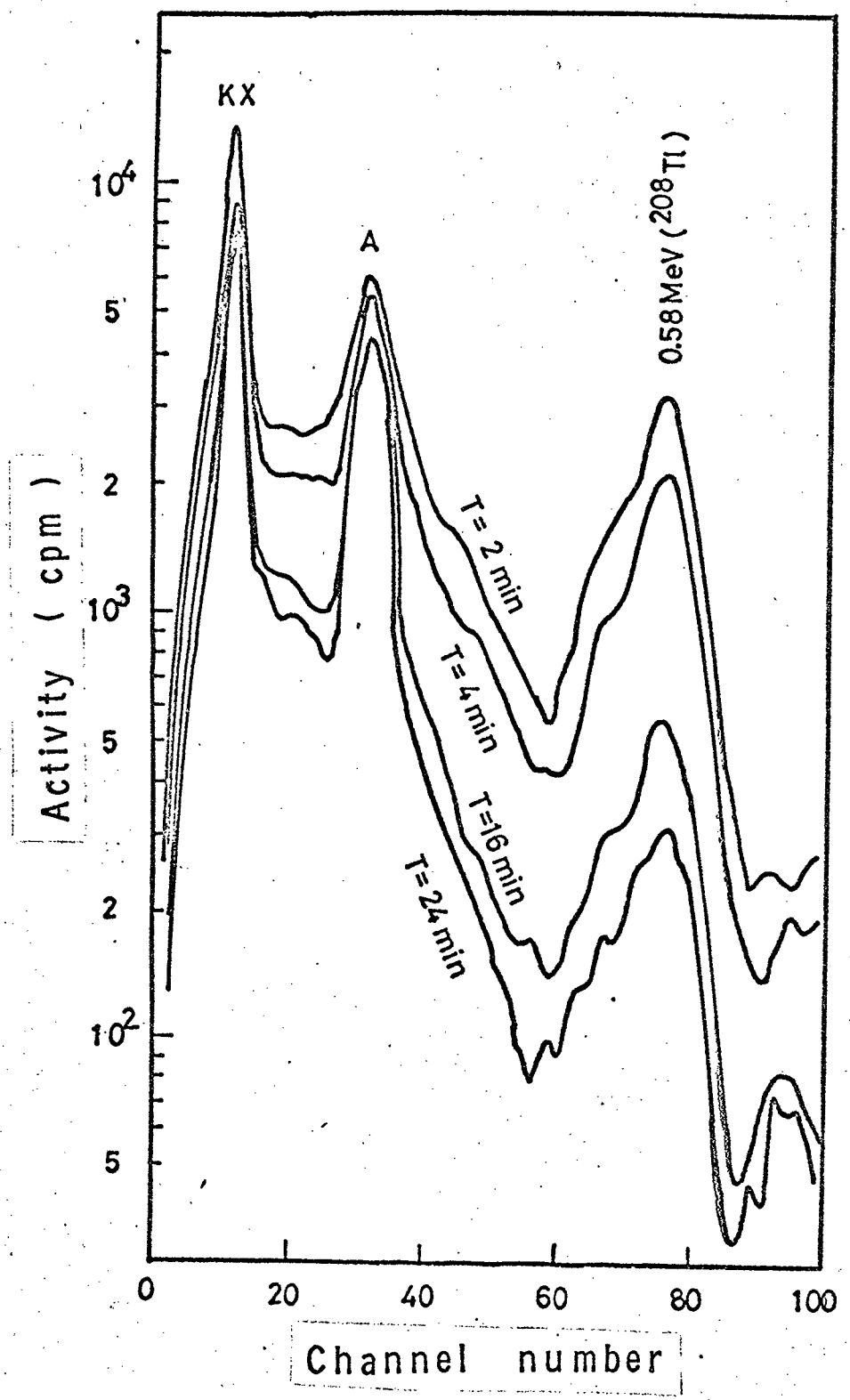

Fig. 2.3 Variation of γ-ray spectra of nuclides deposited on target brought by differences in cooling time T

2-3 Results and Discussion

2-3-1 Effect of the Target Voltage V_1 with Grid Removed

As the target voltage V_1 between the source and the target was changed from 0 to -1500 V, the activities on the target changed as shown in Fig. 2.4. The activity of ^{212}Pb (A) deposited on the target is seen to increase rapidly up to -100 V, after which the rise eases off. On the other hand, that of ^{208}Tl(B) on the target is seen to increase gradually up to -500 V beyond which it tends to saturate. The resulting ratio between ^{208}Tl and ^{212}Pb (B/A) decreases up to -50 V and then increases sharply up to -500 V. The ratio B/A on the target exceeded that of RdTh source beyond -500 V.

2-3-2 Effect of Differences in Time Allowed for Electro-Deposition with Grid Removed

The time allowed for electro-deposition was varied up to 2 hrs, with a constant applied voltage V_1. The results are shown in Fig. 2.5.

The activity of ^{208}Tl is seen to present a saturation plateau in the range from 5 to 20 min, after which it increases again linearly. The plateau starts at a point about twice the half-life of ^{208}Tl, indicating the establishment of radioactive equilibrium of the ^{208}Tl on the target. The increase of ^{208}Tl activity above the plateau value after 30 min could be attributed to the appearance of the daughter nuclide of the deposited ^{212}Pb on the target ($^{212}Pb \xrightarrow{\beta^-} {}^{212}Bi \xrightarrow{\alpha} {}^{208}Tl$) and added to ^{208}Tl directly deposited on the target from RdTh source.

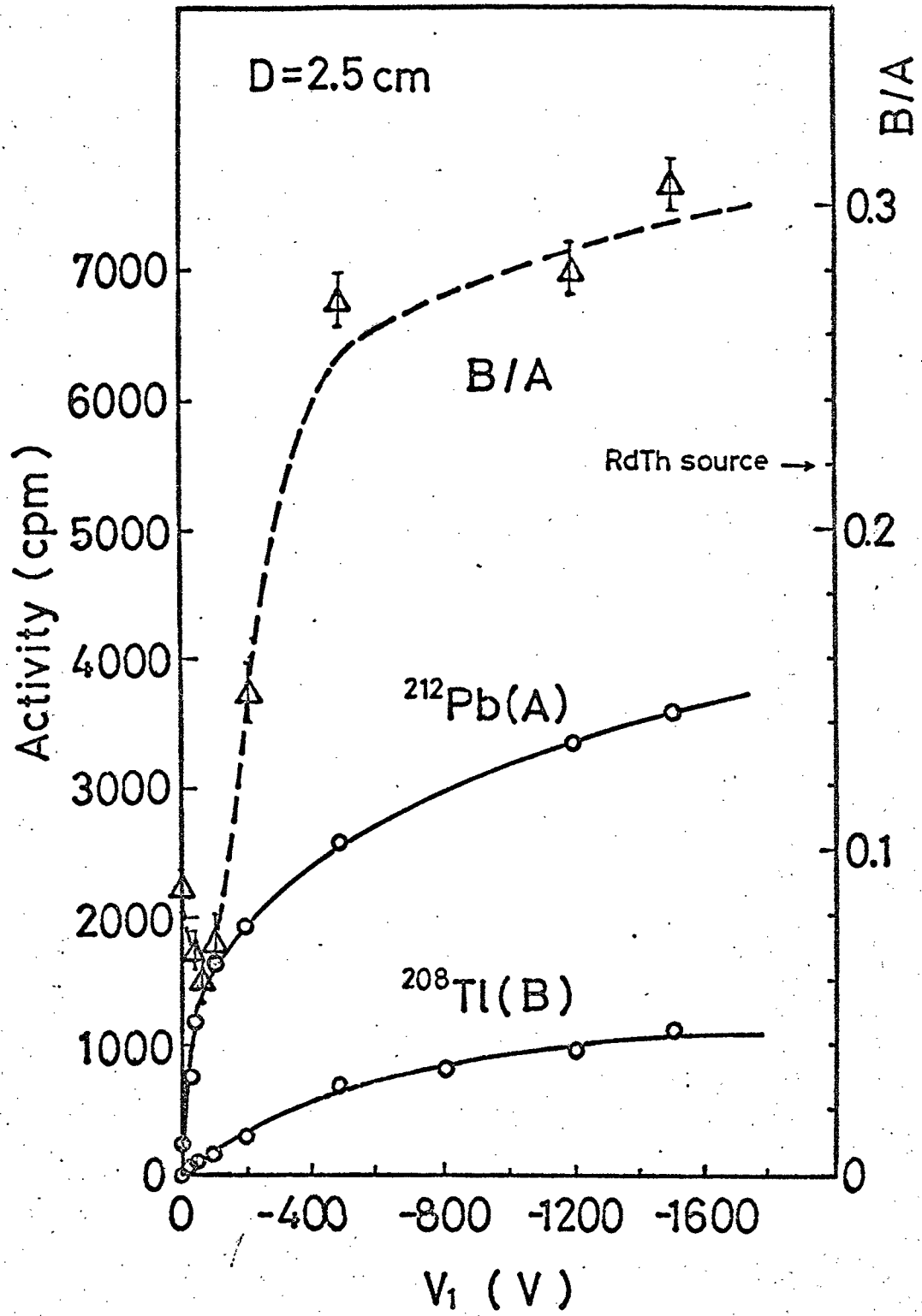

Fig. 2.4 Effect of differences in target voltage V_1 on target activity, with grid removed

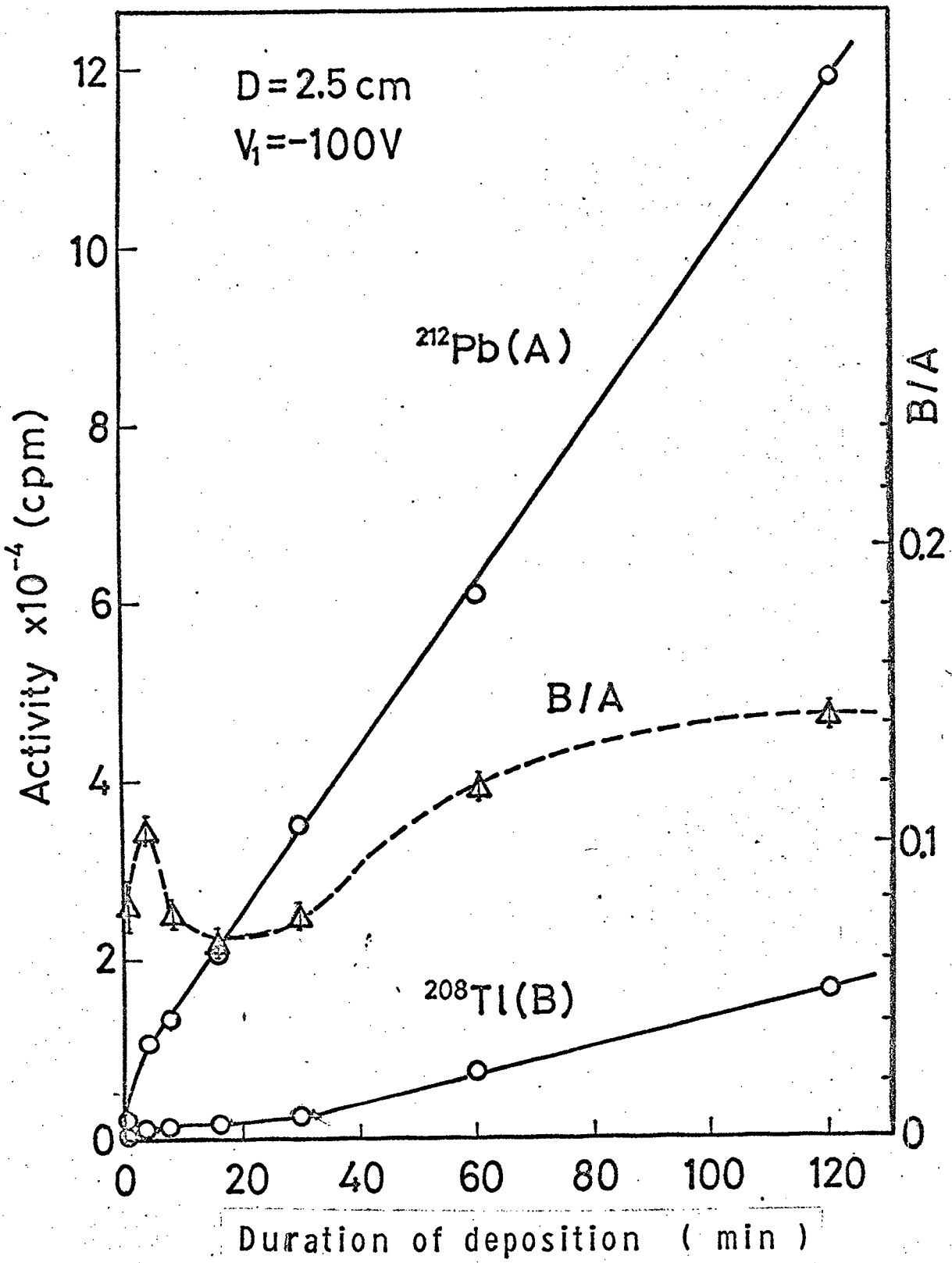

Fig. 2.5 Effect of differences in duration of deposition, with grid removed

On the other hand, the activity of ^{212}Pb increases linearly with the time allowed for deposition. This increase can be considered due to the daughter nuclides of ^{220}Rn ($RdTh \xrightarrow{\alpha} {}^{224}Ra \xrightarrow{\alpha} {}^{220}Rn \xrightarrow{\alpha} {}^{216}Po \xrightarrow{\alpha} {}^{212}Pb$), which had been transferred to the vicinity of the target by diffusion, and thereupon attracted by the electric field to the target, thereby supplementing the activity of the directly electro-deposited ^{212}Pb. The activity of ^{212}Pb did not reveal a plateau in the range up to several hours of electro-deposition. It should however be expected to enter a plateau region in about 18 hours, which is about twice the value of the half-life of ^{212}Pb ($T_{1/2}$ = 10.6 hr). Such a behavior has also been reported by Shinagawa et al[5].

2-3-3 Effect of the Differences in the Target Voltage V_1 with Grid Installed

The grid was set in the capsule and the voltage V_1 between the source and the target was varied up to -1500 V with grid voltage V_2 = 0 V at D = 2.5 cm and d_{SG} = 1.5 cm. The results are shown in Fig. 2.6.

The pattern is similar to Fig. 2.4, except that the activity on the target is seen to be roughly half for ^{212}Pb, while for ^{208}Tl it is seven times greater than with the grid removed. This indicated that one-seventh of the ^{208}Tl on the target had passed through the grid net, and the remaining six-seventh of what had deposited on the target had originated from the grid, where ^{212}Pb had primarily deposited from the RdTh source to yield ^{212}Bi and to emit ^{208}Tl by α

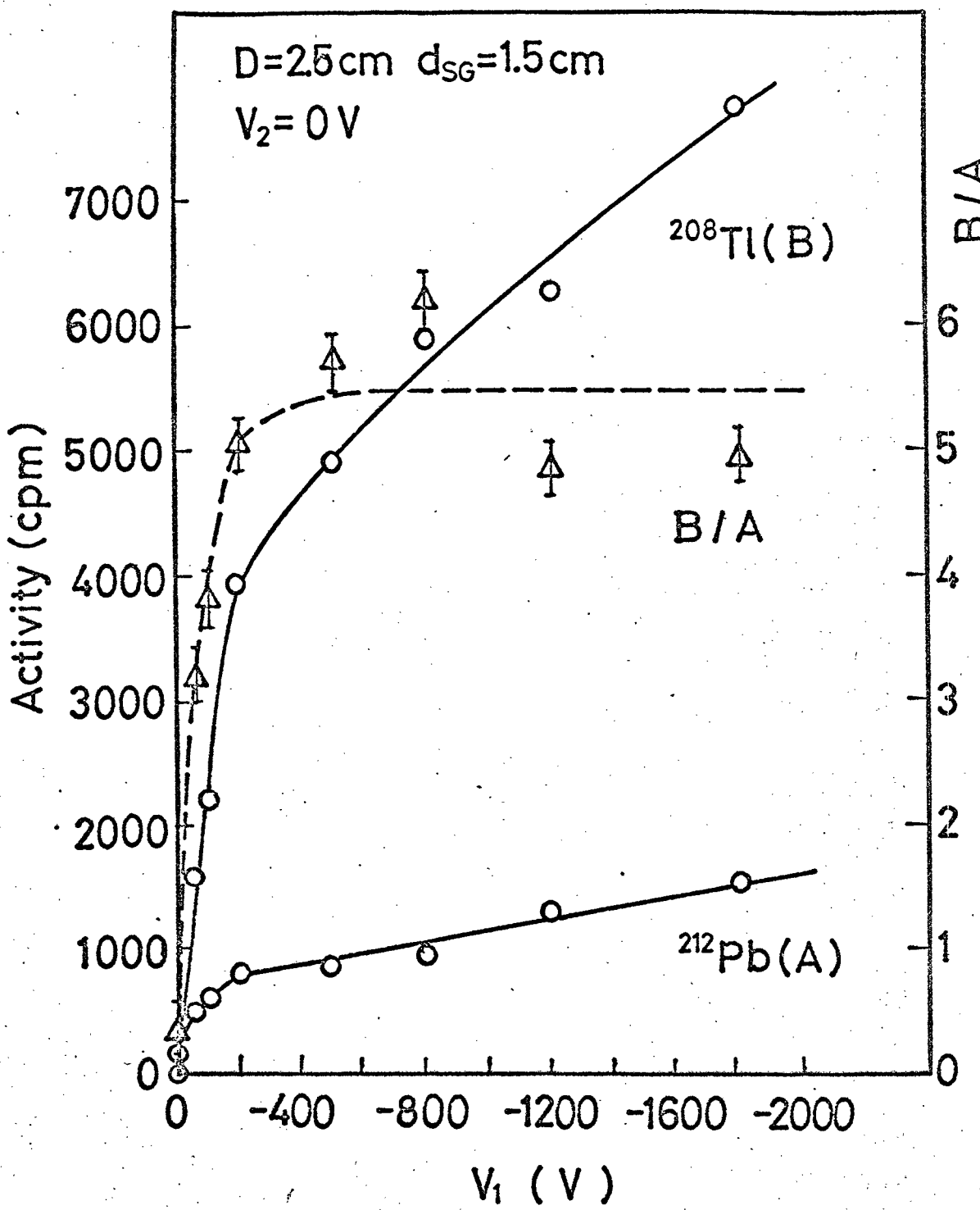

Fig. 2.6 Effect of differences in target V_1 on target activity with grid installed but not charged

recoil.

2-3-4 Effect of Differences in the Target Voltage V_3 with Grid Installed

The target voltage V_3 between the grid and the target was changed from +400 to -1500 V with grid voltage held constant at V_2 = +500 V, and with the distances D = 2.5 cm and d_{SG} = 1.5 cm. The results are shown in Fig. 2.7. Despite the positive charge of the grid in reference to the source, the activity of ^{212}Pb on the target is seen to have increased with the target voltage V_3 and then to have tended to saturate.

2-3-5 Effect of Differences in the Grid Voltage V_2

In order to examine the effect of changing the grid voltage, the potential difference V_2 between the source and the grid was varied from 0 up to 1500 V, with V_3 held constant at -100 V, D = 2.5 cm and d_{SG} = 1.5 cm. The results are shown in Fig. 2.8. The activities of ^{208}Tl and ^{212}Pb on the target decrease gradually with increasing grid voltage of V_2. At V_2 = 1500 V the former is four-fifth of the level at V_2 = 0 V, while the latter is reduced by half. The relatively small shield effect of the grid net for ^{212}Pb can be attributed to the activity of the deposited ^{212}Pb being reinforced by the effect of the diffusion of ^{220}Rn (cf. Fig. 2.7).

2-3-6 Effect of Differences in the Interval between the Target and the Source

The interval D between the target and the source was changed with no voltage applied. The results, shown in Fig. 2.9, reveal that the active deposits on the target de-

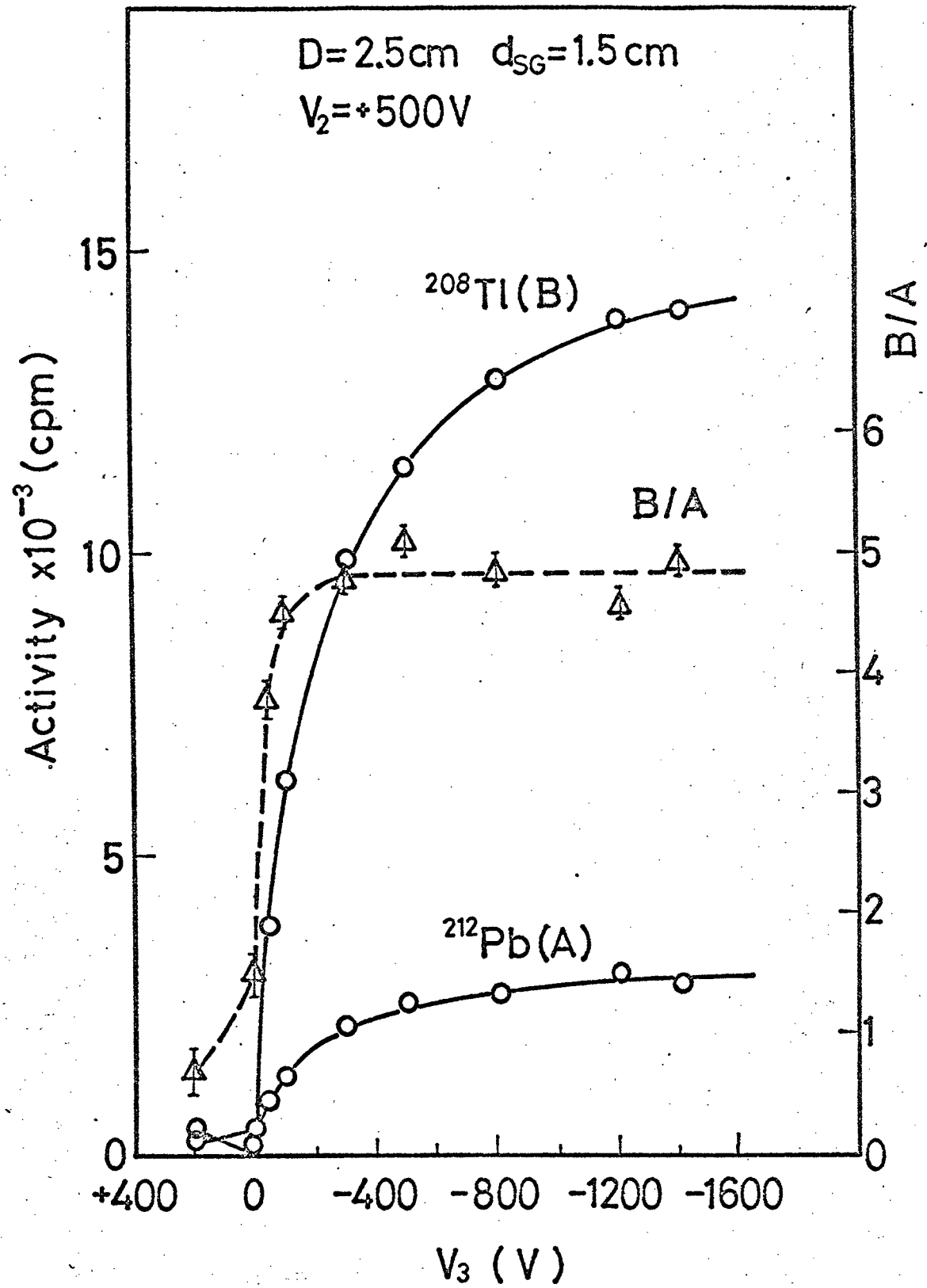

Fig. 2.7 Effect of differences in target voltage V_3 on target activity with grid installed and positively charged

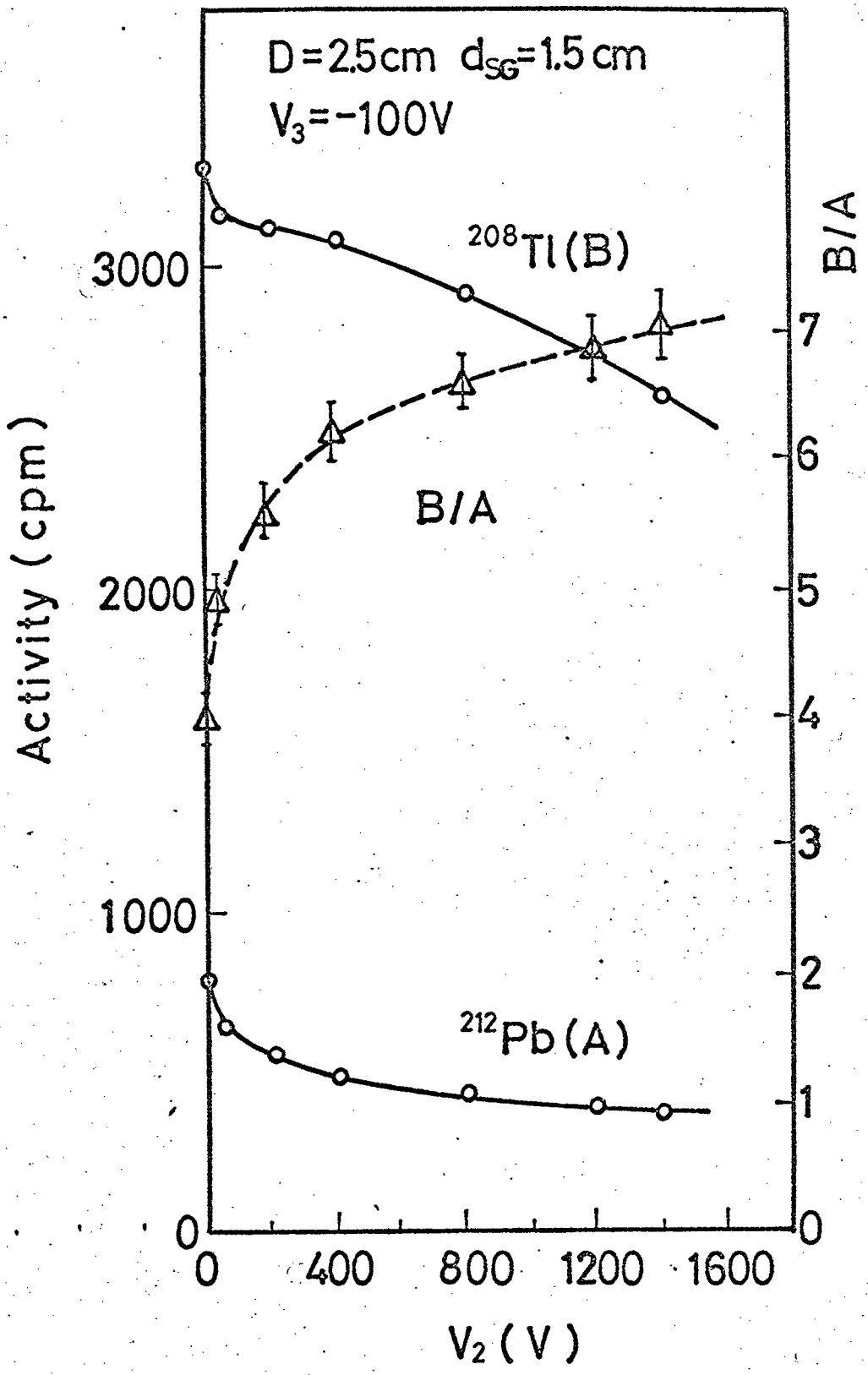

Fig. 2.8 Effect of differences in positively charged grid voltage V_2

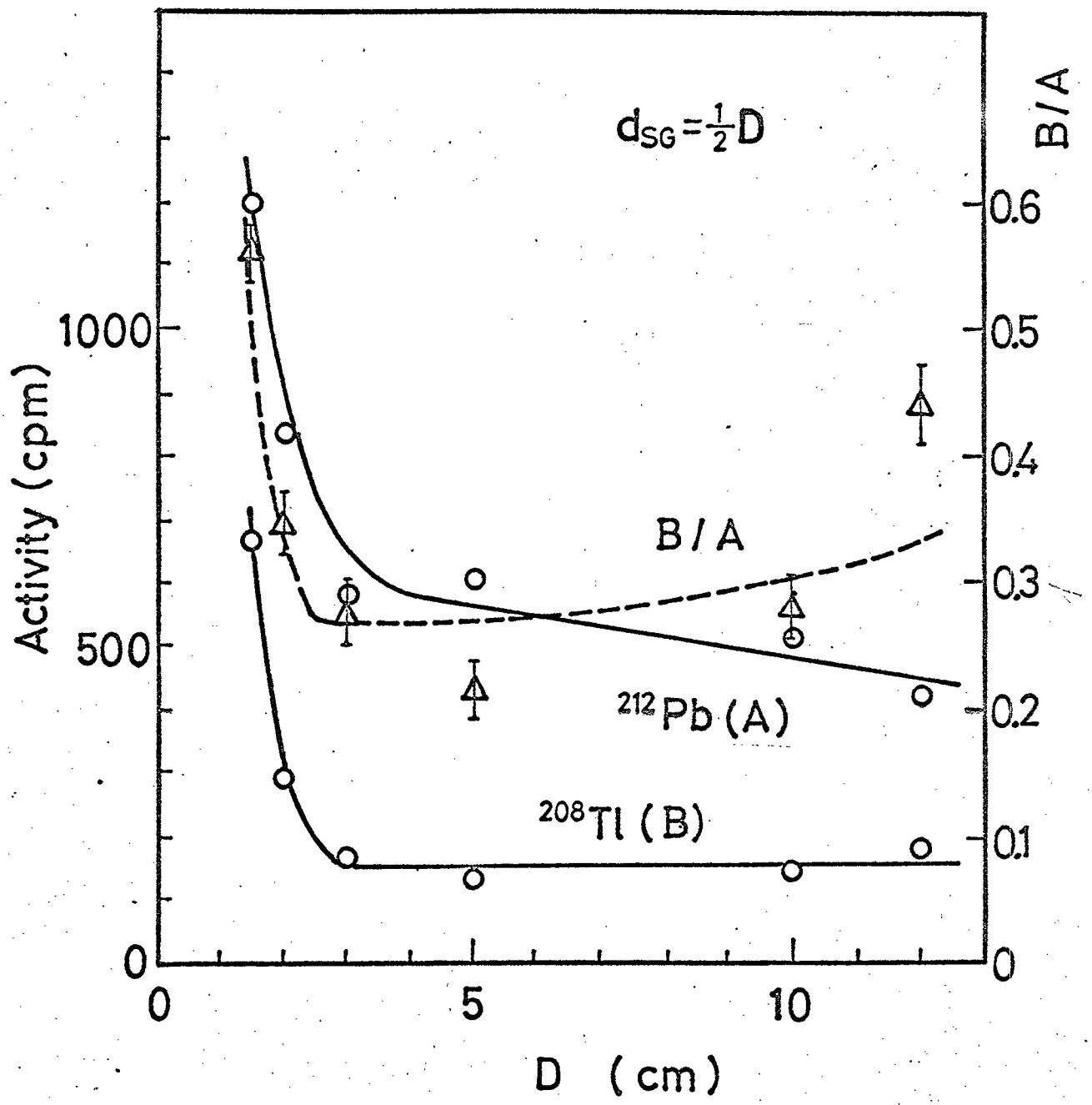

Fig. 2.9 Effect of differences in source-target interval D with no voltage applied

creased rapidly up to 2.5 cm beyond which point it remained almost unchanged. In order to examine the influence of the electric field, the activity of ^{208}Tl deposited on the target was measured, with the interval D changed from 2 to 15 cm, and the target voltage V_1 from -50 to -400 V. The results are shown in Figs. 2.10 and 2.11. Up to about 10 cm, the activity is in proportion to the applied electric potential (Fig. 2.10). In Fig. 2.11, the activity is seen to decrease exponentially with the distance D and the curve becomes steeper as the applied potential is made more deeply negative.

The active deposits on the target at D = 15 cm or more may have been caused chiefly by the diffusion of ^{220}Rn as in the case of V_1 = 0 V, because it is unaffected by electromigration, as may be expected for a rare gas.

2-3-7 Distribution of the Active Deposits on the Target

Photograph 2.1 shows the autoradiographical distribution of radioactive deposits on the target at V_1 = -1500 V, D = 2.5 cm, d_{SG} = 1.5 cm, and with the grid installed, but with no applied potential. The distinct net-like image proves that the recoil atoms emitted from the source slit had flown linearly and were screened by the grid net. The meshes of the net in central zone of the image agree precisely with those of the actual grid, while in the periphery the meshes are somewhat deformed and smaller. Moreover, the radioactivity on the backside surface of the target was only very slightly smaller than on the front face. These phenomena attest the parallel flux constituted by the substrate par-

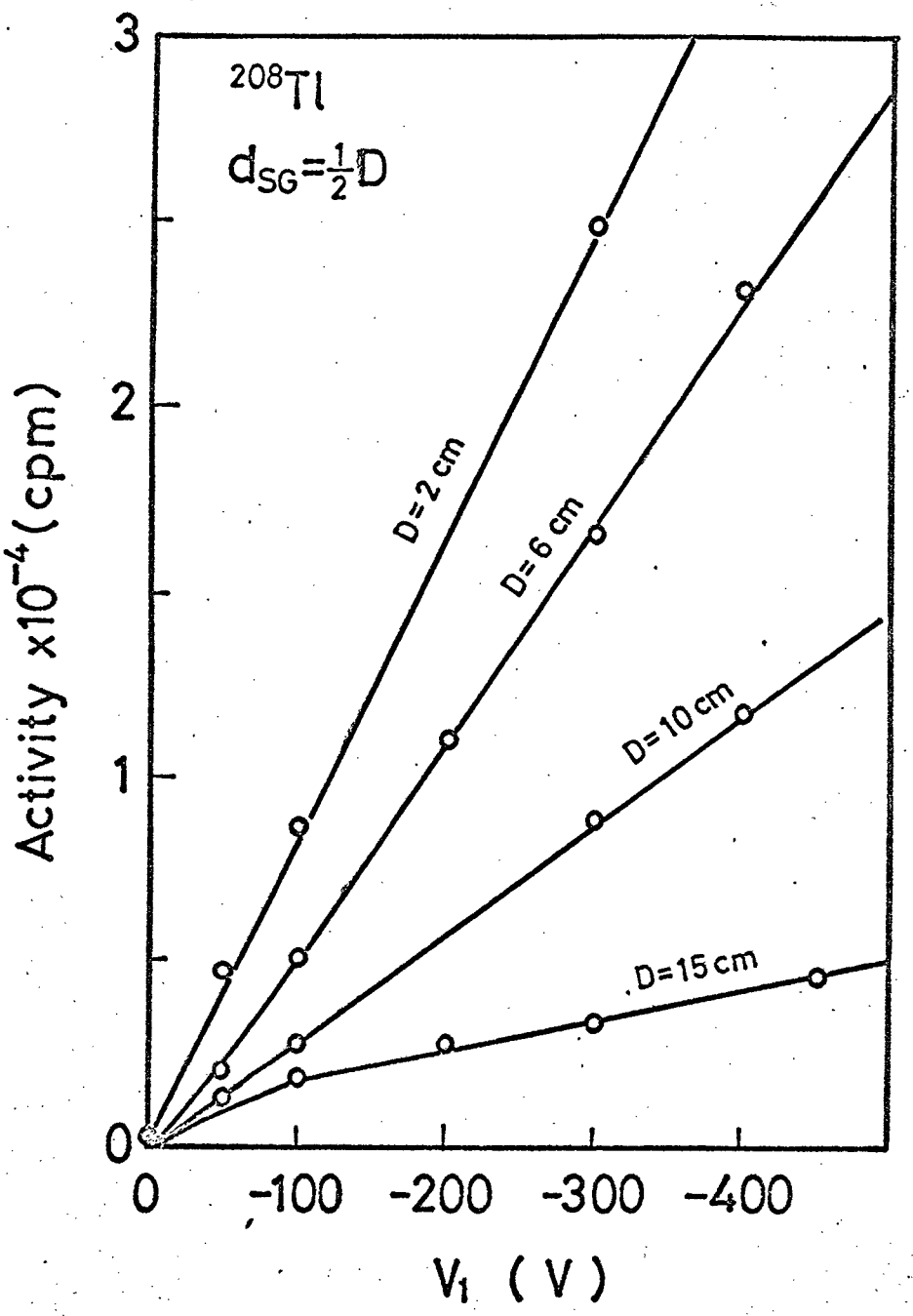

Fig. 2.10 Variation of deposited activity of ^{208}Tl brought by differences in target voltage V_1, with source-target interval D as parameter

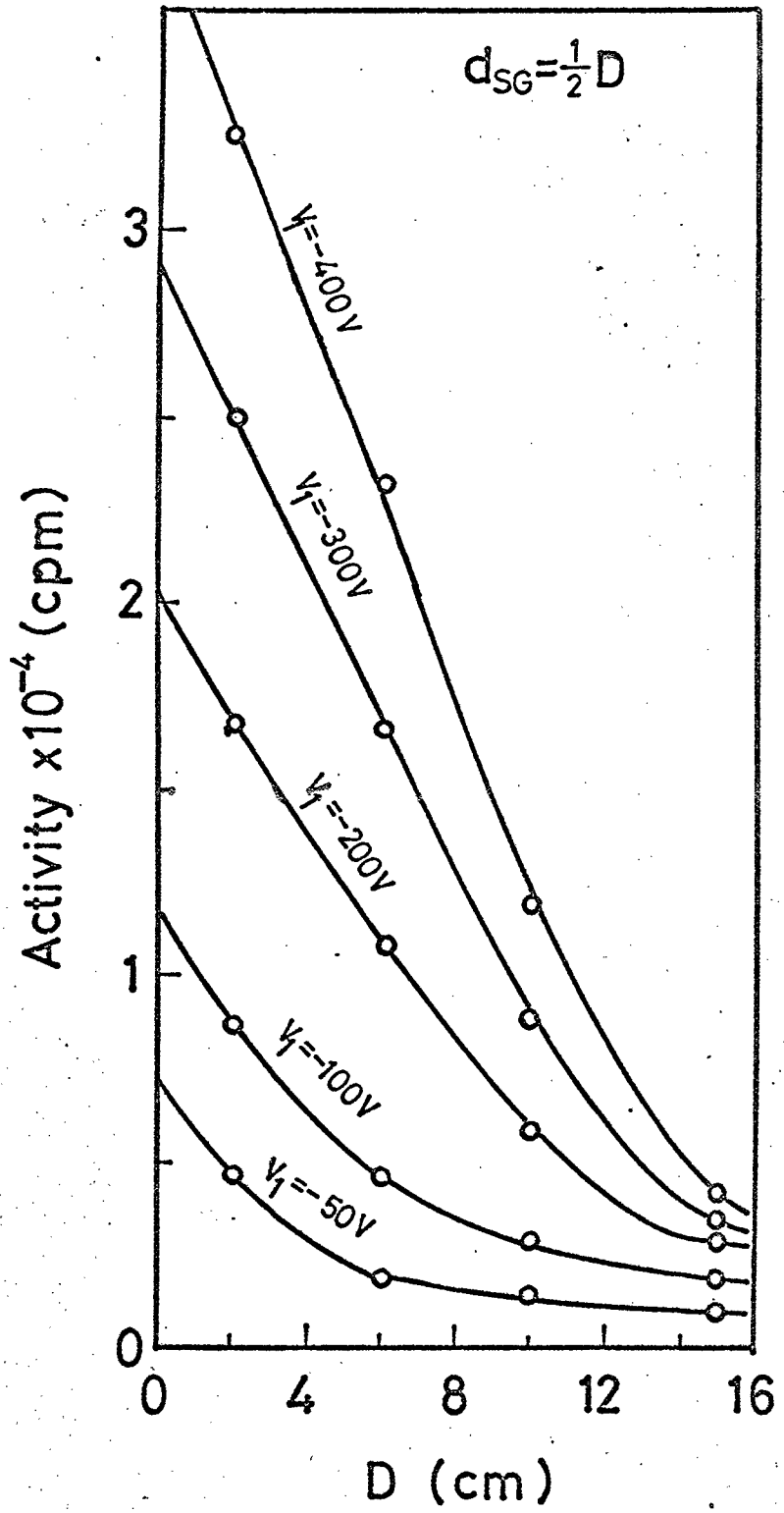

Fig. 2.11 Variation of deposited activity of ^{208}Tl brought by differences in interval D, with target voltage V_1 as parameter

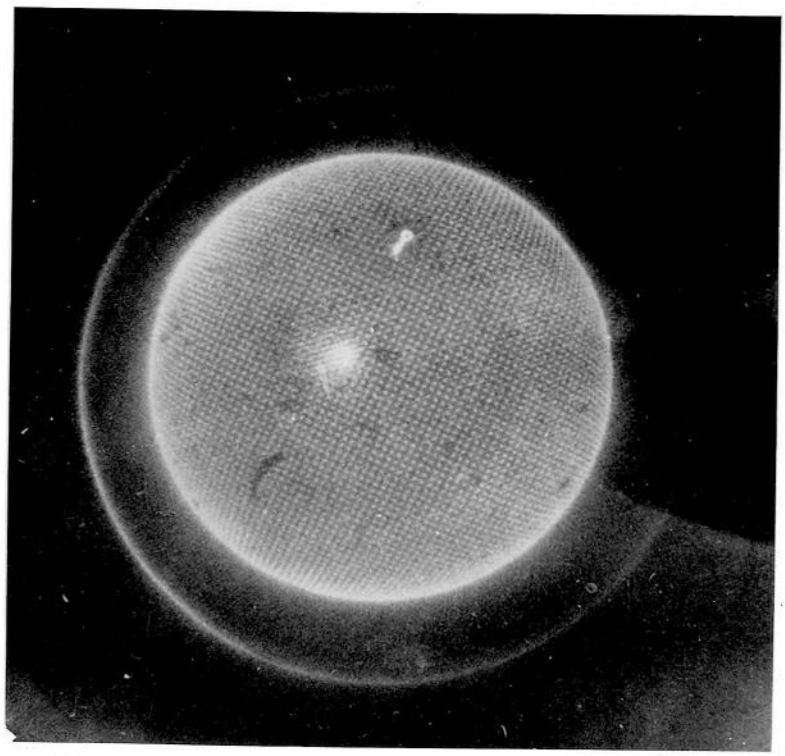

Photo. 2.1 Auto radiographical distribution pattern of radioactive deposit on target x 2

(V_1 = -1500 V, D = 2.5 cm, d_{SG} = 1.5 cm)

ticle, and prove the linearity of the mass-transfer. The diameter of the grid was 4 cm, but that of the image was 3 cm, indicating that there was some converging effect, the reasons for which remain to be investigated. Since the image of the grid was clearly projected on the target, the recoil atoms emitted from the source slit will have reached the target through the grid, driven by the electric force.

When the grid voltage V_2 was +500 V, the image of the grid on the target was not as sharp as when V_2 = 0 V. This phenomenon could be explained as the result of the positively charged recoil particles being repulsed by the grid and thus being hindered in their passage through the net of the grid.

2-3-8 Considerations on Electro-Deposition Process

In the thorium decay series, the daughter nuclides that have large recoil effect by α decay, are ^{208}Pb, ^{212}Pb, ^{216}Po and ^{208}Tl. Since ^{208}Pb is a stable nuclide, it cannot be estimated by radiochemical method. As for ^{216}Po, its extremely short half-life ($T_{1/2}$ = 0.158 sec) makes it very difficult to measure. The relatively short half-life of ^{208}Tl ($T_{1/2}$ = 3.1 min), also does not suit it to the electro-deposition process. Lastly, ^{212}Pb has a convenient half-life of 10.6 hr, and its deposition process has been reported by several authors[2],[5]. It has been considered in most cases that ^{220}Rn, which is a descendant of ^{232}Th, ^{228}Th or ^{224}Ra, deposits on the metal target transferring from the source by diffusion (being a rare gas), and subsequently produces ^{212}Pb of transient equilibrium.

In the present work, an α-ray spectrometer was not used, and the activity of ^{220}Rn on the target could not be confirmed. However, it would be expected that, when there was no target voltage applied (cf. Fig. 2.9), there would be a primary ^{220}Rn gas deposition on the target and a secondary ^{212}Pb production, but when a negative target potential was applied (cf. Figs. 2.10 and 2.11), direct electro-deposition of ^{212}Pb would have priority over the diffusion of ^{220}Rn. It would appear that most of the ^{216}Po and ^{220}Rn remained within the source cover, and ^{212}Pb was selectively emitted through the pin hole due to the recoil of α decay at the source, and thus hit the target. The increase of ^{208}Tl deposited on the target when the grid was present may indicate that some of ^{212}Pb on the grid had turned into ^{212}Bi by β^- decay, and ^{208}Tl had recoiled onto the target due to α decay of ^{212}Bi. In order to confirm this grid effect, further experiments were carried out.

After letting ^{212}Pb deposit on the negatively charged grid from the RdTh source, and with transient equilibrium established between ^{212}Pb and its descendants, the source was removed from the capsule. Subsequently a negative potential was applied to the target against the grid net. The results are shown in Figs. 2.12 and 2.13.

In Fig. 2.12, the γ-ray spectrum reveals the presence solely of ^{208}Tl, and that of the mother nuclide ^{212}Bi produced by the β^- decay of ^{212}Pb is not discernible, indicating that, in contrast with the recoil effect of α decay, that of

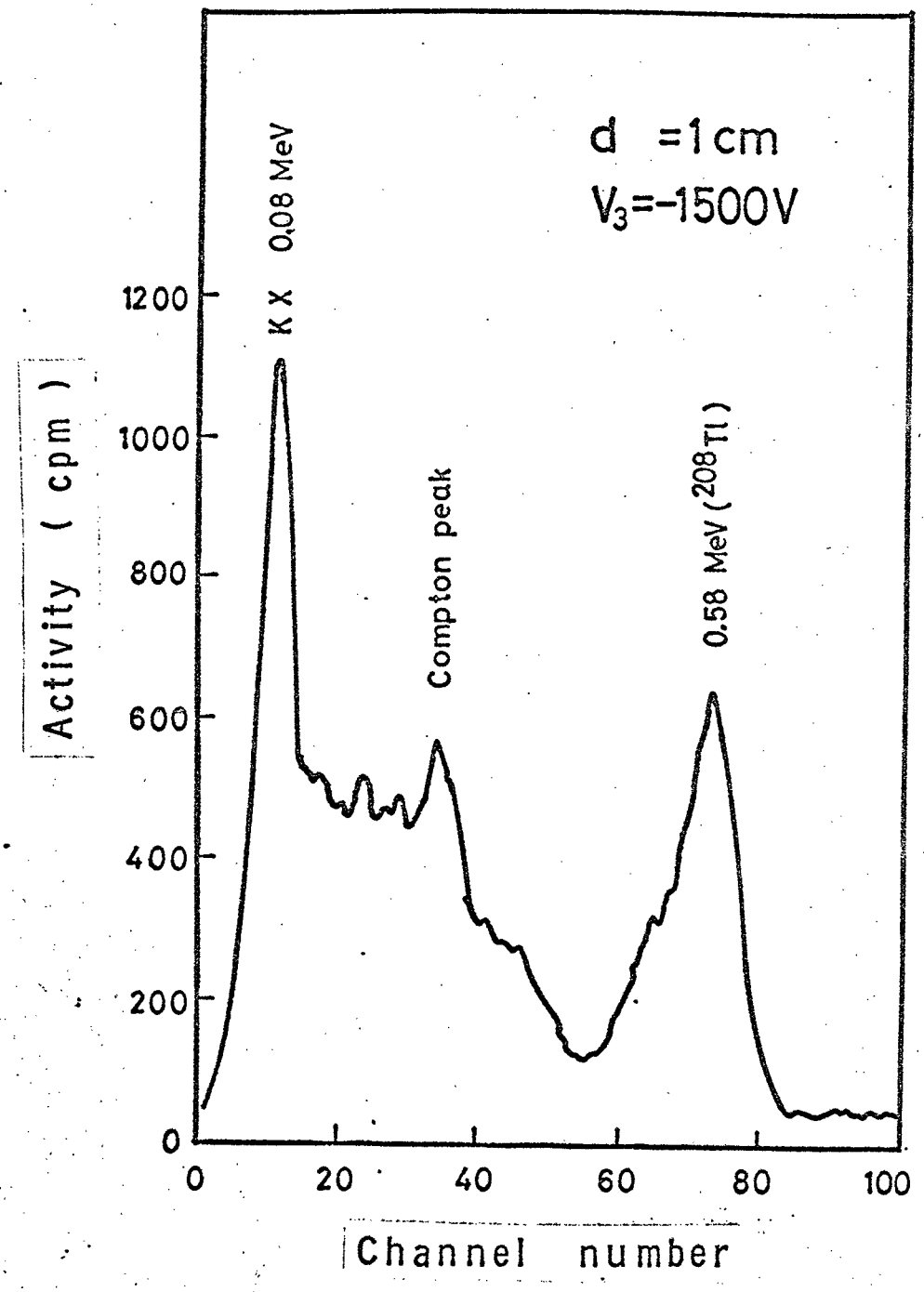

Fig. 2.12 Gamma-ray spectrum of deposit which had passed from grid to target

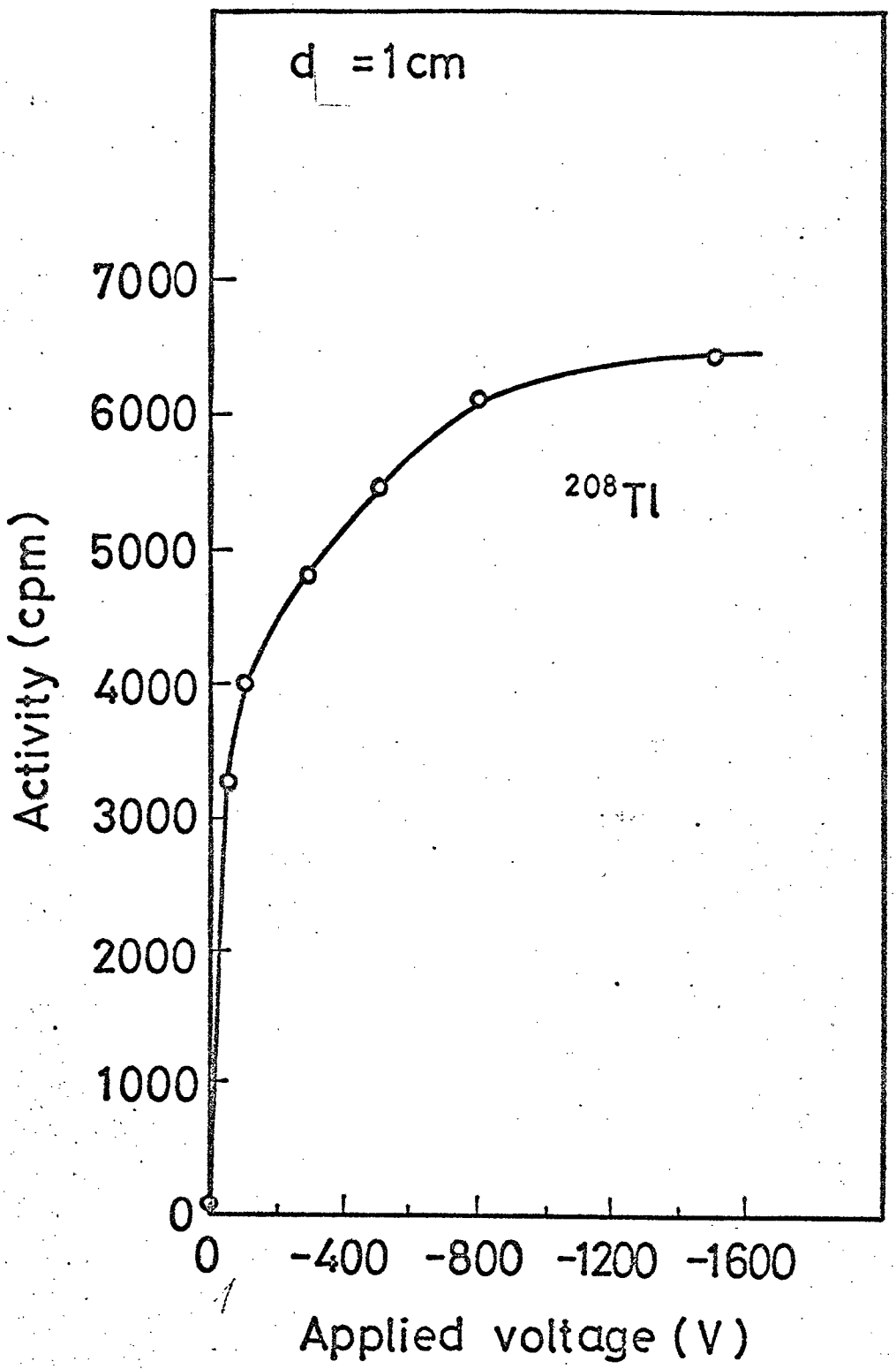

Fig. 2.13 Variation of target activity of ^{208}Tl deposited from grid net brought by differences in target voltage after removal of RdTh-source

β^- decay is too small to let the decay product reach to the target.

The variation of the amount of ^{208}Tl deposited on the target from the grid due to change of the voltage applied to the target is presented in Fig. 2.13. It is seen that the saturation plateau of activity is approached at a target potential beyond -1000 V. The amount of detected ^{208}Tl depends on the target voltage, and beyond -1000 V most of the ^{208}Tl in radioactive equilibrium with ^{212}Bi ($T_{1/2}$ = 60.5 min) would appear to have been trapped by the target.

2-4 Conclusion

The present chapter gives on the results obtained with different conditions of electro-deposition of daughter nuclides in the decay chain of thorium, using RdTh as source. The conditions varied were, in particular, the electrode potential, which was changed in a range covering both negative and positive potential, and with an intermediate grid either installed or removed. Measurements on the active deposits obtained on the target indicated that, when no potential was applied to the target, the deposition process depends on one of the daughter nuclides, ^{220}Rn, while under negative potential applied to the target, it depends on the recoil atoms with positive charges produced by α decay. The recoil atoms are driven from the source toward the target both by the energy of recoil and by Coulomb's force.

In the case where the electric field is strong enough,

the recoil atoms with positive charge travel to the target along the electric field under atmospheric pressure. The behavior under pressures below atmospheric and the mechanism of mass-transfer from the source to the target will be given in next chapter.

References

(1) Takemi,H., Asai,N. and Shinagawa,M.:
J. Nucl. Sci. Technol., 10, 155 (1973).

(2) Siegbahn,K.: "Alpha-, Beta- and Gamma-Ray Spectroscopy", Vol. 1, p. 401 (1965), North Holland Amsterdam.

(3) Briand,J.P., Chevallier,P.:
Nucl. Instrum. Methods, 80, 309 (1970).

(4) Ghiorso,A., Sikkeland,T., Walton,I.R. and Seaborg,G.T.:
Phys. Rev. Letters, 1, 17 (1958).

(5) Shinagawa,M., Furushima,K. and Mizumoto,Y.:
J. Nucl. Sci. Technol., 5, 408 (1968).

(6) Covell,D.F.: Anal. Chem., 31, 1785 (1959).

Chapter III. Effect of Pressure on Mass-Transfer in Gaseous Electro-Deposition[1]

3-1 Introduction

As for the mass-transfer mechanism in the electro-deposition process of thorium decay series, it has been considered that the diffusion of ^{220}Rn, which is one of rare gases, is predominant over alpha recoil effect, because the range of recoil atoms due to alpha decay is very small, for instance, 6.65×10^{-3} cm of ^{208}Tl in air at 760 mmHg pressure. The $^{212}Bi \xrightarrow{\alpha} {}^{208}Tl$ decay has been interested being complicated in the chemical result: for example, in aqueous system, it has been shown that about 70 % of Tl appears in the univalent and 30 % in the trivalent state[2]. Meyer has recently reported that the charge spectrum of $^{208}Tl^{n+}$ due to internal conversion lies between +5 and +20 with a mean charge of +12[3].

The fractional separation of ^{212}Pb and ^{208}Tl from RdTh source, using a capsule equipped with three electrodes under the normal pressure is reported in the preceding chapter. The deposition process depended on the species of recoil atoms with positive charges produced by alpha decay and on the negative potential applied to the target.

In this chapter, the purpose is to examine the mass-transfer under pressures below atmospheric, using ^{212}Pb source deposited on the Al plate. As the result, the relation between the deposited nuclide on the Al target and the electric field in the range of 10 ~ 760 mmHg is reported,

comparing with that of in the discharge range of the pressure or in the higher vacuum.

3-2 Experimental

Figure 3.1 shows the apparatus used for the experiment, i.e.a glass capsule containing five electrodes (12) and vacuum line. The plate of source or the target was made of Al foil supported with a rim ring of stainless steel (3 cm inner diam. 0.5 cm thick), of which stem was fixed with one of five electric terminals for optional use installed in the wall of a glass capsule (6 cm diam., 20 cm long). The capsule was constructed with two parts ground to fit together and easy for rearrangement of the fixed electrodes. The interval and the applied potential difference among the electrodes were from 1 to 10.5 cm and up to 1000 V D.C., respectively.

The ^{212}Pb source used was prepared by electro-deposition on the Al plate from a RdTh source[4]. After the source activity became in radioactive equilibrium, the target plate was set in the capsule. The daughter nuclides of ^{212}Pb were electro-deposited on the target surface under the different experimental conditions. The relative amounts of electro-deposits were measured by γ-ray spectrometer (NaI(Tl) crystal, 1" x 1") and by autoradiography. In the case of deposited nuclide ^{208}Tl ($T_{1/2}$ = 3.1 min), corrections of such as time taken for electro-deposition, for cooling, and for measurements were made, and the activities at end of elec-

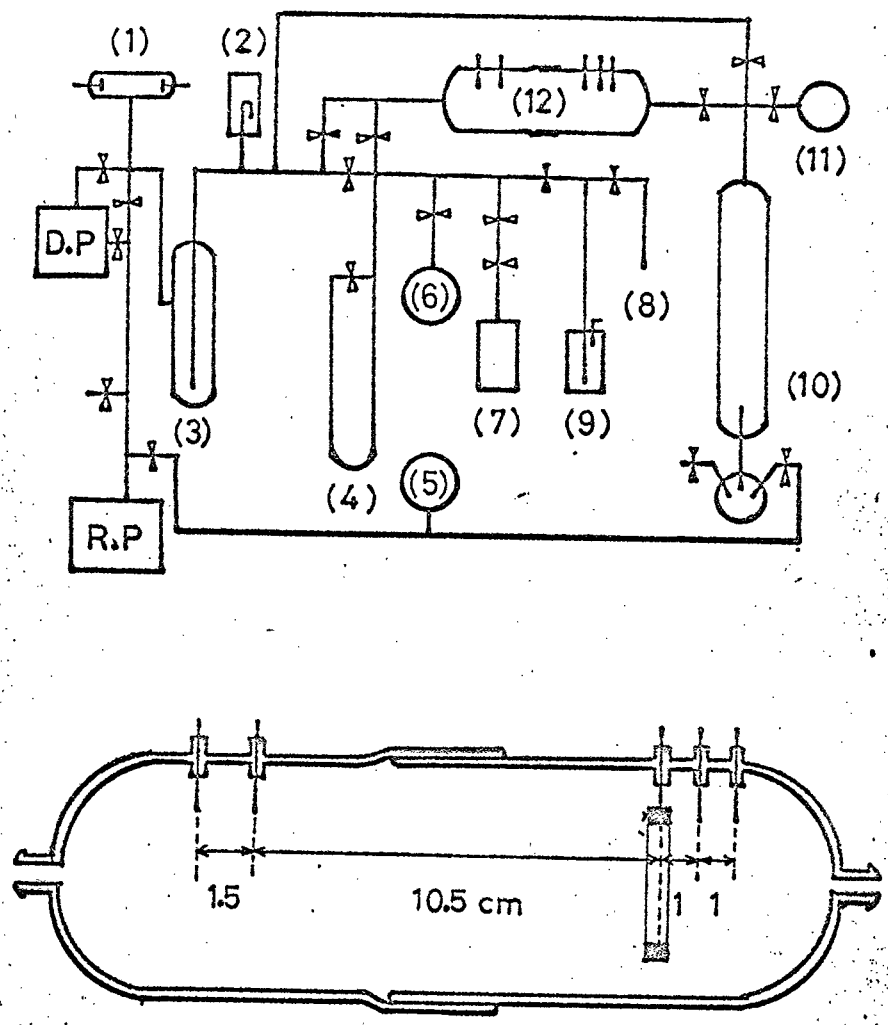

Fig. 3.1 Experimental arrangement

(1) Geissler's tube (2) ionization vacuum gauge (3) trap (4) manometer (5),(6) reservoir (7),(8) gas conduit (9) Hg bubbler (10) Toepler pump (11) gas sampler (12) glass capsule

tro-deposition were estimated. The values thus obtained were considered to represent the activities of deposited nuclides, and were adopted in the ensuing description.

3-3 Results and Discussion

When the pressure in the capsule was changed from several to 10^{-2} mmHg under a negative potential applied to the target, a discharge phenomenon happened. Gamma spectrum of the deposits thus obtained on the target was identical with that of the source ^{212}Pb and its decay nuclides. It was inferred that electrons produced by the discharge irradiated the source to make the radionuclides contained sublimate and move to the target along the electric field. Therefore, in further experiment, omitting the above discharge range of pressure, the following two regions were chosen as the experimental condition; i.e. the low vacuum of $10 \sim 760$ mmHg and high vacuum range of less than 10^{-3} mmHg.

3-3-1 Electro-Deposition under Low Vacuum

The deposited nuclide on the target under the pressure of $10 \sim 760$ mmHg reveals the presence of ^{208}Tl only by γ-spectrometry. The variations of deposited activity of ^{208}Tl according to the inverse pressure (1/P) with the negatively applied D.C. potential on the target as parameter are shown in Fig. 3.2. In the case of high applied potential, the dependence of deposited activity on pressure is seen to be smaller than that in low one. The variations of deposited activity of ^{208}Tl according to the applied potential with

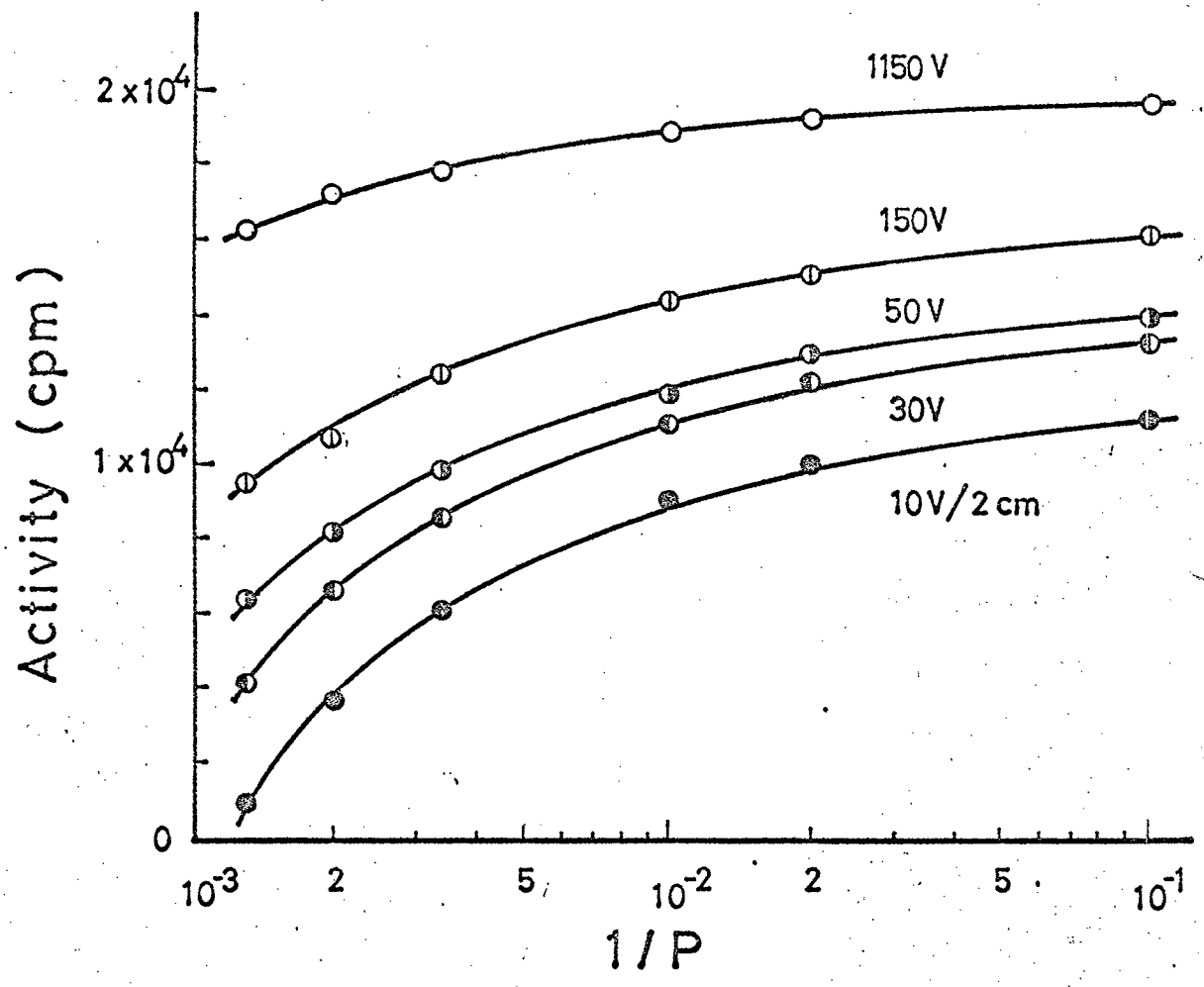

Fig. 3.2 Variations of deposited activity of ^{208}Tl according to the 1/P value, with applied D.C. potential as parameter (source(+), target(-) and interval 2 cm)

the pressure as parameter are shown in Fig. 3.3. It is seen that in each pressure, the deposited activity (A) is related to the logarithm of the applied potential (V) by the following equation

$$A = a \log V + b .$$

The inclination (a) in above equation becomes smaller with decreasing of the pressure. Extrapolating this tendency to the discharge region, it is easily known that (a) becomes zero, agreeing with the fact that the transfer of ^{208}Tl is independent of the applied potential. The range of recoiling atom of α-decay, however, must be longer with decreasing of the pressure. The applied potential V_c (V/2 cm) at A = 0 in the above equation (cf. intercepts with abscissa in Fig. 3.3) is related to the pressure of P (mmHg) by the following equation

$$V_c = 1.0 \times 10^{-5} P^2 + 2.5 \times 10^{-4} P + 1.2 \times 10^{-2} \quad (P \geqq 10).$$

The value of V_c might have the meaning of the critical potential for transference of ^{208}Tl by Coulomb attraction in each pressure. In the case of the potential less than V_c, ^{208}Tl emitted from the source may undergo simply the diffusion after exhausting its recoil energy. As the range of an α-racoil atom must be smaller than when electrostatically attracted, ^{208}Tl nuclide may move not so far from the source layer due to recoil and while it possesses some part of its initial charges, it may transfer up to the target along the electric field when the field potential is higher than the critical. In the experiments of Figs. 3.2 and 3.3, the

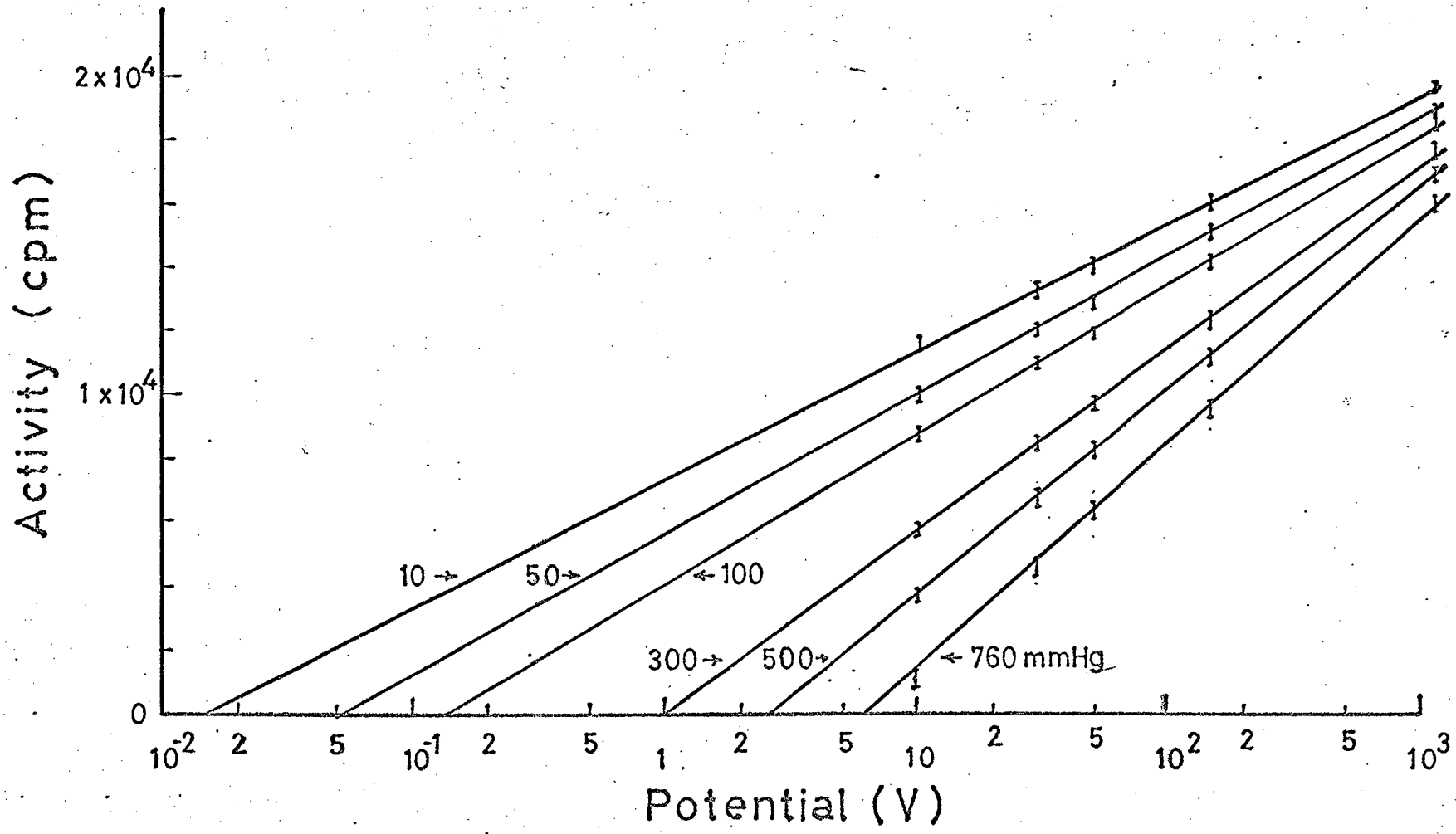

Fig. 3.3 Variations of deposited activity of ^{208}Tl according to applied potential, with pressure as parameter (source(+), target(-), and interval 2 cm)

distance between the source and the target is 2 cm, in which condition the diffusion contributes in minor extent (cf. Fig. 2.9). In Fig. 3.3, the lines converge at about 10000 V/2 cm. A negative factor for the mobility of ^{208}Tl is thought to come into play, which is caused by the collision with surrounding gas. In a certain pressure it may equilibriate with the attraction by applied potential. Therefore, even under more than 760 mmHg, the recoil atom associated with α-decay would be expected to transfer up to fairly long distance under the higher electric field.

3-3-2 Electro-Deposition under High Vacuum

The deposited activity under high vacuum of less than 10^{-3} mmHg as a function of applied potential is shown in Fig. 3.4. It is seen that the activity does not depend on the applied potential, but the value is smaller than that at 10 mmHg, indicating that the α-recoil energy of ^{208}Tl amounting 116 keV is large enough to transfer to the target without the influence of the applied potential used in the present experiment at D = 2 cm. The deposited nuclide on the target is surveyed by autoradiography with X-ray film. In the case of low vacuum, the autoradiographical pattern was the same in size as source (2.2 cm in diam.) but under high vacuum it is seen being enlarged extending all over the target (3 cm in diam.). Consequently, in connection with mass-transfer of the recoil atom associated with α-decay under high vacuum, the flight by recoil must be predominant over the electric attraction. The daughter nuclides of ^{212}Pb

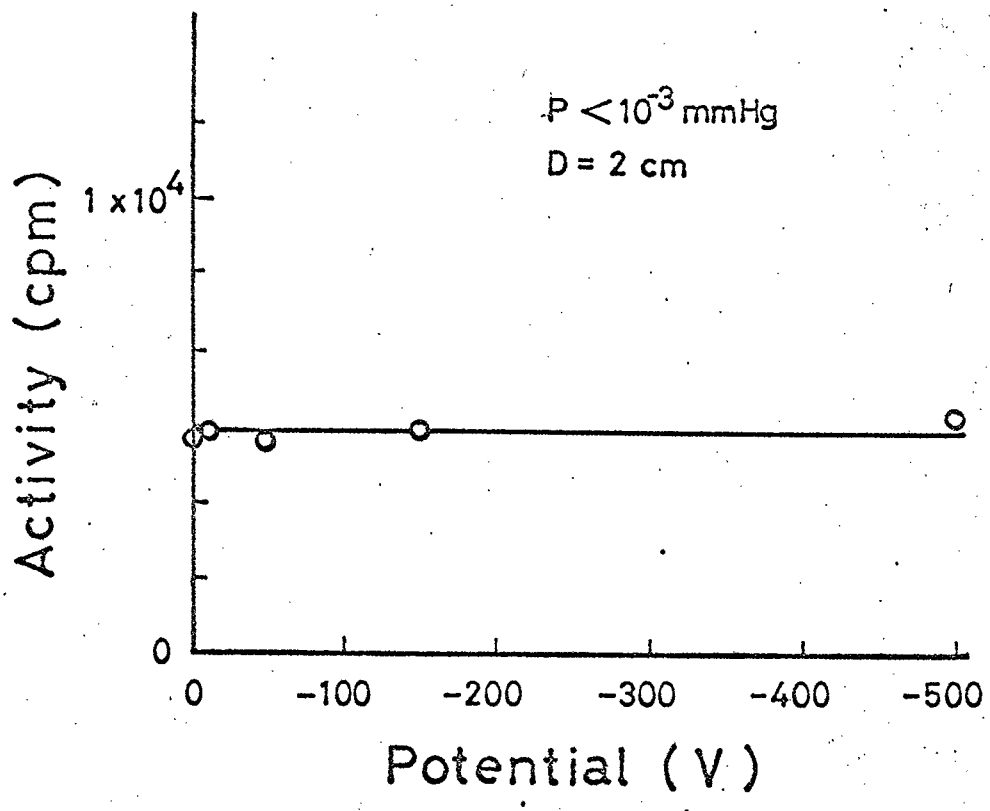

Fig. 3.4 Effect of applied potential on target activity (source(+), target(-))

deposited on the target are not clearly observed except ^{208}Tl by γ-spectrometry. So, as supplemental examination α-track method with celluloid film is helpful as seen in next chapter. The pattern obtained by α-track method at high negative applied potential to the target is different from that at no applied potential. The α-emitting nuclide thus observed is considered to be ^{212}Bi which has come to the target as it is or as parent ^{212}Pb. The transference of the ^{212}Bi on the target must be small in amount because of the weakness of the recoil energy of β^- decay. The transference of ^{212}Pb may be explained that at a restricted high temperature region due to the α-recoil coexisted in the source ^{212}Pb arises in a form which must be regarded as a supersaturated lead vapour, and then travels to the target along the electric field. This explanation is consistently referred with the results reported by several authors on the contamination of α-recoil atoms on the surface of semiconductor detector[5]~[7].

3-4 Conclusion

The electro-deposited nuclide from ^{212}Pb source under pressures below atmosphric is found to be mostly ^{208}Tl. When the pressure is 10 ~ 760 mmHg, ^{208}Tl transfers to the cathode target along the electric field, depending on the applied potential. However, under vacuum region higher than 10^{-3} mmHg the amount of the activity on the target depends on the solid angle from the source. The recoil atoms except

^{208}Tl are observed on the target in discharge condition and the strong electric field under high vacuum.

References

(1) Takemi,H., Azuma,H. and Shinagawa,M.:
To be published in J. Nucl. Sci. Technol.

(2) McKay,H.A.C.: "Principles of Radiochemistry", p-456 (1971), Butterworths, London.

(3) Meyer,J., Paulus,J.M. and Adde,J.Ch.:
Radiochim.Acta, 17, 76 (1972).

(4) Takemi,H., Asai,N. and Shinagawa,M.:
J. Nucl. Sci. Technol., 10, 155 (1973).

(5) Bowen,V.T., Wong,K.M. and Noshkin,V.E.:
J. Marine Res., 29, 1 (1971).

(6) Wong,K.M.: Anal. Chim. Acta, 56, 355 (1971).

(7) Hashimoto,T.: Radiochem. Radioanal. Letter,
8, 25 (1971).

Chapter IV. On Solid State Track Detector of Celluloid Film

This chapter is concerned with the interaction between alpha particles and celluloid film. Celluloid is one of the most interesting and useful substances as solid state track detector. Its ionization threshold is the lowest among the presently known track detectors.

4-1 Celluloid Film for Several Alpha Emitters of RdTh Daughter Nuclides[1],[2]

4-1-1 Introduction

Since a method of solid state track detector was reported by Fleischer et al., many dielectric materials have been used in several disciplines, including nuclear physics and chemistry[3]. The application of this technique may be expected considerably if they can be used to discriminate the nuclear charged particles of different energies. Somogyi et al. have reported the relation between the particle energy and the diameter of track under a certain etching condition [4]~[6].

In this section, the alpha track pattern of several α-emitting sources with nuclides of RdTh decay series was examined with celluloid film on the basis of the track formation technique (See 4-1-3). Alpha spectrum was easily obtained by variant thickness of absorber piling up thin films

on the detector film and by chemical etching of the detector film with variant duration. This track method was also applied to measure the alpha radiogram of RdTh daughter nuclides separated by focusing chromatography and to detect the radiocolloid.

4-1-2 Experimental

As a thin alpha source, electro-deposited ^{212}Pb on nickel plate from RdTh source was used in a glass capsule[7]. The celluloid film used in this experiment was manufactured by the Daicel Co. Ltd. and had 25 w/o camphor in cellulose nitrate. Between the α-source and a celluloid film (100 micron in thickness) there placed several sheets of thin film absorber (Saran Wrap, polyester film, 10.0 ± 0.7 micron in thickness, 1.7 g/cm^3 in density) and a plastic plate with a hole at the center of these films as shown in Fig. 4.1.1. Through the hole alpha particles are collimated to enter at right angles to the detector film. After the irradiation the celluloid film were etched for 10 ~ 300 min with 5 M sodium hydroxide solution at 50°C, being inspected intermittently its surface for the developed track patterns by an optical microscope.

On focusing chromatographic separation of RdTh daughter nuclides, cathodic compartment of the apparatus was filled with 0.05 M sodium triphosphate solution (pH = 5) as a complex forming reagent while anodic one was filled with a mixture solution of 0.05 M in HCl as a complex decomposing rea-

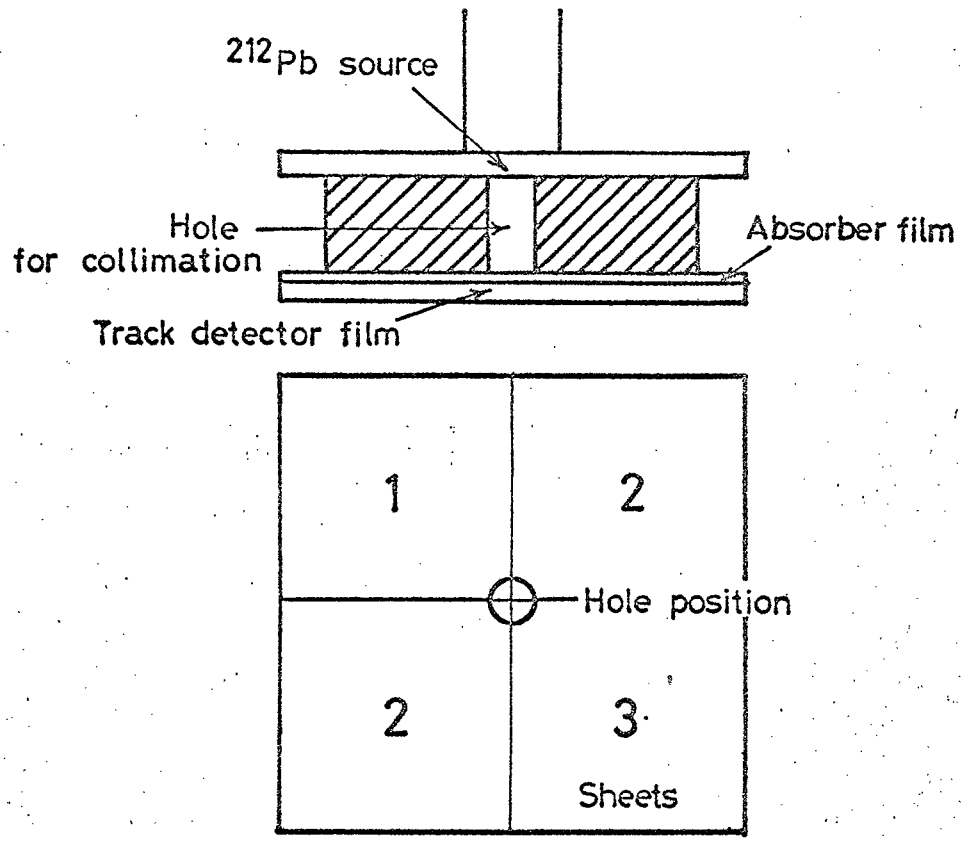

Fig. 4.1.1 Arrangement of solid state track detector film under ^{212}Pb source-hole-absorber

gent and 0.05 M NaCl as an ionic strength conditioner. About 0.02 ml of RdTh solution was dropped on a sheet of Tōyō filter paper strip No. 50 (2 x 26 cm), at an area of 1 cm width in the center. After the electromigration was conducted for 20 min under a potential gradient of D.C. 700 V/22 cm, the strip was taken out, dried an infrared lamp, and was examined for the radioactive distribution on it by α-track method. It was carried out with close contact of celluloid film at one side of the paper strip in parallel with autoradiographical Fuji Medical X-ray film at another side. The irradiated celluloid film was etched in 5 M sodium hydroxide solution at 50°C for 60 min. Then, the chromatographic patterns made of the alpha tracks due to the separated daughter nuclides of RdTh were compared with their corresponding autoradiograms on the X-ray film.

In order to examine alpha emitting nuclides in the solution, a liquid drop containing RdTh nuclides in radioactive equilibrium was dropped on the celluloid film. After several hours the film was washed with distilled water and examined by means of the track method as above mentioned.

4-1-3 Chemical Etching of the Latent Track on the Plastics

The trail produced by the charged particle on the plastics film can be developed by using a suitable chemical reagent to make tracks easily visible by optical microscopy[3]. The energy distribution of the charged particle entered in plastics have been clarified by measuring the range of

charged heavy particle[8] and the growth of the hole diameter versus the etching time. The latter method which has been extensively developed by Somogyi et al.[4]~[6] and known to be simple and quick is adopted in this study. Their results in the chemical etching of the latent tracks are summarized as follows.

The length of the primer damage region is correlated to the total energy of the charged particle, and the width of that to local energy loss of the particle, which is approximately proportional inversely to the energy. So, when a particle enters at right angles to the surface, at low particle energy a large hole will be created and at high energy a small one. If it is chemically etched the enlargement of the hole diameter and length of primer channel are good measures of particle energies.

In the case of the particle having the values of the energy E and of R(E) less than the critical ones E_c and $R(E_c)$ on the surface of the detector, the growth of the hole diameter arises from the commencement of the chemically etching (ref. (a) and (a') in Fig. 4.1.2). The growth rate of the hole diameter depends on the rate primary ionization[9] or restricted energy loss[10] of a charged particle.

In the case of the particle of the critical range under the surface of the detector, the track appears after the etching time t(E) defined by the formula as follows (ref. (b) in Fig. 4.1.2),

$$t(E) = \left[R(E) - R(E_c) \right] / V_B$$

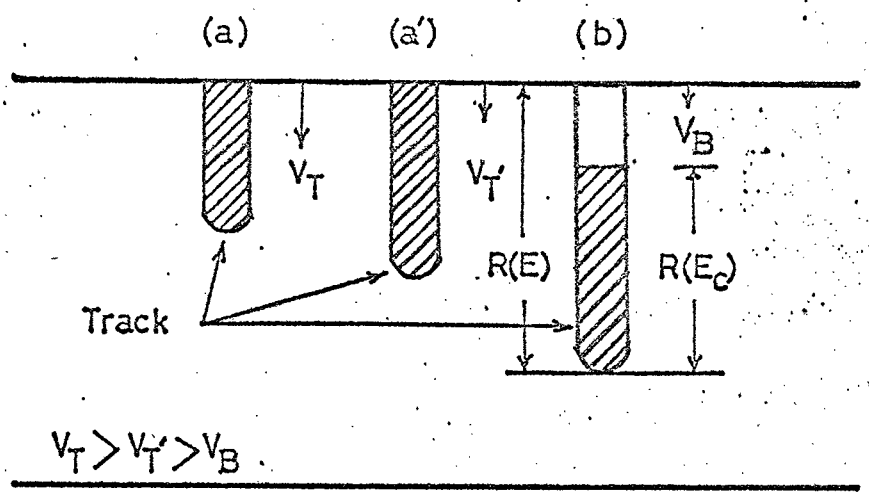

Fig. 4.1.2 Schematic diagram of track formation according to Somogyi et al.[4]

V_T, V_T' : etching rate inside the track

V_B : bulk etching rate on the detector surface

where V_B is the bulk etching rate on the detector surface.

4-1-4 Results and Discussion

4-1-4-a Alpha Track Spectrum

Alpha track diameter growth on the celluloid film in the case of 4.5 mg/cm^2 thickness of absorber is shown as a function of the etching time in 5 M sodium hydroxide solution at 50°C in Fig. 4.1.3. Their photographic patterns under an optical microscope are shown in Photo. 4.1.1. As seen in Fig. 4.1.3 and Photo. 4.1.1, the tracks of small diameter appear after about four hours of etching time. This is due to the α-particle of ^{212}Po nuclide (8.78 MeV) derived from the ^{212}Pb source which have been prepared by electro-deposition and in radioactive equilibrium with ^{212}Bi and ^{212}Po. While, the track appeared at the beginning of the chemical etching is due to the α-particle of ^{212}Bi nuclide (6.05 MeV).

Let us consider this experimental results according to the track formation as shown in Fig. 4.1.2. The α-track of ^{212}Po nuclide corresponds to (b) and that of ^{212}Bi nuclide to (a), respectively. It is understood on seeing that the rising point of α-track growth curve of ^{212}Po in Fig. 4.1.3 is several hours later than that of ^{212}Bi. Moreover, the rising of ^{212}Bi is steeper than that of ^{212}Po in Fig. 4.1.3, agreeing with that the etching rate of lower α-energy is larger than that of high α-energy as Somogyi et al. reported and mentioned above[6]. This fact is also the example of

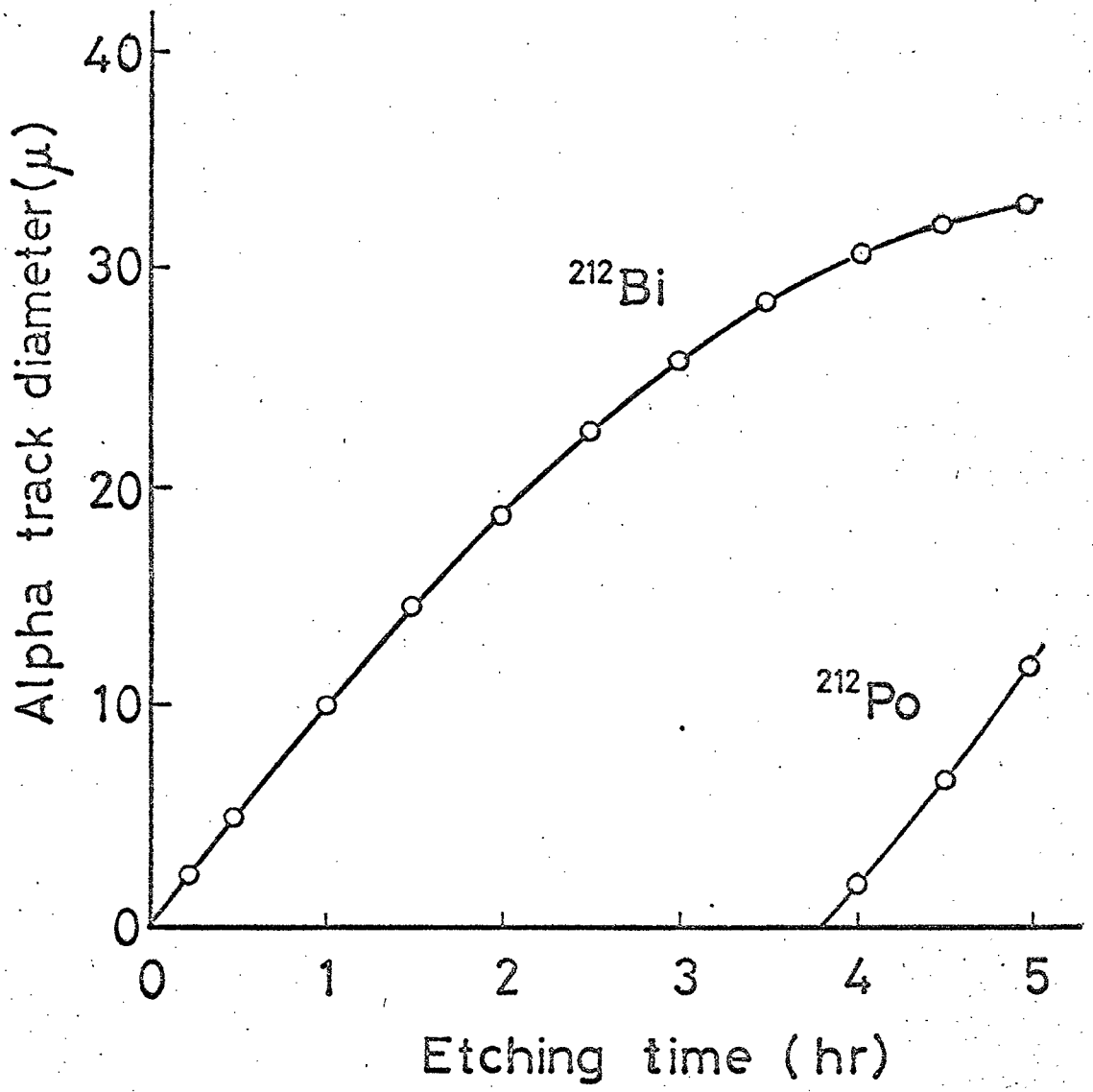

Fig. 4.1.3 Growth curves of α-track diameter of ^{212}Bi and ^{212}Po derived from ^{212}Pb source as function of etching time (absorber of 4.5 mg/cm^2 in thickness, 5 M NaOH at 50°C)

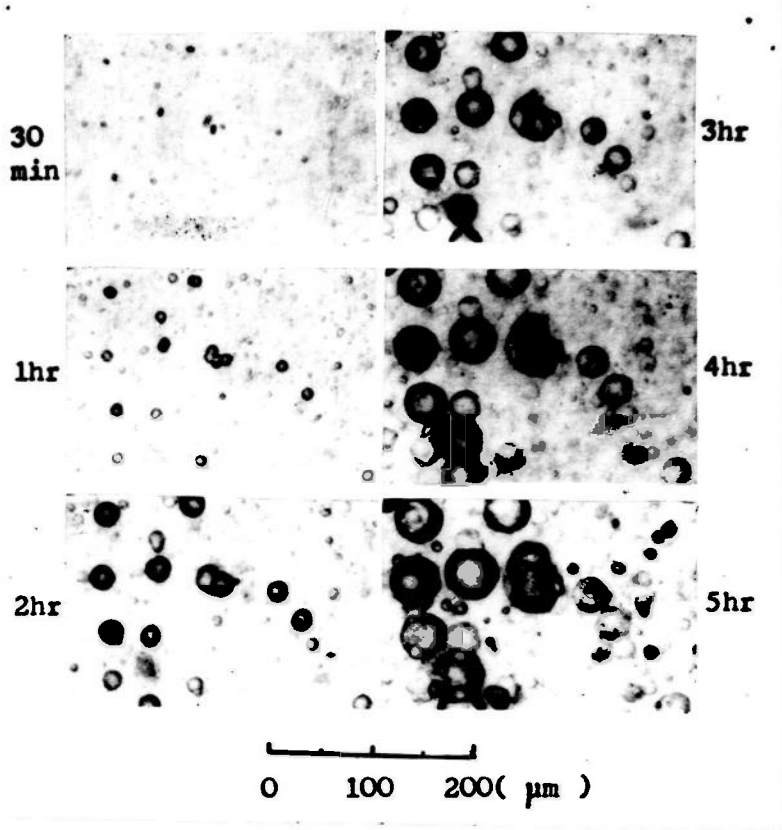

Photo. 4.1.1 Variation of α-track pattern as function of etching time under absorber of 4.5 mg/cm^2 in thickness (5 M NaOH at 50°C)

(a) and (a') in Fig. 4.1.2 corresponding to the larger etching velocity V_T for ^{212}Bi track and smaller $V_{T'}$ for ^{212}Po track, each within the critical registration range. However, the α-track growth of ^{212}Bi is seen to be almost saturated at about more than four hours of etching time, while that of ^{212}Po increases rapidly as shown in Fig. 4.1.3. Increasing the etching time to follow the tracks is not always advisable because not only the thin celluloid film is hardly stable for more than several hours' etching but also time consuming.

To overcome difficulties the sheets of thin absorber film were changed up to five sheets and put between the ^{212}Pb source and the celluloid detector film during the alpha particle irradiation as shown in Fig. 4.1.1. After the irradiation, the surface of the detector was etched for one hour in 5 M sodium hydroxide solution at 50°C and counted the number of α-tracks per unit area under an optical microscope. The results are shown in Fig. 4.1.4. There are two groups of α-tracks of different α-energies, which are good agreement with the α-spectrum measured with a grid ionization chamber (Osaka Denpa). The first peak is due to 6.05 MeV α-particle of ^{212}Bi and the second is due to 8.78 MeV of ^{212}Po. This method to obtain alpha spectrum changing the thickness of absorber is simple and quick. So, it is convinced to be useful for the study of α-emitting nuclide.

4-1-4-b Application of Focusing Chromatography

Photograph 4.1.2 shows alpha track pattern registered

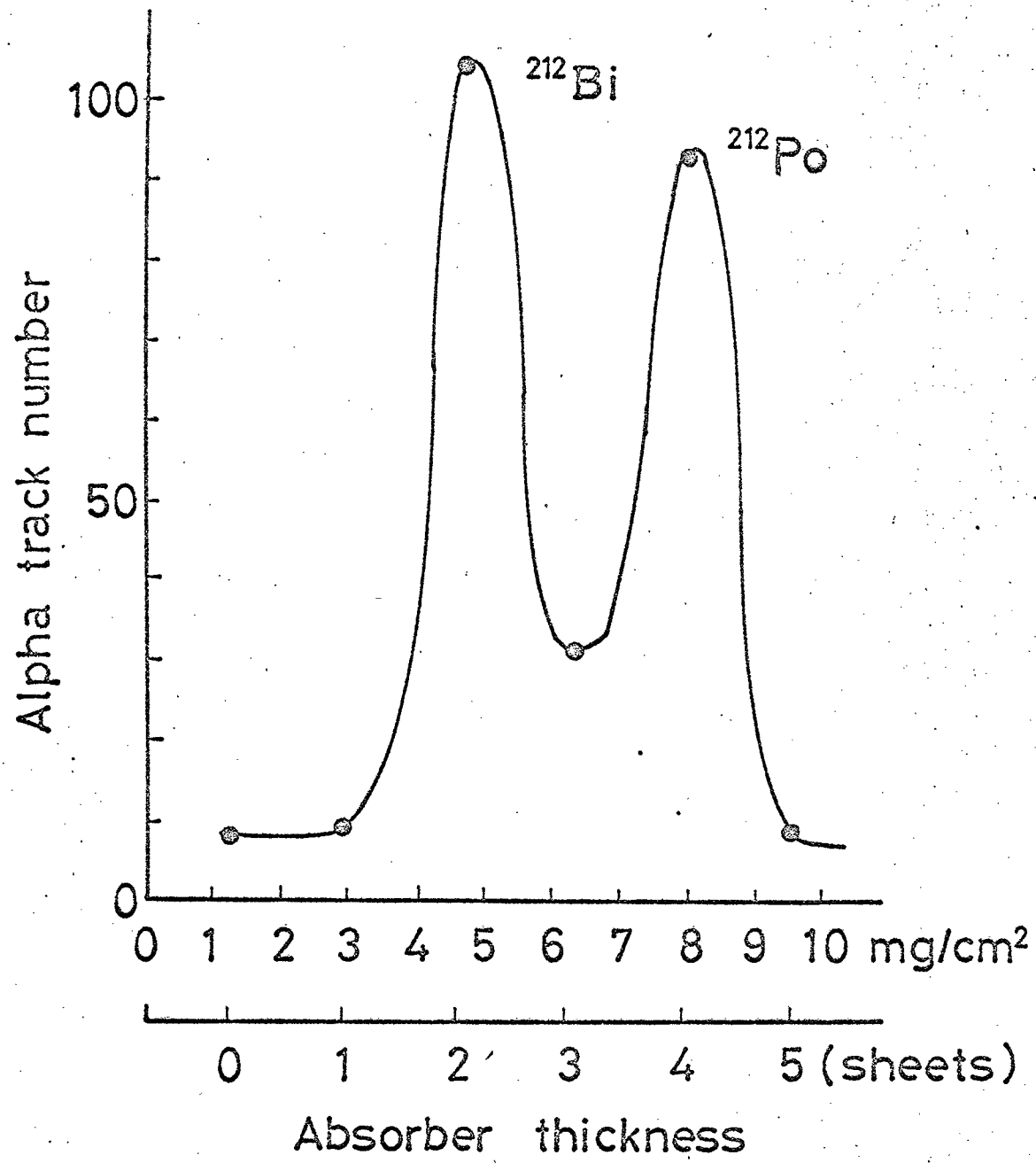

Fig. 4.1.4 Alpha track spectrum

Spots are by track detector , solid line is by grid ionization chamber. (^{212}Pb source, 5 M NaOH at 50°C for 1 hr)

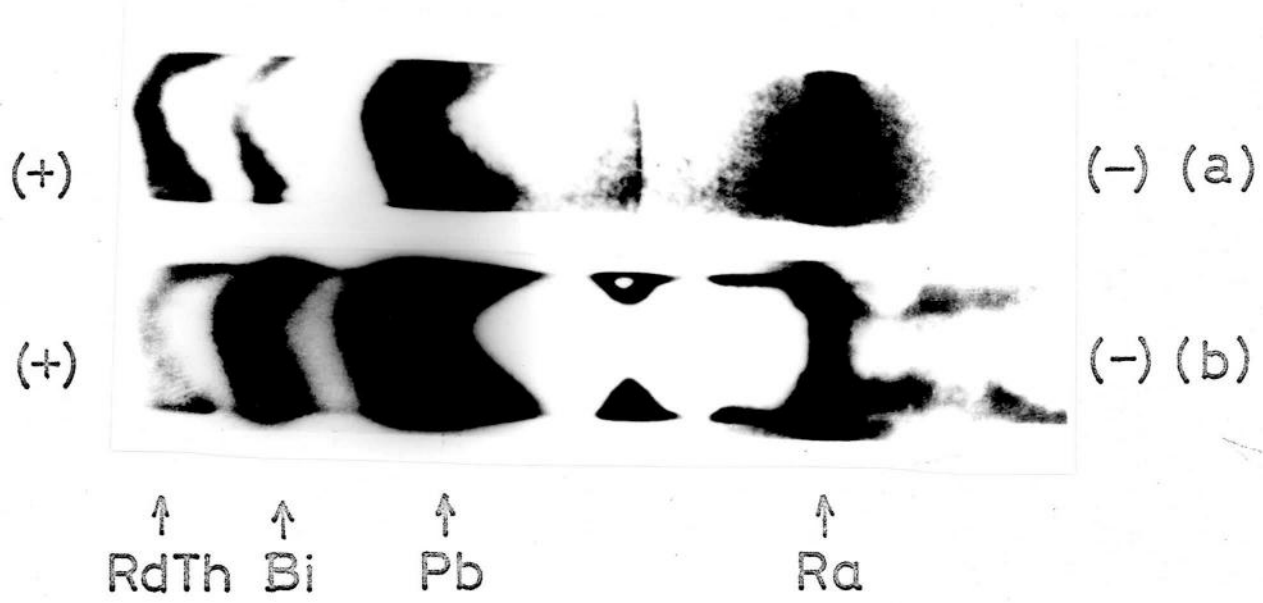

Photo. 4.1.2 Alpha track pattern (a) and its corresponding autoradiograph (b) of RdTh series according to a strip of focusing chromatography

on the celluloid film (a) and its corresponding autoradiograph with X-ray film (b) by the focusing chromatographic separation of RdTh series, where RdTh, ^{212}Bi, ^{212}Pb and ^{224}Ra are oriented in respective bands. The former appears clearly comparing with the later, since it is insensitive to β-rays of each daughter nuclide, particularly in the patterns of RdTh. Half-life of each isolated radioactive nuclide has been examined and identified by counting timely the number of α-tracks. In the case of obtaining the intensity of radioactivities by means of the number of α-tracks, care must be taken that the number of α-tracks is changed under the etching conditions applied[11]. Typical example of the decay curve of ^{212}Pb taken by α-track method at 5 ~ 10 μm in the diameter of α-track is shown in Fig. 4.1.5. The energy distribution of the alpha radiogram on paper strip may be obtained by the change of the thickness of absorber as mentioned above, but the discrimination of α-energy was poor comparing with that of collimated α-source because the incident angles to the detector film of alpha particles with different energies are isotropic. Using the X-ray film having the celluloid film as base material, the fractional detection of radioactive nuclides containing α- and β-rays is possible[12].

Incidentally, the features of translucency observed on etched surface of irradiated plastics having high density of α-tracks have been recently investigated[13]. Alphagraphy as well as fissionography will be useful in many scientific

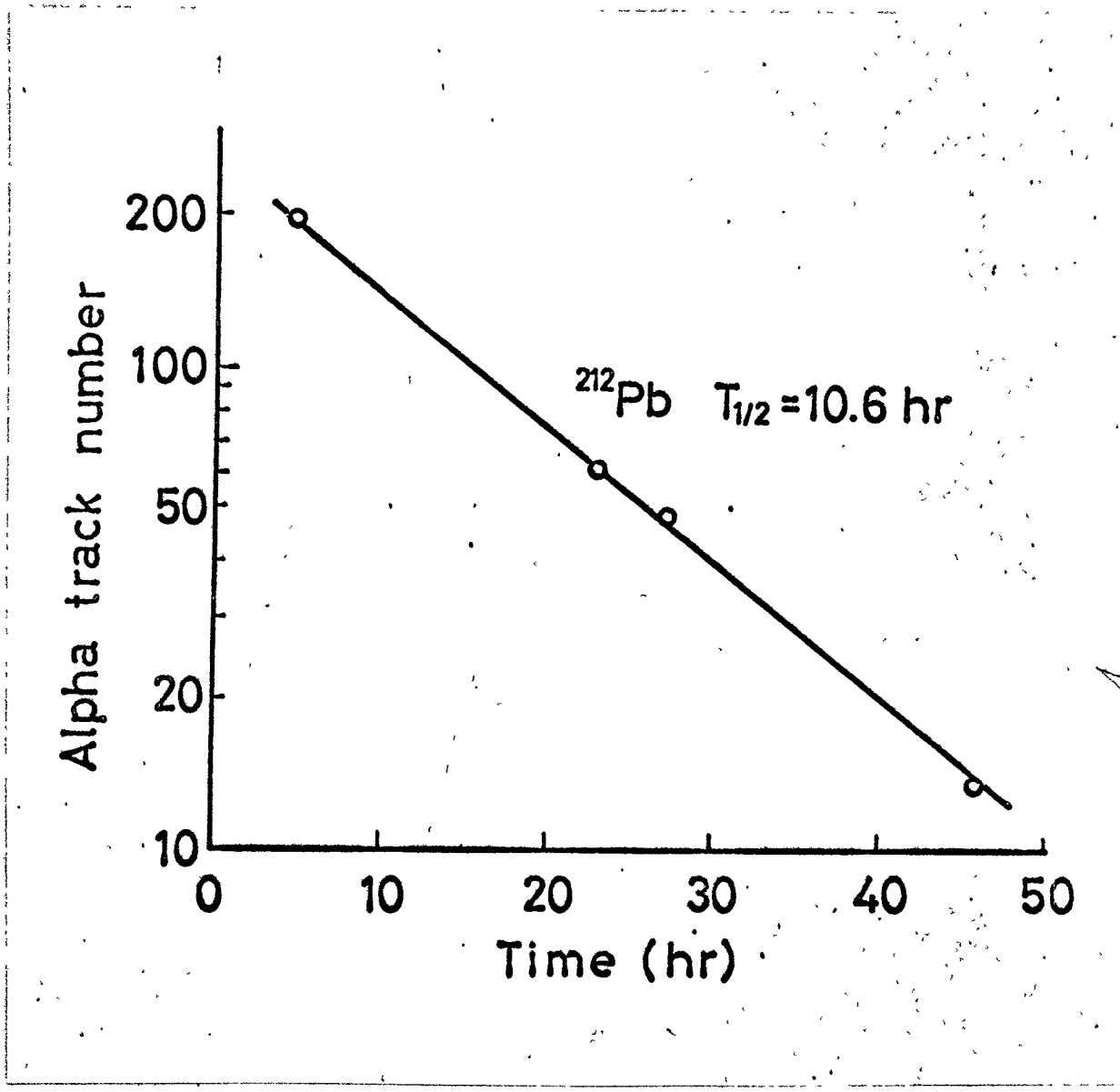

Fig. 4.1.5 Decay curve of ^{212}Pb, taken by alpha track method

fields.

4-1-4-c. Detection of Radiocolloid

Alpha track pattern was obtained using a drop of RdTh solution fallen upon the surface of the polyester absorber on the celluloid film detector as shown in Photo. 4.1.3. It is seen that α-tracks radiate from a point in a form like a star. This pattern can be considered to be the radiocolloid of RdTh decay series as has been reported by Chamié[14]. The diameter of radiocolloid obtained by α-track method was several times smaller than his results by microphotography.

4-1-5 Conclusion

Using alpha particle track detector of celluloid film, alpha spectrum is easily obtained as a curve of track number versus absorber thickness. The recommended technique is to use several sheets of polyester thin films as absorber to cover the celluloid detector before collimated irradiation. The α-track pattern obtained by the track method makes the detection feasible for thick α-emitting source and a radiocolloid without the influence of sun light, β- and γ-rays.

References

(1) Shinagawa,M., Takemi,H., et al.: "Proceedings of the 9th Japan Conference on Radioisotopes", B/2-3, p.226 (1969), Tokyo. (in Japanese)

(2) Takemi,H., Kinaga,Y., Ōsumi,K. and Shinagawa,M.: Technol. Report, Osaka Univ., 23, No. 2 (1973).

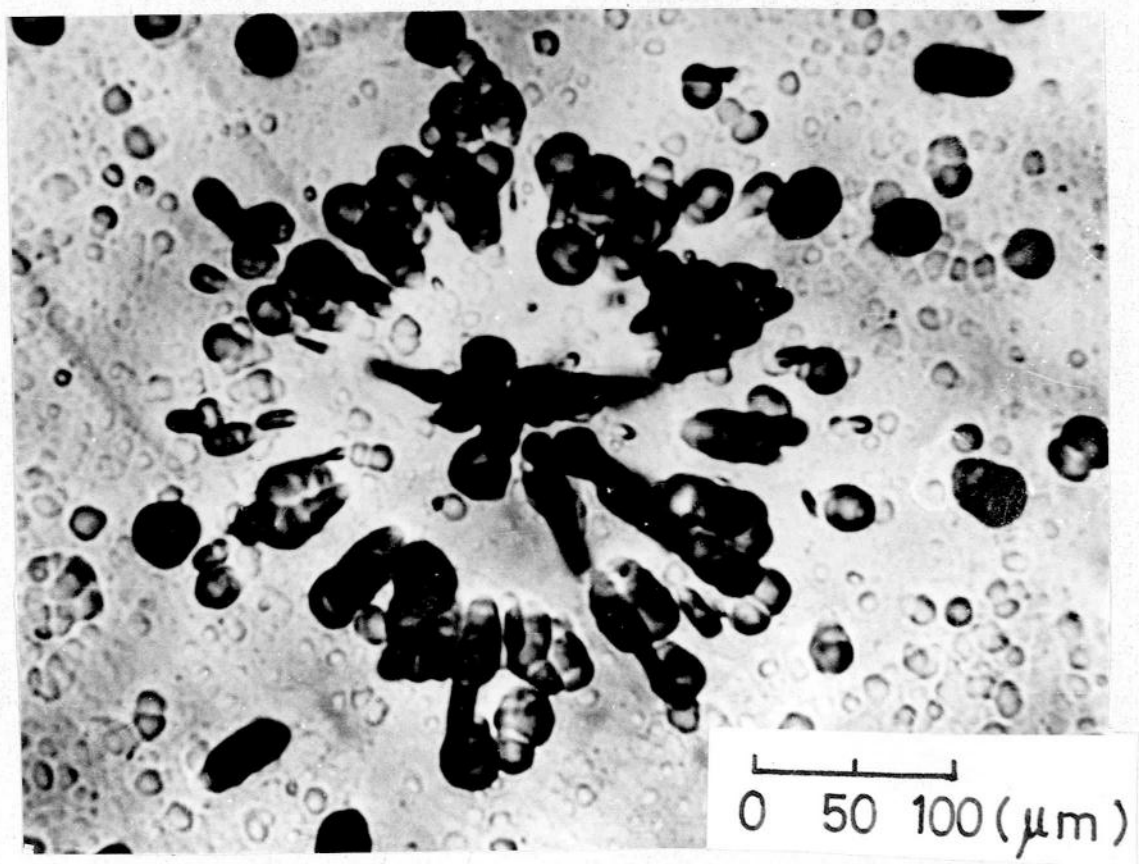

Photo. 4.1.3 Alpha track pattern of RdTh daughter nuclides foming a radiocolloid (absorber of 2.8 mg/cm^2 in thickness, 5 M NaOH at 50°C for 1 hr)

(3) Fleischer,R.L., Price,P.B. and Walker,R.M.:
Ann. Rev. Nucl. Sci., 15, 1 (1965).

(4) Somogyi,G.: Nucl. Instrum. and Methods, 42, 312 (1966).

(5) Somogyi,G., Várnagy,M. and Petö,G.: ibid., 59, 229 (1968).

(6) Somogyi,G., Schenk,B., Várnagy,M., Meskó,L and Valek,A.: ibid., 63, 189 (1968).

(7) Takemi.H., Asai,N. and Shinagawa,M.
J. Nucl. Sci. Technol., 10, 155 (1973).

(8) Price,P.B., Fleischer,R.L., Peterson,D.D., O'Ceallaigh, C., O'Sullivan,D. and Thompson,A.:
Phys. Rev., 164, 1618 (1967).

(9) Fleischer,R.L., Price,P.B., Walker,R.M. and Hubbard, E.L.: ibid., 156, 353 (1967).

(10) Benton,E.V. and Nix,W.D.:
Nucl. Instrum. and Methods, 67, 343 (1969).

(11) Hashimoto,T. and Iwata,S.:
Japan Analyst, 18, 1382 (1969). (in Japanese)

(12) Shinagawa,M. and Furushima,K.:
1971 Fall Meeting on Chemistry and Chemical Engineering in Atomic Energy, A-6.

(13) Somogyi, G. and Srivastava,S.:
Int. J. Appl. Radiat. Isotopes, 22, 289 (1971).

(14) Chamié,M.C.: Comptes rendus, 189, 1277 (1927).

4-2 Effect of Gamma Irradiation on Celluloid Film and Related Influence on the Registration of Alpha Tracks[1]

4-2-1 Introduction

The usefulness of the solid state track detector depends primarily on its ability to register heavy particle ion tracks without being affected by a dense background of less highly ionizing radiation that does not leave tracks[2]. It has been found that the registering sensitivity depends not only on the type of detector but also on the etching contions applied[3]~[7]. For determining the registering sensitivity, Katz, Monnin and Benton have pointed out that, for more accurate interpretation of experimental data, the distribution of the σ-electrons along the particle trajectory must be taken into account as well[7]. From this point of view, it was indicated that the dose required for etchable damage formation along a particle trajectory should be the same as that required for γ-irradiation damage. Measurements of bulk etching rate for γ-irradiated cellulose nitrate showed that a dose exceeding 1×10^6 rads was required to produce significant enhancement of etching rate above the value found for the normal, unirradiated material[7].

The effect of γ-irradiation on celluloid film is given in this section. This effect has been examined by weighing a piece of the plastic film before and after etching under various conditions and by measuring the optical density of UV light transmitted through the film. The sensitivity of

α-track registration of the γ-irradiated films was also estimated by examining the appearance of α-track under the optical microscope according to etching time.

4-2-2 Experimental

The celluloid film used in this experiment was manufactured by the Daicel Co. Ltd. and had 25 w/o camphor in cellulose nitrate, recognized as one of the most radiation sensitive materials[8]. This film (200 μ thick i.e. 1.32 g/cm^3) was irradiated with ^{60}Co γ-rays at the Institute of Scientific and Research, Osaka University. The dose rates obtained with the irradiation arrangement shown in Fig. 4.2.1 were approximately $2 \sim 7 \times 10^5$ rads/hr. The total absorption dose of the film was set between 1×10^6 and 3.5×10^7 rads. At doses above these values, the film was found to decrease its thickness by several percent, and it became too brittle to be applied as a solid state track detector. After γ-ray irradiation, these films were cut into pieces of equal area (50 mm x 40 mm) and then etched together with unirradiated film in a sodium hydroxide solution. After drying for 15 hours in a silica gel desiccator, the pieces were weighed by a balance reading down to one tenth of a milligram, to determine the average decrease of thickness of the material etched. Compatible results were obtained by re-etching the same piece several times.

The optical density of UV light transmitted through the γ-irradiated film was measured by a Shimazu UV-200, double

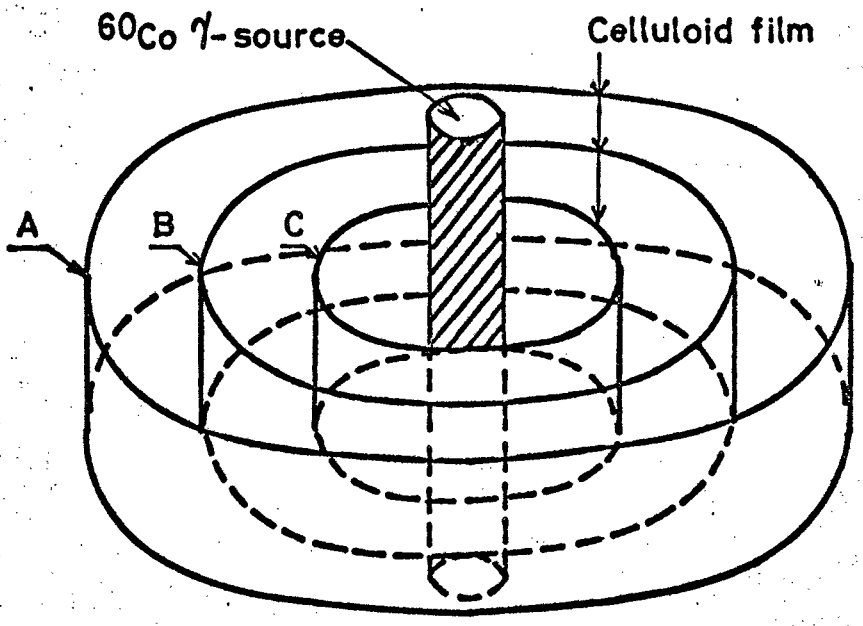

Fig. 4.2.1 Arrangement of celluloid films for γ-irradiation with ^{60}Co γ-rays

The dose-rates are approximately 7 x, 3.5 x and 2 x 10^5 rads/hr at the positions A, B and C.

beam spectrophotometer.

In order to examine the registering sensitivity of γ-irradiated film, a sample film was irradiated with α-particles of different energies incident perpendicularly on the film surface. The α-particles were obtained from a ^{212}Pb source in radioactive equilibrium with ^{212}Bi and ^{212}Po. The ^{212}Pb was electro-deposited on a nickel plate from a RdTh source[9], and the α-particles were passed through various thicknesses of air layer and thin polyester films to attenuate their energy. These films were then etched in 6 M sodium hydroxide solution at 50°C, and intermittently observed under an optical microscope to detect the appearance of tracks.

4-2-3 Results and Discussion

4-2-3-a Concentration of Etchant

To determine the etching parameters, e.g. concentration of etchant and temperature of etching process, first the bulk etching rate in $mg/cm^2 \cdot hr$ (corresponding to half the weight loss per cm^2 of the film after etching) was estimated by changing the concentration of sodium hydroxide solution at 50°C using a film irradiated to a γ-dose of 1.0×10^7 rads. The results are shown in Fig. 4.2.2. It can be seen that the bulk etching rate for the unirradiated film (A) depended linearly on the concentration of sodium hydroxide solution, while that for the γ-irradiated film (B) was saturated at above 7 M of sodium hydroxide solution. The ratio

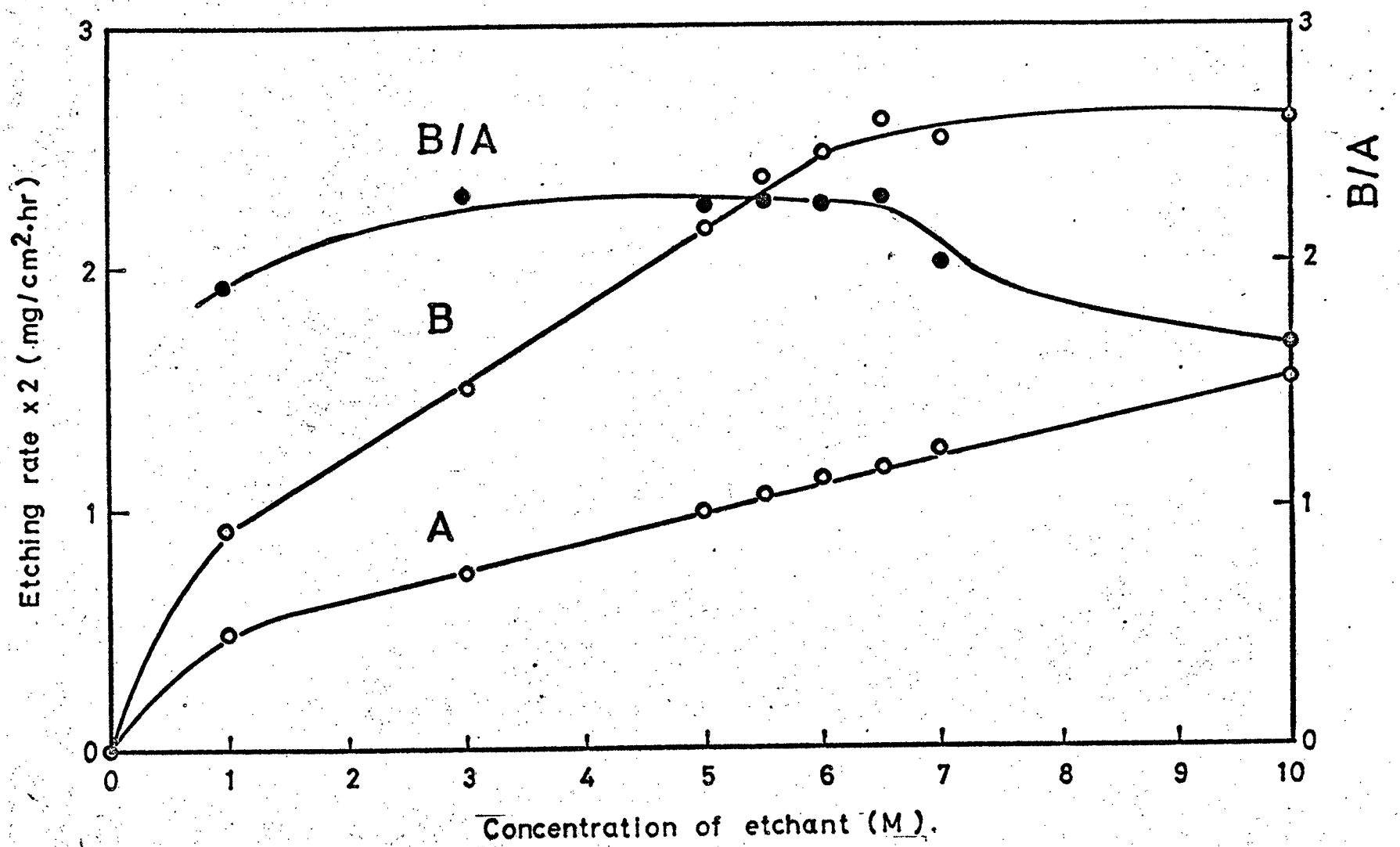

Fig. 4.2.2 Etching rate dependence of γ-irradiated celluloid film on concentration of NaOH solution at 50°C

A: unirradiated celluloid film

B: γ-irradiated film, absorption dose 1 x 10^7 rads

of these bulk etching rates B/A was revealed to be constant between 3 M and 6.5 M sodium hydroxide solution. For the ensuing experiments, it was decided that 6 M sodium hydroxide solution would be the most suitable as solution for etching the γ-irradiated film.

4-2-3-b Temperature of Etchant

Each γ-irradiated film was etched in a 6 M sodium hydroxide solution by changing its temperature from 30 to 80°C. The results are shown in Figs. 4.2.3 and 4.2.4. It can be observed in Fig. 4.2.3 that the bulk etching rate at each temperature depended on γ-dose above 3×10^6 rads. This effect indicates that celluloid film can be utilized as dosimeter for high dose γ-ray irradiation. The ratio of bulk etching rate between that of the γ-irradiated film and that of the unirradiated film is plotted in Fig. 4.2.4 as function of etching temperature for each γ-absorption dose. It is revealed that the ratio has a maximum value at about 50°C, where the radiation damage induced in the celluloid film can be considered to be the most accentuated. The etching time had to be shortened when the temperature of the etching solution was high, because of the fading effect of the celluloid reported by Hasegawa at al. (softening point of this film: 70 ± 5°C). The maxima observed in Fig. 4.2.4 suggest that the radiation damage caused by higher γ-absorption dose could have been partially faded during the high temperature etching, and that beyond a certain temperature this negative factor for the etching became predominant.

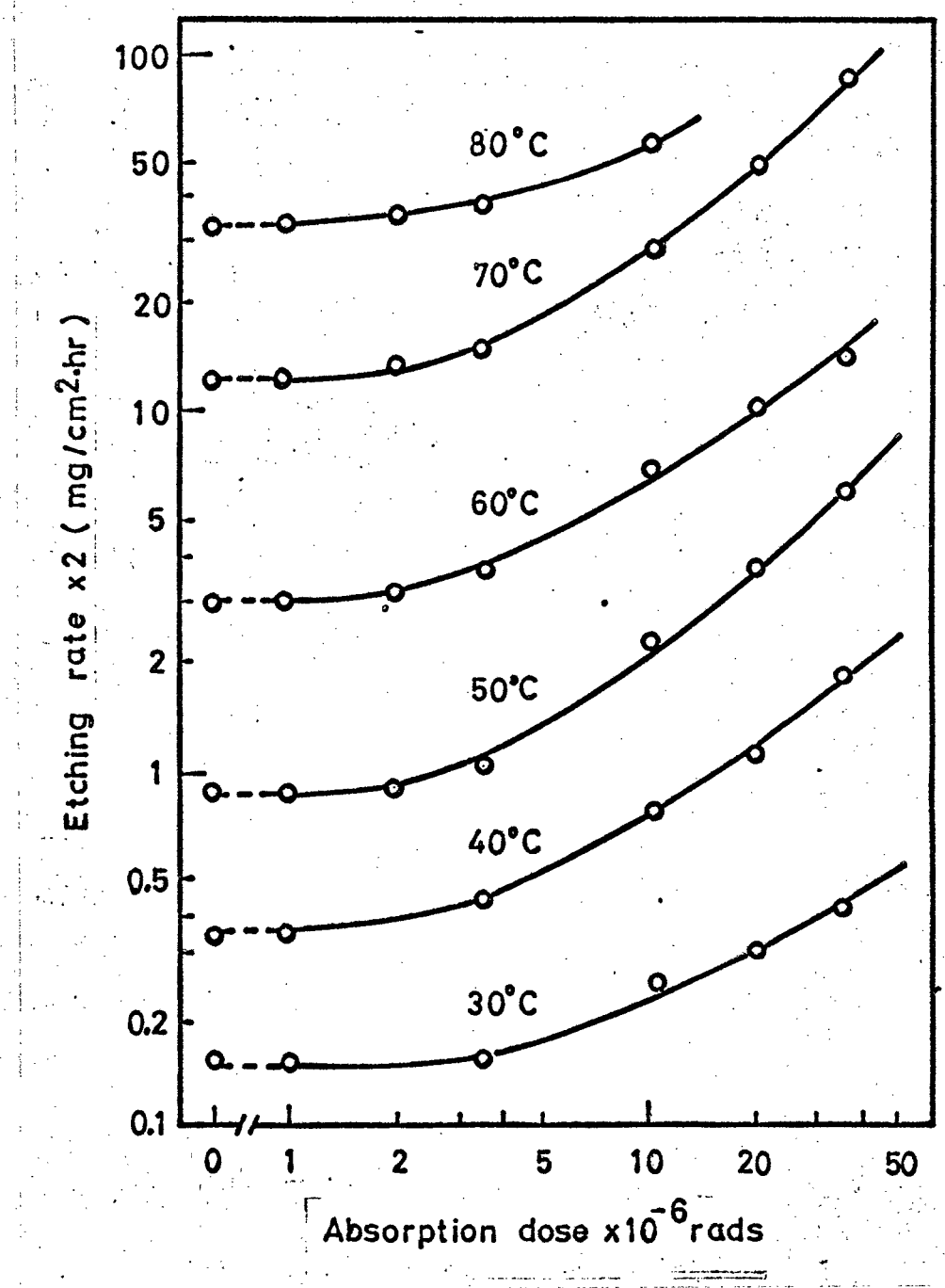

Fig. 4.2.3 Etching rate dependence on γ-absorption dose (rads) at different temperatures of 6 M NaOH solution

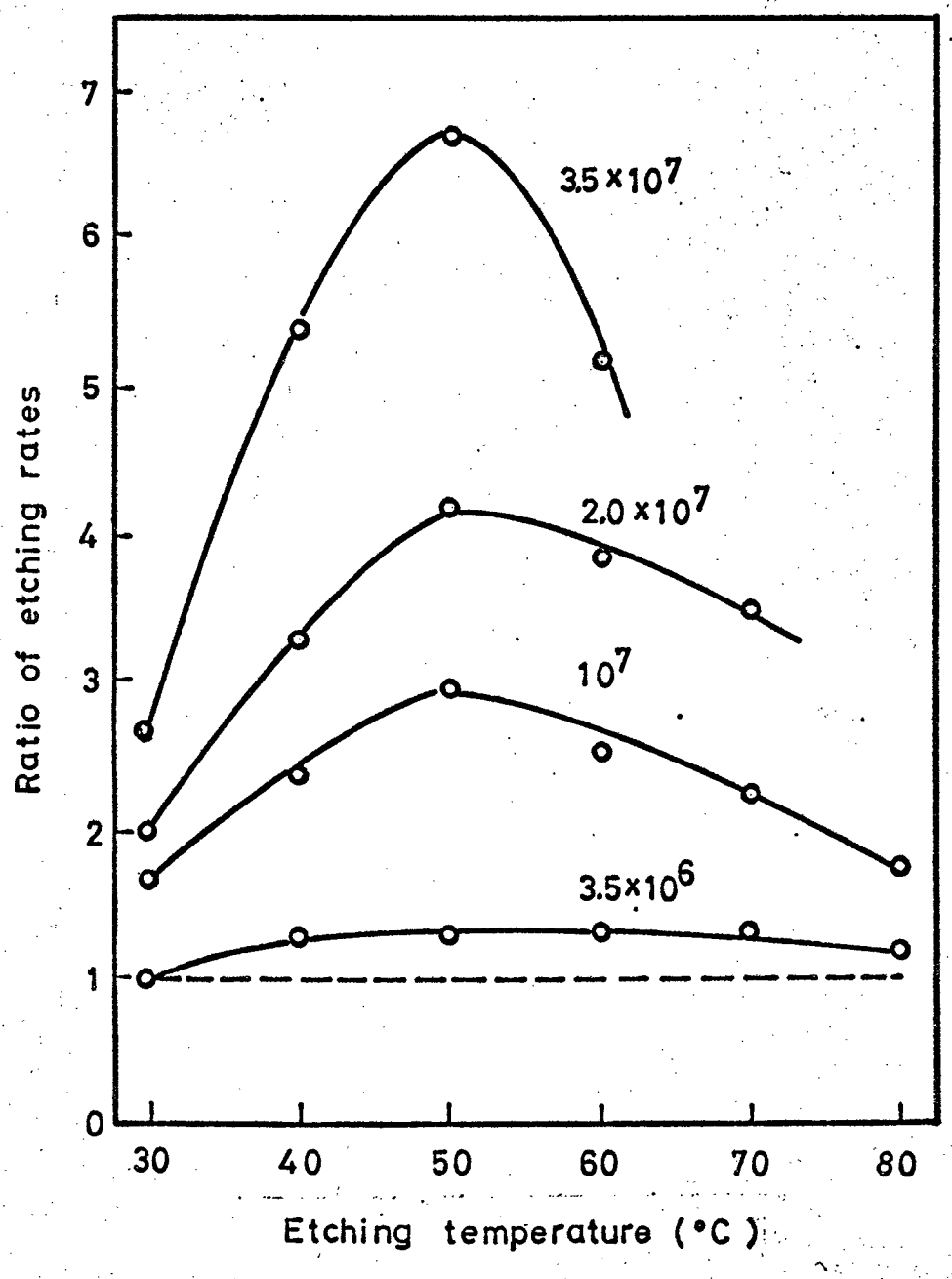

Fig. 4.2.4 Ratio of etching rates between γ-irradiated film and unirradiated film as function of temperature of 6 M NaOH solution. Doses are in rad.

By using 6 M sodium hydroxide solution the best etching condition was at 50°C, which agreed precisely with what had been reported by Somogyi et al. as the optimum condition for developing the α-track[10].

The free energy of activation for the chemical etching process was also estimated. It has been previously shown by Benton et al.[11] that the etching rate can be expressed by the relation

$$V_B = D \exp\left[-(F_A - F_B)/kT\right] ,$$

where V_B: Bulk etching rate

D : Constant

F_A: Free energy of activated complex

F_B: Free energy associated with bulk polymer and etchant

k : Boltzmann constant

T : Temperature of reactant in °K.

The activation free energy ΔF_B^* is equal to $(F_A - F_B)$. By plotting ln V_B versus 1/T as shown in Fig. 4.2.5, $\Delta F_B^*/k$ can be found as the slope of the straight line. The ΔF_B^* values obtained for several γ-irradiated films in 6 M sodium hydroxide solution are shown in Table 4.2.1. The activation free energy for a dose of 3.5×10^7 rads was found to be about 18 percent higher than that for unirradiated film. At the same time, it can be seen from Fig. 4.2.5 that the etching rate is enhanced with increase in the dose of pre-irradiation. These tendencies can be attributed to the degradation of the celluloid film and/or the decrease of

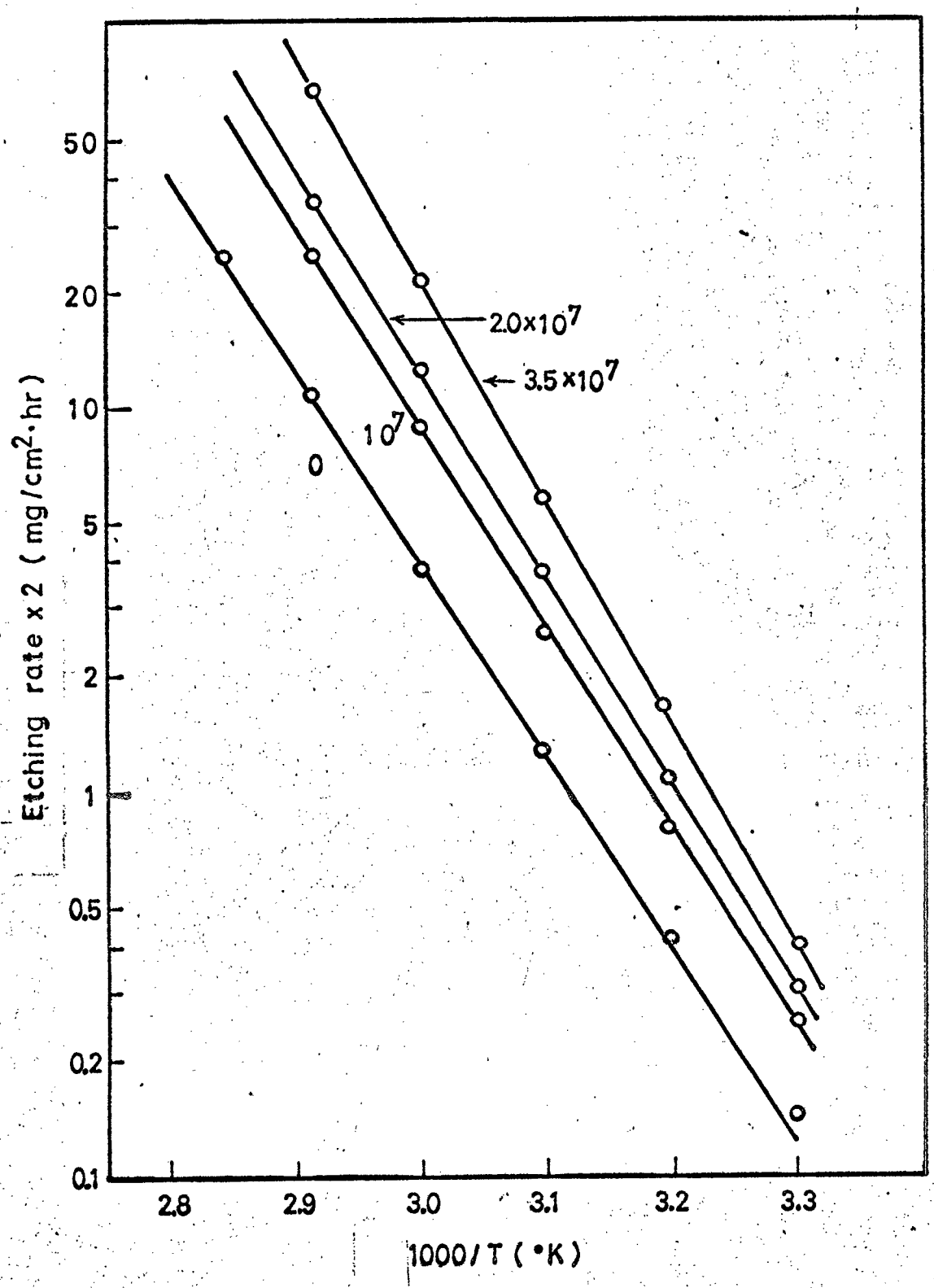

Fig. 4.2.5 Etching rate dependence of γ-irradiated films on temperature of 6 M NaOH solution
Doses are in rad.

Table 4.2.1 Activation free energy according to treatment of film

Treatment	ΔF_B^*
Unirradiated	0.99 eV
1.0×10^7 rads	1.04 eV
2.0×10^7 rads	1.10 eV
3.5×10^7 rads	1.17 eV

camphor content due to γ-irradiation. Therefore, the optical property of the celluloid film before the etching has been investigated in order to observe the latent damage.

4-2-3-c Optical Measurement

The optical density of UV light transmitted through the γ-irradiated film was measured. The results are shown in Fig. 4.2.6. The optical density of unirradiated film decreased sharply at about 320 mμ upon increasing the UV wavelength. As the γ-absorption dose of a film increased, the UV light absorption curve of the film shifted towards the longer wavelengths. This fact might be applied to the dosimetry of γ-ray irradiation together with the gravimetric method mentioned above. Such a change of the optical quality of a film may be ascribed to the degradation of the polymer by γ-irradiation. The radiolytic species might be changed by altering the atmospheric conditions during γ-irradiation. Particularly, the presence of oxygen in the surrounding atmosphere had been found to cause a significant increase in the α-track etching rate[7]. The results as shown in Fig. 4.2.6 were obtained under ordinary atmosphere.

4-2-3-d Sensitivity of Alpha Track Registration

In order to examine the α-track registering sensitivity on the γ-irradiated celluloid film, pieces of the film were irradiated with α-particles of different energies (3.0, 4.5 and 5.8 MeV).

Let us denote by R(E) the real range of α-particle having energy E, and by $R(E_c)$, the range of the α-particle

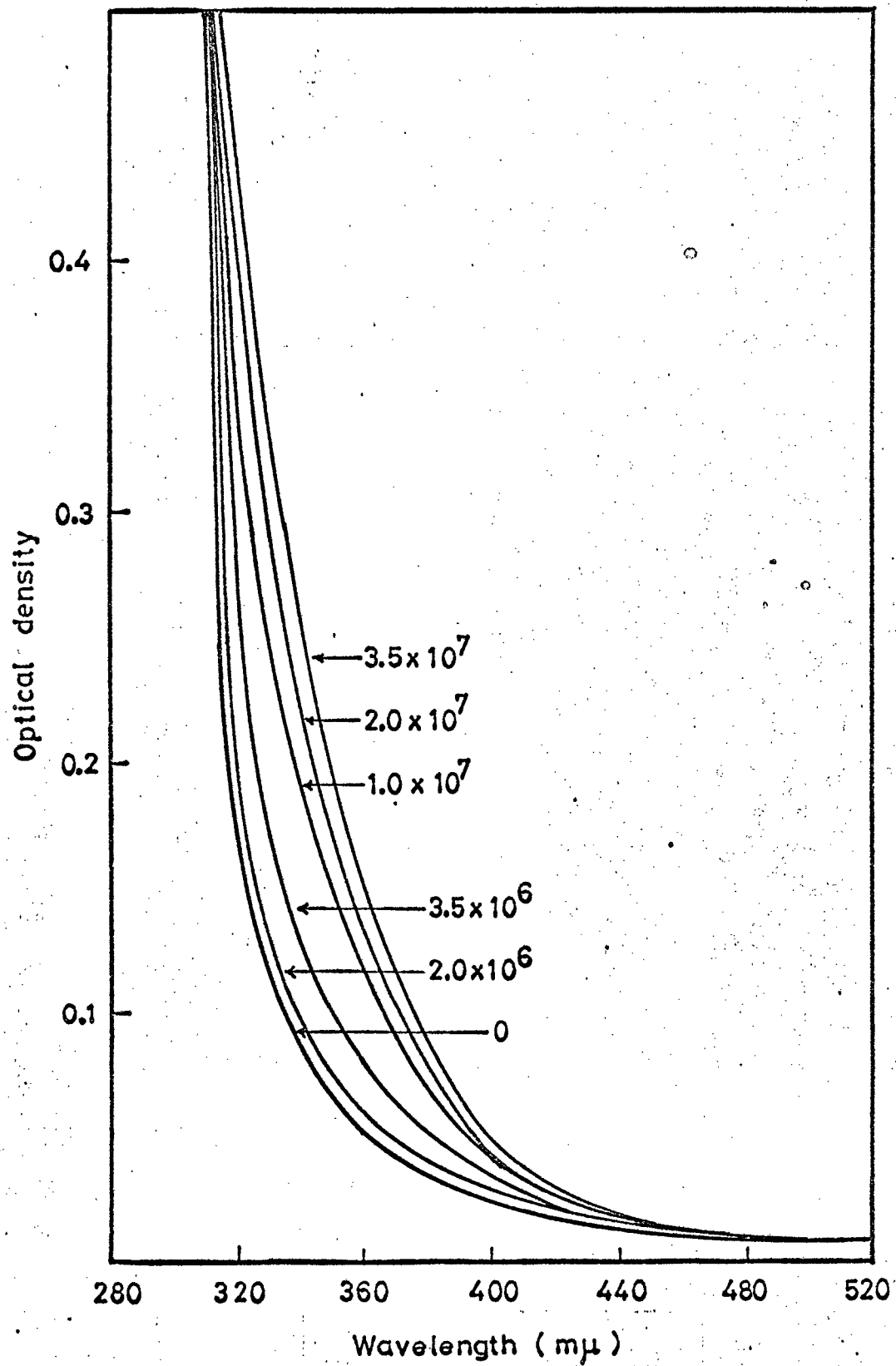

Fig. 4.2.6 Optical density of celluloid film irradiated with ^{60}Co γ-rays as function of UV wavelength

Doses are in rad.

having the critical registration energy E_c. If $R(E) > R(E_c)$, the region of range $R(E) - R(E_c)$ may be etched with the same rate of bulk etching, V_B. The time (t) required for α-track appearance on the etching is defined by the formula

$$t = \left[R(E) - R(E_c) \right] / V_B .$$

The variation of α-track diameter for the film pre-irradiated with a γ-dose of 2×10^7 rads is shown as function of the etching time in 6 M sodium hydroxide solution at 50°C in Fig. 4.2.7. Using both the V_B values obtained in Fig. 4.2.3 and the t values obtained as the intercepts of the abscissa in Fig. 4.2.7, $R(E) - R(E_c)$ is calculated by the above equation. The dependence of this value on α-particle energy is shown in Fig. 4.2.8, from which can be seen that the critical registration energy (cf. intercepts with abscissa in Fig. 4.2.8) decreases with the γ-absorption doses of the celluloid film.

If the units are normalized, the value of the ordinate of Fig. 4.2.3 and the slope of the line in Fig. 4.2.7 can be compared with each other as a measure of etching rate. The bulk etching rate (V_B) is found to be larger than that of the α-track (V_T) above about 5×10^6 rads. Therefore, the γ-ray pre-irradiation of celluloid film is not a suitable treatment insofar as concerns α-track registration, because of the decrease of the ratio V_T/V_B. Yet, the pretreated film has the advantage that latent tracks of α-particles exceeding the critical energy can be developed more quickly than in the case of non treated film.

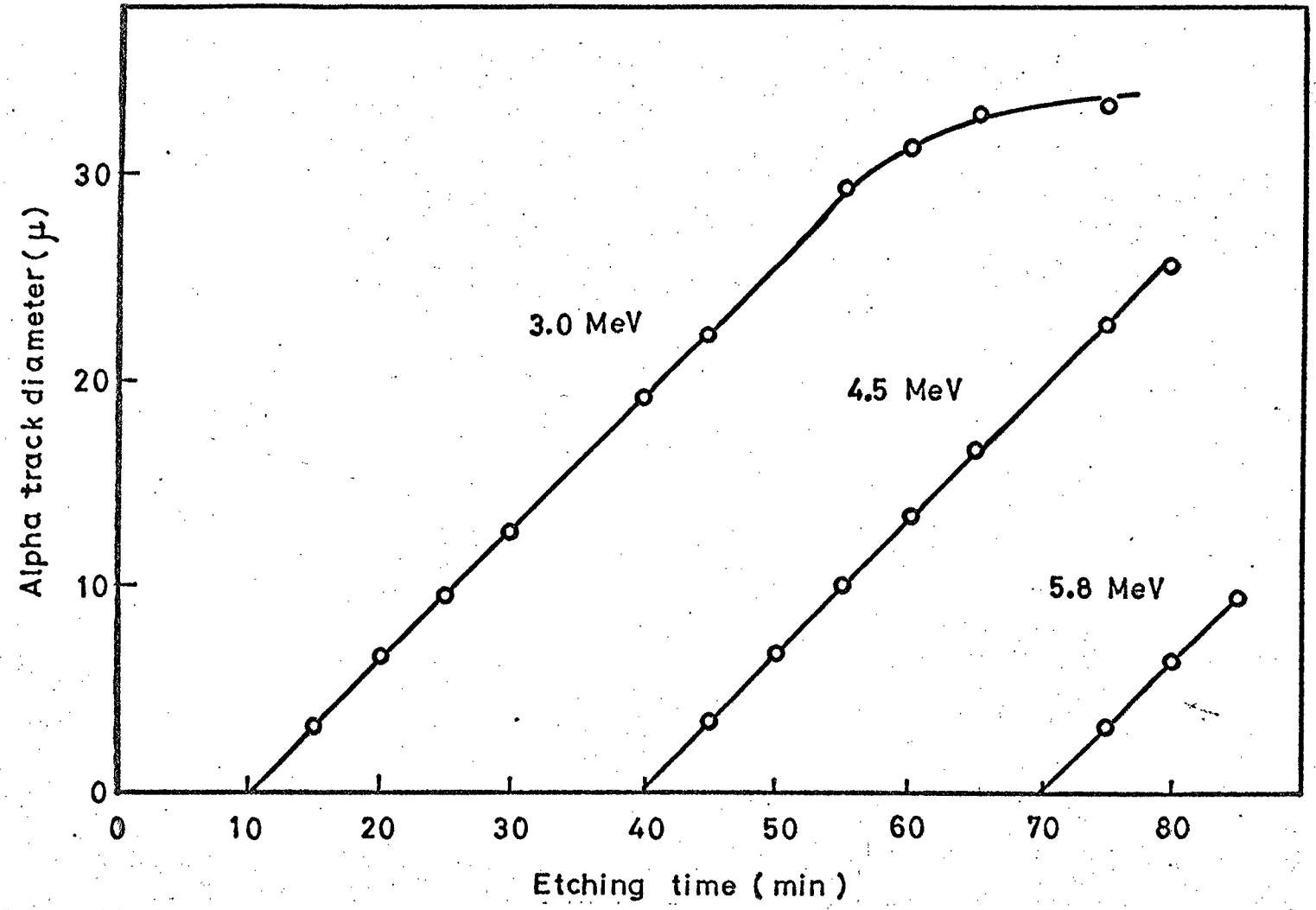

Fig. 4.2.7 Growth curve of α-track diameter on γ-irradiated film irradiated to 2 x 10^7 rads as function of etching time
The incident angles to the film of α-particle with several energies have been collimated at right angles. The etching condition is 6 M NaOH solution at 50°C.

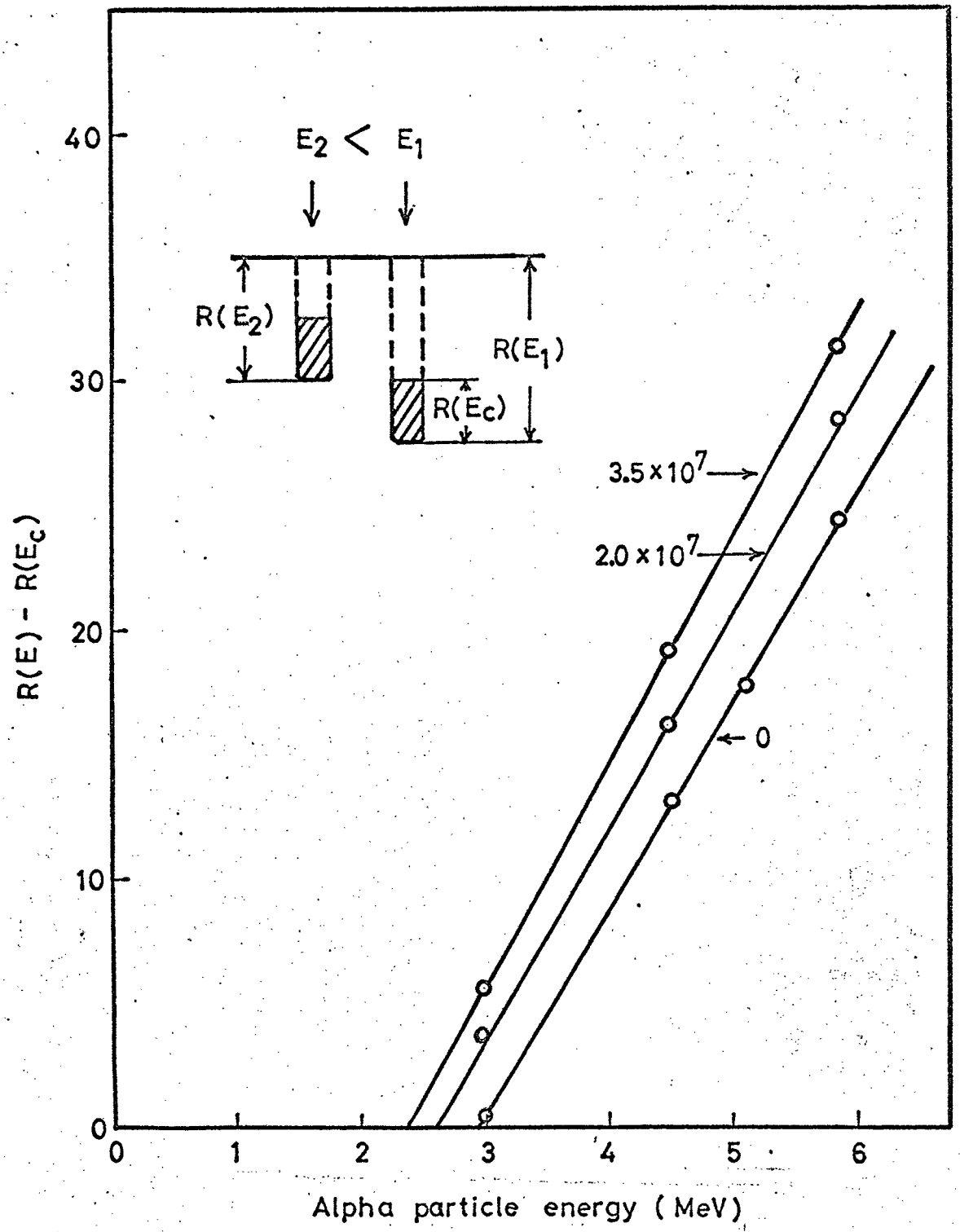

Fig. 4.2.8 Range $R(E) - R(E_c)$ from film surface to α-track appearance as function of α-particle energy E
The incident angle is perpendicular. The etching condition is 6 M NaOH solution at 50°C.
Doses are in rad.

4-2-4 Conclusion

Gamma-irradiation produces radiation damage i.e. latent tracks in the celluloid film. The optimum etching condition was found to be 6 M sodium hydroxide solution at 50°C, and the activation free energy of the γ-pretreated film increased slightly with the γ-absorption dose. The UV light absorption curve of the film shifted towards the longer wavelength side with the γ-absorption dose. These measurements have indicated the possibility of applying the celluloid film to dosimetry of high γ dose.

The sensitivity of the γ-irradiated film for α-track registration was examined, and it was found that its critical energy decreased with the absorption dose in γ-pretreatment. Such a change of critical registration energy of solid state track detectors should be taken into account when registering heavy particles under high γ-ray background.

References

(1) Takemi,H., Kinaga,Y. and Shinagawa,M.:
J. Nucl. Sci. Technol., 10, 215 (1973).

(2) Fleischer,R.L., Price,P.B. and Walker,R.M.:
Ann. Rev. Nucl. Sci., 15, 1 (1965).

(3) Benton,E.V. and Collver,M.M.:
Health Phys., 13, 495 (1967).

(4) Somogyi,G., Várnagy, M. and Petö,G.:
Nucl. Instrum. and Methods, 59, 299 (1968).

(5) Becker,K.: Health Phys., 16, 113 (1969).

(6) Somogyi,G., Várnagy,M. and Medveczky,L.:
Rad. Effects, 5, 111 (1970).

(7) Benton,E.V.: ibid., 2, 273 (1970).

(8) Hasegawa,H., Matsuo,M., Yamakoshi,K. and Yamakawa,K.:
Radioisotopes, 17 (9), 11 (1968).

(9) Takemi,H., Asai,N. and Shinagawa,M.:
J. Nucl. Sci. Technol., 10, 155 (1973).

(10) Somogyi,G. and Srivastava,D.S.:
Int. J. Appl. Radiat. Isotopes, 22, 289 (1971).

(11) Frank,A.L. and Benton,E.V.: Rad. Effects, 2, 269 (1970).

Chapter V. On Hydrazine Formation with Boron Compounds Added[1]

5-1 Introduction

There are a number of points of similarity between the radiolysis of liquid ammonia and that of water [2],[3]. The primary products of the radiolysis of liquid ammonia are H_2, N_2H_4, $\cdot H$ (or e_{am}^-) and $\cdot NH_2$ corresponding to H_2, H_2O_2, $\cdot H$ (or e_{aq}^-) and $\cdot OH$ from water, respectively. The major radiolytic differences between ammonia and water, on the other hand, lie in their primary radiation chemical action, and the decomposition and formation yields of their derivatives.

Particular interest has been focused on the formation of hydrazine in the liquid ammonia system, the yield of which is generally very small and strongly dependent on the type of irradiation and the dose [2] ~ [8]. The G-value for hydrazine formation in the ^{60}Co γ-radiolysis of liquid ammonia has been reported to be about $0.2 \sim 0.003$ [2] ~ [5]. By irradiation with fission fragments, there have been indications that the $G(N_2H_4)$ value may be as high as $1.5 \sim 0.1$ [6]. Both in-pile and fission fragment irradiations of liquid ammonia have been studied by Landsman et al.[7], who have found the G-value to be 0.11 and 1.10, respectively. Since the G-value of hydrazine rapidly decreases with increasing dose, the maximum G-value is attained only at a relatively small total dose of energy[8].

On the other hand, the γ-radiolysis of aqueous solution

of ammonia has been studied by only a small number of investigators[9] ~ [11]. Sorokin et al.[9] and Sakumoto[10] have reported that the yield of hydrazine depends on the concentration of ammonia, and that it has a maximum value at 50 mole percent. In frozen ammonia-water system at 77°K, the yield of the $\cdot NH_2$ radical, which may be a main precursor of hydrazine, has also been reported as a function of the ammonia concentration by Al-Naimy et al.[11].

The present chapter covers the results obtained from a basic study on the effect of the $^{10}B(n,\alpha)^7Li$ reaction on hydrazine formation in an ammonia-water system containing a boron compound. The LET value in the $^{10}B(n,\alpha)^7Li$ reaction is high (about 280 keV/μ) in a medium of unit density. When a boron compound is dissolved in the system, the average kinetic energy of 2.33 MeV of the reaction is completely absorbed in the surrounding medium. In this connection, the reaction $^{235}U(n,f)F.F.$ should be the most suitable as source of high LET radiation[12], for its energy release amounting to about 170 MeV, but this aspect will be discussed later on. The result of ^{60}Co γ-ray irradiation of the same system will also be treated in comparison with that of pile irradiation.

5-2 Experimental

5-2-1 Sample and Irradiation

A known amount of ammonium boron fluorate (NH_4BF_4) or else ethylamino boron trifluoride ($C_2H_5NH_2BF_3$) was dissolved in an aqueous solution of ammonia, and put in a quartz am-

poule (10 mm i.d.), which was attached to a vacuum line for degassing at dry ice temperature. After repeated degassing, the ampoule was sealed and irradiated with pile radiation or with ^{60}Co γ-rays. All chemical reagents used were of G.R. grade. The pile irradiation was carried out in one of the three columns of KUR (Research Reactor Institute, Kyoto University, 5 MW): The pneumatic tube (Pn-2), which had a thermal neutron flux density of 2.7×10^{13} cm^{-2} sec^{-1} with an accompanying γ-exposure rate of 1.1×10^{8} R/hr; the slant column (Slant), of 3.9×10^{12} cm^{-2} sec^{-1} neutron flux and 4.0×10^{7} R/hr γ-exposure rate; and the thermal column (E-2) of 8.8×10^{10} cm^{-2} sec^{-1} with less than 10^{5} R/hr. A ^{60}Co source with an exposure-rate of $2.1 \sim 5.6 \times 10^{5}$ R/hr, in the Institute of Scientific and Research, Osaka University, was used for the γ-irradiation. In order to study the higher dose-range and dose-rate effects at fixed neutron flux, the irradiations were carried out at concentrations of the boron compound ranging up to 4.35 mol/o. Since the boron compounds used were soluble in aqueous ammonia solution, the energy of the nuclear reaction could be considered to be completely absorbed in the medium. The absorption dose resulting from the $^{10}B(n,\alpha)^{7}Li$ reaction could be determined simply by externally monitoring the thermal neutron flux at the position of irradiation, knowing the boron content of the sample. The flux depression at the sample containing boron was less than one percent, so that it could be neglected in this case. Table 5.1 shows the dose-rate resulting from the neutron

Table 5.1 Dose rates from $^{10}B(n,\alpha)^{7}Li$ reaction of 1 mg of natural boron, and γ dose rates in ammonium hydroxide solution, in three columns of KUR

Column	$^{10}B(n,\alpha)^{7}Li$ dose-rate(eV/ml·min)	γ dose-rate(eV/ml·min)
Pn-2	1.5×10^{20}	1.2×10^{20}
Slant	2.1×10^{19}	4.1×10^{19}
E-2	4.8×10^{17}	$<1.5 \times 10^{17}$

capture process of 1 mg of natural boron in the three columns used in the KUR.

5-2-2 Analytical Procedure

For the determination of hydrazine, the irradiated ampoules were frozen in dry ice with alcohol and then crushed. Some of the irradiated samples were allowed to dissolve in hydrochloric acid. The hydrazine produced was analyzed spectrophotometrically by means of a Hitachi Recording Spectrometer (EPS-3T) on suitable aliquots, using p-dimethylaminobenzaldehyde[13]. Nitrogen and hydrogen were determined with a Hitachi RMU-5B mass spectrometer.

5-3 Experimental Results

5-3-1 Irradiation in ^{60}Co γ-ray Cell

The ^{60}Co γ-radiolysis of an aqueous solution of ammonia up to 24.5 M was carried out at room temperature. The yields of hydrazine showed a constant concentration of 0.7 μg/ml in the region of 6 ~ 16 M at 1 x 10^{20} eV/ml. This value of hydrazine yield agreed with that obtained previously with 11 M ammonia solution at about 6 x 10^{20} eV/ml[10]. In further experiments, 15 M ammonia solution was used in consideration of the following points: (a) the yield of hydrazine therein was thereby expected to approach that in the case of liquid ammonia[9],[10], (b) little variation in ammonia concentration in the solution was expected during the irradiation and (c) the concentration was suitable for the standpoint of reactor safety.

5-3-2 Irradiation in Pile

The sample of 15 M ammonium hydroxide solution was exposed to a constant γ-absorption dose of 1×10^{20} eV/ml in either of the two columns Pn-2 and Slant, or else in the ^{60}Co γ-ray cell. Since the accompanying γ-rays and fast neutrons in the E-2 column were much smaller than in the Slant, the irradiation in the former could be regarded as a pure thermal neutron exposure. The irradiation in the E-2 was carried out until the estimated neutron dose was equal to that obtained in the Slant. The resulting yields of hydrazine in μg per ml of 15 M ammonium hydroxide solution are shown in Table 5.2. It can be seen that the hydrazine yield in the Slant was about twice that in the ^{60}Co γ-cell. This can be explained as follows. Addition of the hydrazine yield in the E-2 to that in the ^{60}Co γ-cell, would be expected to give the aggregate effect of both thermal neutron and gamma rays, which should equal the yield obtained in the Slant.

The yield of hydrazine in the Pn-2 at dry ice temperature was ten times that in the Slant. Temperature dependence of hydrazine formation in the γ-radiolysis of liquid ammonia has been reported by Sorokin et al. who give the values of $G(N_2H_4) = 0.18$ at $-70^{\circ}C$ and $G(N_2H_4) = 0.01$ at $15^{\circ}C$[9]. In the case of the aqueous ammonia solution, the temperature dependence is smaller than in liquid ammonia.

5-3-3 Irradiation in Pile with $^{10}B(n,\alpha)^{7}Li$ Reaction

As shown in Fig. 5.1, the N_2H_4 concentration increased

Table 5.2 Hydrazine yields in 15 M ammonium hydroxide solution at 1 x 10^{20} eV/ml dose

Column	N_2H_4 μg/ml NH_3 solution	G-value	Temperature
Pn-2	15.5 ± 0.1	0.29	Dry ice temp.
Slant	1.3 ± 0.1	0.024	Cooling water temp. (~40°C)
E-2	0.5 ± 0.1	0.0094	Room temp.
^{60}Co γ	0.7 ± 0.1	0.013	Room temp.

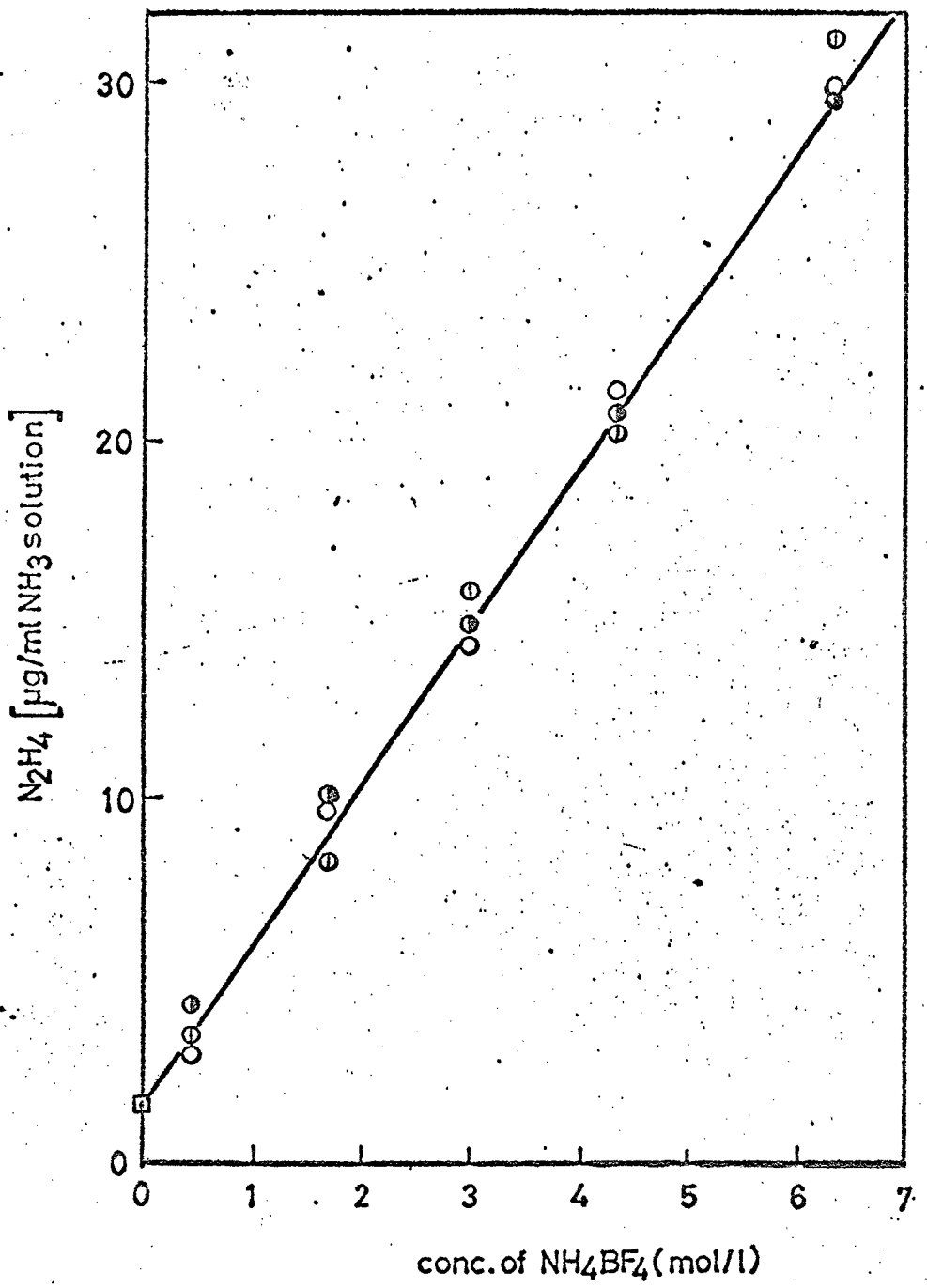

Fig. 5.1 Effect of $^{10}B(n,\alpha)^7Li$ reaction on 15 M ammonium hydroxide solution

Yield of N_2H_4 according to concentration of NH_4BF_4

○: 10 min ◑: 20 min ◕: 40 min

with the amount of NH_4BF_4 added as boron compound, but it was independent of the duration of irradiation. In the case of $C_2H_5NH_2BF_3$, however, the N_2H_4 yield increased up to 5 x 10^{21} eV/ml and then decreased as seen in Fig. 5.2. Thus, the boron compound appears to have acted chemically as well as radiologically according to its chemical form. In order to study the purely chemical effects of the boron additives, ^{60}Co γ-radiolysis was carried out. The results obtained with several different kinds of additives are shown in Table 5.3. It can be seen that isopropanol, which is known to be a strong radical scavenger[4], contributes particularly to increasing the hydrazine yield. The presence of ionic compounds such as NH_4BF_4 or NH_4Cl also contributed somewhat to increasing the yield, although these compounds had been reported to be either noneffective or else inhibitive in action for N_2H_4 yield in liquid ammonia[4],[8].

Figure 5.3 shows the yields of hydrogen and nitrogen as a function of the total absorption dose for the case with and without NH_4BF_4 addition in 15 M ammonium hydroxide solution in the Slant. No effect of the additive is discernible for the yields in the lower dose range. In the higher doses, the effect of the additive is manifested in the form of deviation from linearity. The yield ratio H_2/N_2 is plotted against the total absorption dose in Fig. 5.4. The value of this ratio is seen to saturate at 4.8 above 1.5 x 10^{21} eV/ml in the case of 15 M ammonium hydroxide solution, and at 5.2 above 2.5 x 10^{21} eV/ml in the case of the same solu-

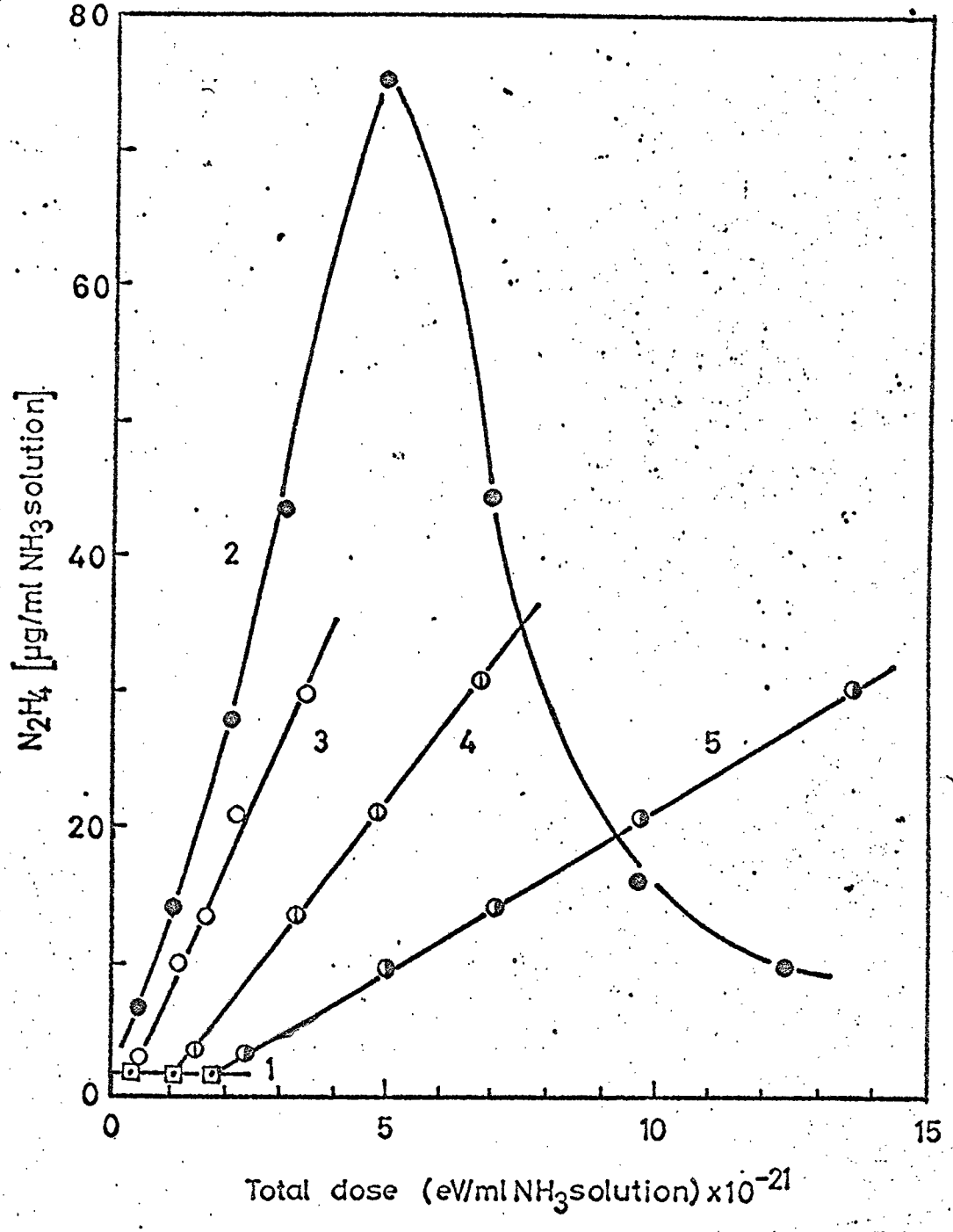

Fig. 5.2 Effect of $^{10}B(n,\alpha)^{7}Li$ reaction on 15 M ammonium hydroxide solution
Dose dependence of N_2H_4 concentration obtained with $C_2H_5NH_2BF_3$ or NH_4BF_4 as boron source
Irradiated in the Slant column of KUR.
1: ⊡ No additive 2: ◉ $C_2H_5NH_2BF_3$
3: ○ NH_4BF_4 10 min 4: ◐ NH_4BF_4 20 min
5: ◉ NH_4BF_4 40 min

Table 5.3 Effect of additives on hydrazine yield in γ radiolysis of 15 M ammonium hydroxide solution at 3.8×10^{20} eV/ml dose

Additive	mol/o	N_2H_4 μg/ml NH_3 solution
None		0.70
C_2H_5OH	3	0.90
$(CH_3)_2CHOH$	0.25	4.55
	3	6.85
CCl_4	3	0.80
NH_4BF_4	0.25	0.83
	3	1.55
$C_2H_5NH_2BF_3$	0.25	1.20
	3	1.83
NH_4Cl	0.25	0.77
	3	1.22
$(CH_3)_2CHOH$*	0	1.9
	0.3	64.5
	1	67.5
	3	28.0

* Pile radiolysis of 15 M ammonium hydroxide solution at 4.0×10^{20} eV/ml dose in the Slant column.

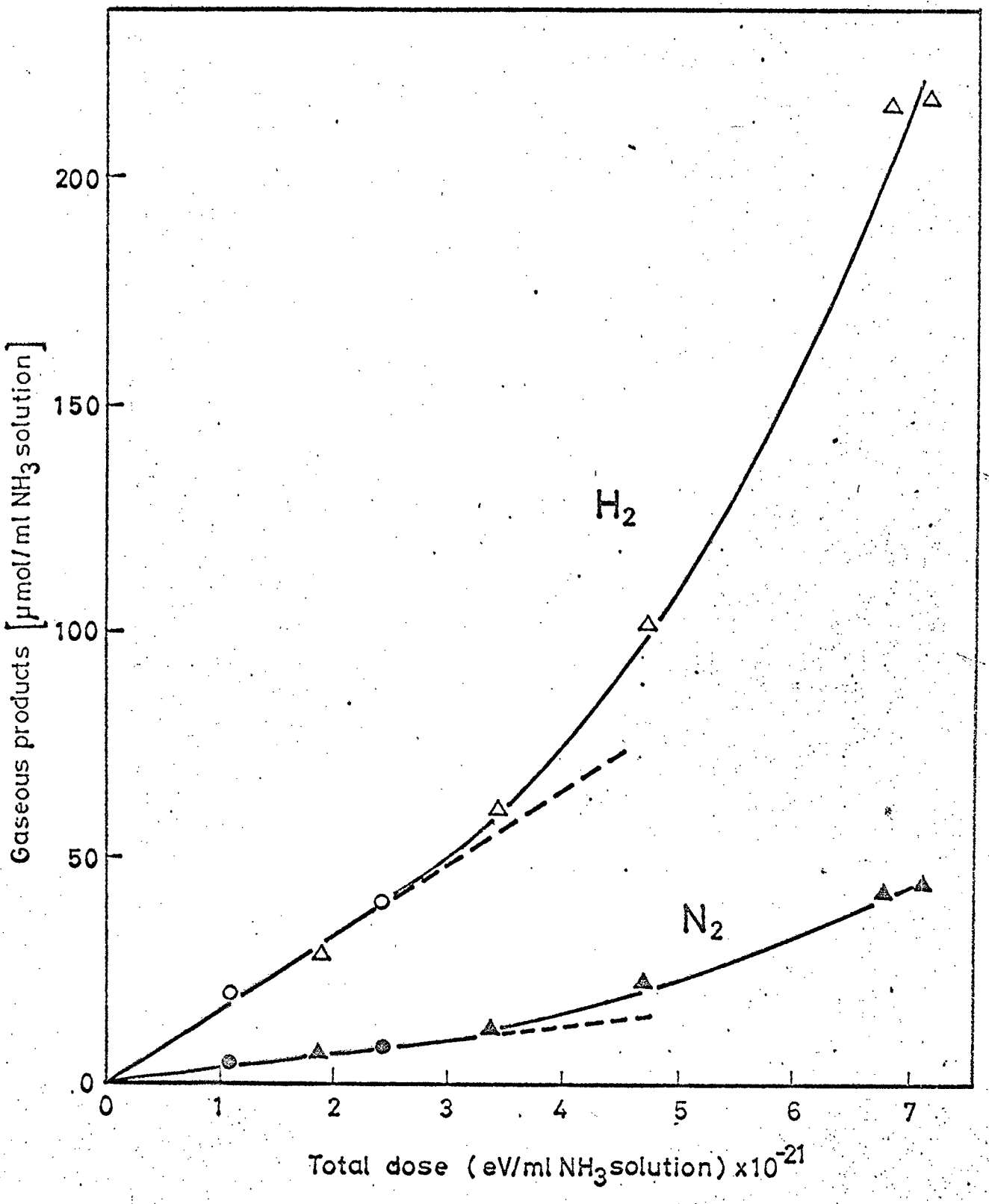

Fig. 5.3 Yields of gaseous products from 15 M ammonium hydroxide without additive (O) and with NH_4BF_4 (Δ) in the Slant
O,Δ: H_2 ●,▲: N_2

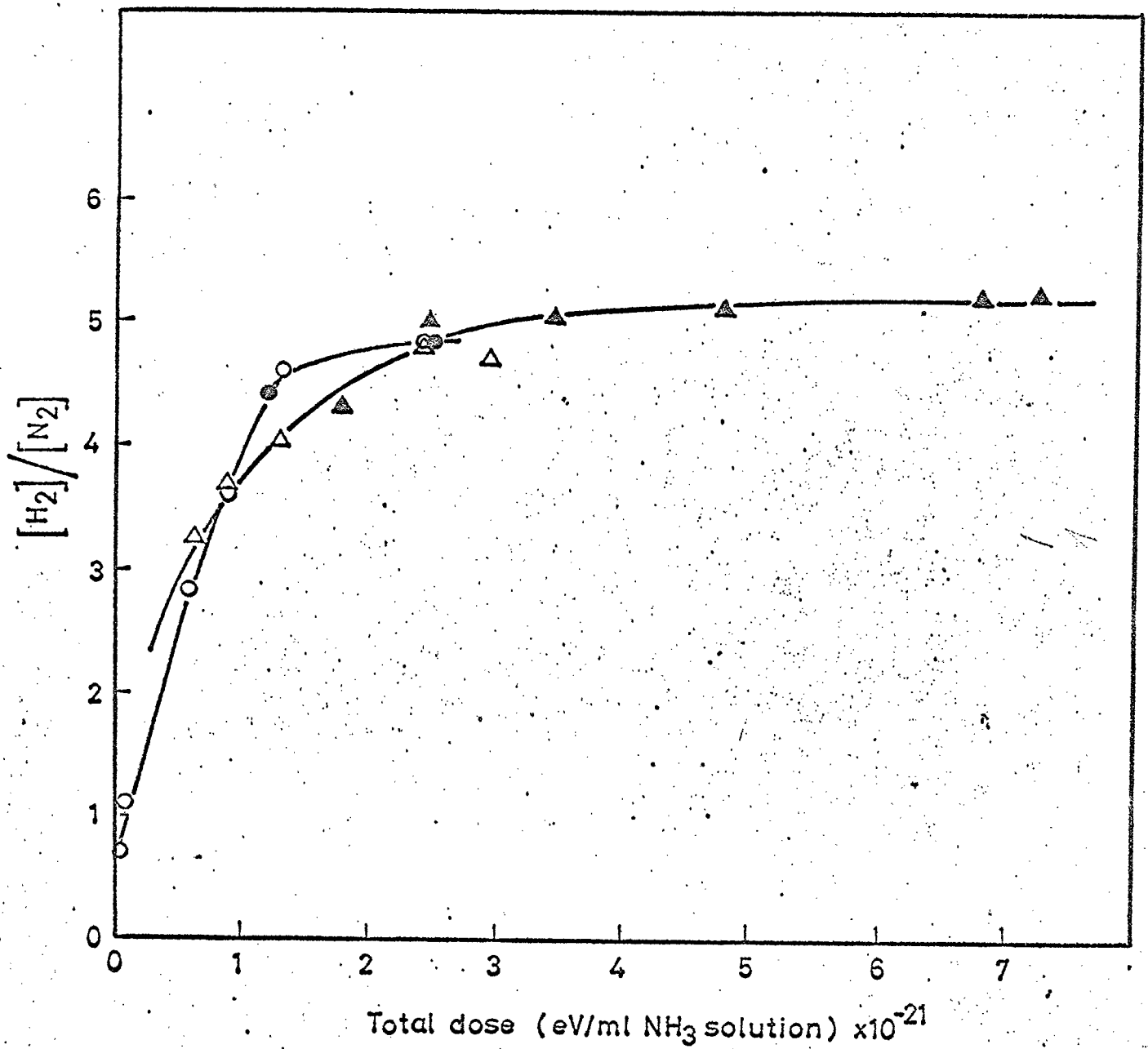

Fig. 5.4 The ratio of H_2-yield over N_2-yield produced by irradiation of 15 M ammonium hydroxide without additive (○) and with NH_4BF_4 (△)

●, ▲ : in Slant

○, △ : in ^{60}Co γ-cell

tion with NH_4BF_4 additive. The black circles and triangles in Fig. 5.4 show the data obtained in the Slant and the white symbols those from the ^{60}Co γ-cell. The difference in conditions of irradiation appears not to affect the ratio of H_2/N_2 to any significant extent. The ratio is seen to be distinctly larger than the value of about 3 which was found in the case of liquid ammonia[3]. This indicates that the water present in the system plays an important role on the ratio.

5-4 Discussion

The formation of hydrazine during the radiolysis of liquid ammonia has been extensively discussed[3],[4]. The major source of N_2H_4 formation has been thought to be the dimerization of NH_2 radicals in the particle track:

$$\cdot NH_2 + \cdot NH_2 \longrightarrow N_2H_4. \qquad (1)$$

In an aqueous solution of ammonia, it has been reported that the yields of N_2H_4 as well as of NH_2 radical depend on the concentration of ammonia. Hence, it is naturally considered that hydrazine is produced by the dimerization of NH_2 radicals. As for the mechanism of formation of the NH_2 radical, the results hitherto reported can be summarized as follows (9) ~ (11):

$$\cdot OH + NH_3 \longrightarrow \cdot NH_2 + H_2O, \qquad (2)$$

$$\cdot H + NH_3 \longrightarrow \cdot NH_2 + H_2, \qquad (3)$$

$$H_2O^+ + NH_3 \longrightarrow \cdot NH_2 + H_3O^+, \qquad (4)$$

$$NH_4^+ + e^- \longrightarrow \cdot NH_2 + H_2, \qquad (5)$$

$$NH_3^+ + e^- \longrightarrow \cdot NH_2 + \cdot H. \qquad (6)$$

On the other hand, the hydrazine molecules once formed during their diffusive movement, can be destroyed by reaction with radicals or electrons. The major decomposition reactions that have been suggested are

$$e^- + N_2H_4 \longrightarrow \cdot NH_2 + NH_2^-, \qquad (7)$$

$$\cdot H + N_2H_4 \longrightarrow \begin{cases} \cdot NH_2 + NH_3 \\ \cdot N_2H_3 + H_2, \end{cases} \qquad (8)$$

$$\cdot NH_2 + N_2H_4 \longrightarrow \cdot N_2H_3 + NH_3. \qquad (9)$$

Thus, the hydrazine concentration eventually reaches saturation at a certain dose-level. The calculation of the G-value of hydrazine presented in Table 5.2 is based on the concentration of hydrazine formed at a dose of 1×10^{20} eV/ml. The saturation value of hydrazine concentration depends not only on the LET and other irradiation parameters but also on the type and amount of additives, such as radical scavengers. In the case of γ-radiolysis with 3 mol/o NH_4BF_4 or NH_4Cl added, the N_2H_4 yield increased to a value several times that of the case without additive (cf. Table 5.3). Ionic salt such as NH_4BF_4 or NH_4Cl is a strong electrolyte and furnishes ammonium ion. The ammonium ion thus formed is neutralized with an electron by the reaction (5). This reaction accentuates the decrease of e^-, though this electron reacts with NH_4^+ about 100 times more slowly than with N_2H_4 (14). On the other hand, in pile-radiolysis, the hydrazine yield from 15 M ammonium hydroxide solution with NH_4Cl was reduced to zero.

The effective electron or radical scavenger may compete with hydrazine for the diffusing radicals and protect a hydrazine molecule from decomposition, thus increasing the N_2H_4 yield. The presence of isopropanol has a marked protecting effect as seen in Table 5.3. Isopropanol produces a hydrogen molecule from the reaction with a hydrogen radical. In this case, the high LET radiation favors the hydrogen atoms[15]. With increasing concentration of the additive, the hydrogen radical will also increase in pile-radiolysis, thus to a decrease of the N_2H_4 yield, as indicated in Table 5.3. The results obtained from $^{10}B(n,\alpha)^7Li$ radiolysis in the presence of NH_4BF_4 show that the N_2H_4 yield for a constant concentration of added NH_4BF_4 is independent of the duration of irradiation (cf. Fig. 5.1). An explanation for this can be given when considering that a boron compound such as Lewis acid of the type BF_3 or their NH_3-adduct is formed by the hot atom effect of the $^{10}B(n,\alpha)^7Li$ reaction in the system. It has been reported by Stöcklin et al.[8] on the radiolysis of liquid ammonia in the presence of a Lewis compound NH_3BF_3 that this compound exhibits a strong protecting effect against radiation decomposition of hydrazine. If the added boron compound transforms into a Lewis type compound by the energy of the $^{10}B(n,\alpha)^7Li$ radiolysis and if the product has a life so short as to be present in the system in constant amount during the irradiation, the N_2H_4 yield can be independent of the duration of irradiation.

In the case of $C_2H_5NH_2BF_3$ as additive, the N_2H_4 yield

has a maximum value at 5×10^{21} eV/ml as shown in Fig. 5.2. At comparably low doses, $C_2H_5NH_2BF_3$ is expected to be ruptured to form a hydrazine precursor $\cdot NH_2BF_3$ after one of the two series of reactions

$$C_2H_5NH_2BF_3 + \cdot H \longrightarrow \cdot C_2H_5 + NH_3BF_3 \qquad (10)$$

and $$NH_3BF_3 + \cdot H \longrightarrow H_2 + \cdot NH_2BF_3 \qquad (11)$$

or $$C_2H_5NH_2BF_3 \rightsquigarrow \cdot C_2H_5 + \cdot NH_2BF_3 . \qquad (12)$$

Equation (10) expresses not only the Lewis nature of $C_2H_5NH_2$-BF_3 because it takes up $\cdot H$ to exchange with $\cdot C_2H_5$ (bond energies: N-H 93.4 Kcal/mol, N-C 69.7 Kcal/mol) but also the formation of the Lewis acid NH_3BF_3 as shown by the reaction (11) which takes up another $\cdot H$ radical. This repeated uptake of $\cdot H$ radical is revealed clearly on comparing the curves 2 and 3 in Fig. 5.2 which have been obtained under the same experimental conditions $C_2H_5NH_2BF_3$ and NH_4BF_4. The $\cdot NH_2BF_3$ radical thus formed may produce some adduct of hyrazine:

$$\cdot NH_2BF_3 + \cdot NH_2 \longrightarrow F_3B \cdot NH_2 \cdot NH_2 , \qquad (13)$$

$$\cdot NH_2BF_3 + \cdot NH_2BF_3 \longrightarrow F_3B \cdot NH_2 \cdot NH_2 \cdot BF_3 \qquad (14)$$

The radical $\cdot NH_2BF_3$ is heavier than $\cdot H$ or $\cdot NH_2$, so that it has smaller chance to diffuse out of the track. Thus, C_2H_5-NH_2BF_3 or the accompanying $\cdot NH_2BF_3$ radical eliminates the $\cdot H$ or $\cdot NH_2$ radical which promotes the decomposition of the hydrazine (cf. reaction (8) and (9)), meaning an increase of the N_2H_4 yield.

On the other hand, in the higher doses, such as in the descending part of curve 2 in Fig. 5.2, radiolysis of the

added $C_2H_5NH_2BF_3$ may lead to a rupture of the C-H bond, giving rise to an excessive increase of ·H concentration which can no longer be scavenged by the above mentioned Lewis effect. The surplus ·H radical decomposes the hydrazine to decrease its yield.

5-5 Conclusion

The yield of hydrazine upon radiolysis of 15 M ammonium hydroxide solution was found very small but strongly dependent on the type of irradiation. In the case of ^{60}Co γ-radiolysis, the N_2H_4 yield was smaller than in liquid ammonia. When an ionic boron compound NH_4BF_4 was mixed in ammonium hydroxide solution, the N_2H_4 yield increased but still did not equal the corresponding value in liquid ammonia. The molecular boron compound $C_2H_5NH_2BF_3$ produced the same effect as the ionic compound. In pile-radiolysis can be expected to provide the combined effects of both γ-radiolysis and neutron radiolysis. A boron compound present as additive could produce two results: (a) the hot atom effect of $^{10}B(n,\alpha)^7Li$ reaction and (b) the radical scavenging effect of the resulting Lewis type acid. The NH_4BF_4 appears to provide the Lewis acid in the form of NH_3BF_3. The $C_2H_5NH_2BF_3$ is itself originally of Lewis type, which, by exchanging its $\cdot C_2H_5$ for ·H, produces another Lewis acid NH_3BF_3, thus exhibiting a double scavenging action to protect hydrazine decomposition. On the other hand, at comparatively high doses of irradiation, the free radical ·H produced from

C_2H_5 in the molecule tends to inhibit hydrazine formation and to depress its yield.

References

(1) Takemi,H., Watanabe,A. and Shinagawa,M.: J. Nucl. Sci. Technol., 10, 268 (1973).

(2) Cleaver,D., Collinson,E. and Dainton,F.S.: Trans. Faraday Soc., 56, 1640 (1960).

(3) Dainton,F.S., Skwarski,T., Smithies,D. and Wezranowski, E.: ibid., 60, 1068 (1964).

(4) Schischkoff,D. and Schulte-Frohlinde,D. : Z. Phys. Chem., 44, 112 (1965).

(5) Belloni,J.: J. Chim. Phys., 63, 1281 (1966).

(6) White,E.R.: Int. J. Appl. Radiat. Isotopes, 16, 419 (1965).

(7) Landsman,D.A. and Noble,C.M.: Report AERE M-921 Atomic Energy Establishment, Harwell (1961).

(8) Stöcklin,G., Plott,G. and Heckel,E.: Int. J. Appl. Radiat. Isotopes, 20, 399 (1969).

(9) Sorokin,Yu.A., Tsivenko,V.I. and Pshezhetskii,S.Ya.: Russ. J. Phys. Chem., 37, 1012 (1963).

(10) Sakumoto,A.: Bull. Chem. Soc. Japan, 39, 1349 (1966).

(11) Al-Naimy,B.S., Moorthy,P.N. and Weiss,J.J.: J. Phys. Chem., 70, 3654 (1966).

(12) Steinberg,M.: Nucl. Appl., 6, 425 (1969).

(13) Watt,G.W. and Chrisp,J.D.: Anal. Chem., 24, 2006 (1952).

(14) Anbar,M. and Neta,P.:
Int. Appl. Radiat. Isotopes, 16, 227 (1965).
(15) Imamura,M. and Seki,H.:
Bull. Chem. Soc. Japan, 40, 1116 (1967).

Chapter VI. Summary

Concerning so far mentioned behaviors of recoil atoms associated with α-decay and reactions of $^{10}B(n,\alpha)^{7}Li$ with chemical matrix are summarized as follows.

In chapter I, the brief overview on recoil chemistry and hot atom chemistry is given, before the standpoint of the present study is explained. Gaseous electro-deposition, solid state track detection and chemistry influenced by recoil energy are three main parts, first of which is in chapters II and III, the second and third are in chapter IV and V respectively.

In chapter II, selective gaseous electro-deposition of decay nuclides of thorium is taken up. Measurements on the active deposits obtained at the target indicate that, when no potential is applied to the target, the deposition process chiefly depends on one of the daughter nuclides, ^{220}Rn while under negative potential applied to the target, it mainly depends on the recoil atoms with positive charges produced by α-decay. In the experiment using a capsule with three electrodes under normal pressure starting from the same source ^{212}Pb deposited on the grid net, and ^{208}Tl on the target selectively. The mechanism of the electro-deposition process under electric field with and without a grid is explained by the decay pattern shown by each nuclide.

In chapter III, behaviors of recoil atoms in the electro-deposition under pressure below atmospheric are explained. The results obtained are summarized as follows. (1) The

active deposits obtained on the target under pressure except where a discharge happens is mostly ^{208}Tl. (2) Under pressure range of 10 ~ 760 mmHg, the deposition of ^{208}Tl depends on the electric field, accordingly an experimental equation between the critical electric potential and the pressure is obtained. (3) In the case where the range of α-recoil atoms is large enough to travel from source to target for the mass-transfer, the recoil is prior to the applied potential. (4) In discharge condition, the pattern obtained on the target is identical with that of the source, indicating the evaporation by electron irradiation and the transference along electric field line.

In chapter IV, the interactions of α- and γ-rays with celluloid film,which is one of the most sensitive polymers to the radiation damage, are examined from the point of solid state track detector. The results obtained with this film using α-particle from several α-emitters are summarized as follows. (1) The alpha spectrum is easily obtained as a curve of track number versus absorber thickness. (2) The alpha track pattern obtained by thick source or solutional drop of radiocolloid is easily obtained without the influence of sun light, β- and γ-rays.

The results obtained in regard to the effect of γ-irradiation of celluloid on α-track registration are summarized as follows. (1) Gamma-irradiation produces radiation damage, i.e. the latent tracks in the film at the dose above 2×10^6 rad. (2) The optimum etching condition examined by weighing

a piece of the film before and after etching is found to be 6 M sodium hydroxide solution at 50°C, agreeing with that of α-track. (3) The activation free energy of the γ-pretreated film increased slightly with the γ-absorption dose. (4) The UV-light absorption curve of the film shifts towards the longer wavelength side with the increase of γ-absorption dose. (5) Both the gravimetric and the optical methods suggest the possibility of applying the celluloid film to dosimetry of a high γ-dose. (6) The critical energy decreases with the increase of absorption dose in γ-pretreatment, warning that its variation should be taken into account when registering charged particles under high γ-ray background.

In chapter V, the effect of boron compound additives such as NH_4BF_4 and $C_2H_5NH_2BF_3$ on hydrazine formation in the radiolysis of an aqueous solution of ammonia is examined. The results are summarized as follows. (1) The yield of hydrazine upon radiolysis of 15 M ammonium hydroxide solution is found to be very small but is strongly dependent on the type of irradiation. (2) In the case of NH_4BF_4 added, the yield of hydrazine depends on the boron concentration but does not depend on the irradiation time. (3) Hydrazine formed in the presence of $C_2H_5NH_2BF_3$ has a maximum value at about 5×10^{21} eV/ml absorption dose. (4) The characteristics of the added boron compounds are explained by the hot atom effect of $^{10}B(n,\alpha)^7Li$ reaction and the protecting effect of the resulting Lewis type acid, which inhibit the decomposition of hydrazine by scavenging the H and NH_2.

radicals.

The application of the energy of nuclear transformation to a chemical preparation is hopeful to be developed. In particular, in the case of an active nuclide which consists in a molecule or a compound, we should be taken into account that there are not only an energy source in situ but also an effective centre of hot atom or protecting effect described in chapter V.

Acknowledgements

The author would like to express his greatest appreciation to Professor M. Shinagawa who has guided the author to the present study and has been giving the continuous encouragement and criticisms.

The author would like to express his indebtedness to Professor S. Imoto and Professor S. Kawanishi for their valuable discussions and advices.

The author would like to express his appreciation to Professor T. Suita, Professor T. Sano, Professor Y. Sakurai and Professor T. Sekiya for their kind encouragements.

The author is great thankful to Dr. Y. Kiso, Dr. T.Tamai and Dr. T. Hashimoto of Research Reactor Institute, Kyoto University for constant interest and valuable suggestions and to Professor A. Ohyoshi of Kumamoto University and Dr. T. Yanagi for their kind encouragements.

Furthermore, the author is thankful to the past and present members of Shinagawa-Laboratory for many experimental help and discussions, and for providing a stimulating atmosphere.

List of Papers for the Thesis

(1) Application of Solid-State Track Detector for RdTh Daughter Nuclides and Alpha Particles,
Proceedings of the 9th Japan Conference on Radioisotopes, B/2-3 (1969). (in Japanese)

(2) Selective Gaseous Electro-Deposition of Lead-212 and Thallium-208 from RdTh Source,
J. Nucl. Sci. Technol., 10, 155 (1973).

(3) Effect of Gamma Irradiation on Celluloid Film and Related Influence on the Registration of Alpha Tracks,
J. Nucl. Sci. Technol., 10. 215 (1973).

(4) Effect of the Addition of Boron Compounds on Hydrazine Formation in the Radiolysis of an Aqueous Solution of Ammonia,
J. Nucl. Sci. Technol., 10, 268 (1973).

(5) Solid State Track Detector for Several Alpha Emitters of RdTh Daughter Nuclides,
Technol. Report, Osaka Univ., 23, No. 2 (1973).

(6) Gaseous Electro-Deposition of Thallium-208 from Lead-212 Source,
To be published in J. Nucl. Sci. Technol.

Other Publications

(1) On the Determination of Isotope Ratios of Gallium and Antimony Neutron Activation,
Proceedings of the 7th Japan Conference on Radioisotopes, B/1-6 (1966). (in Japanese)

(2) Half-Life and Gamma-Ray Energies of Lanthanum-144,
J. Nucl. Sci. Technol., 9, 658 (1972).

(3) Gama-Ray Energies and Half-Lives of Praseodymium-148 and -149,
J. Nucl. Sci. Technol., 10, 101 (1973).

(4) 固体飛跡検出器のαトラック
日本原子力学会, 放射線微視的効果専門委員会報告書, 135 (1971)

大阪大学

論　文　目　録

報告番号・甲第1625号　　竹味弘勝

主論文　STUDY ON CHEMICAL EFFECT OF RECOIL PARTICLE
（反跳粒子の化学効果に関する研究）

（主論文のうち印刷公表したもの）

1. 固体飛跡検出器によるRdThの娘核種とそのα線の挙動
第9回　日本アイソトープ会議報文集
昭和44年5月15日

1. Selective Gaseous Electro-Deposition of Lead-212 and Thallium-208 from RdTh Source
（RdTh源からの^{212}Pbおよび^{208}Tlに関する選択的ガス電着）
J. Nucl. Sci. Technol.,　10巻　3号
昭和48年3月25日

1. Effect of Gamma Irradiation on Celluloid Film and Related Influence on the Registration of Alpha Tracks
（セルロイドフィルムにおけるγ線照射効果とそのαトラック記録への影響）
J. Nucl. Sci. Technol.,　10巻　4号
昭和48年4月25日

1. Effect of the Addition of Boron Compounds on Hydrazine Formation in the Radiolysis of an Aqueous Solution of Ammonia
（アンモニア水の放射線照射によるヒドラジン生成におよぼすホウ素化合物の添加効果）
J. Nucl. Sci. Technol.,　10巻　5号
昭和48年　5月25日

（主論文のうち未公表のもの）

1. Solid State Track Detector for Several Alpha Emitters of RdTh Daughter Nuclides

（RdTh 娘核種の 二・三の アルファ放射体に対する 固体飛跡検出器）

大阪大学工学報告　　23巻　2号
昭和48年 9月　　掲載予定

1. Gaseous Electro-Deposition of Thallium-208 from Lead-212 Source

（^{212}Pb 源からの ^{208}Tl の ガス電着）

J. Nucl. Sci. Technol.,　　投稿中